Deltares

Mapping the restoration potential of flat oyster, blue mussel, and horse mussel in the North Sea, Wadden Sea and Southwestern Delta



Mapping the restoration potential of flat oyster, blue mussel, and horse mussel in the North Sea, Wadden Sea and Southwestern Delta

Author(s)
Sebastiaan Mestdagh
Floris van Rees
Devanshi Pathak
Lauriane Vilmin
Loreta Cornacchia
Jelle Rienstra

Mapping the restoration potential of flat oyster, blue mussel, and horse mussel in the North Sea, Wadden Sea and Southwestern Delta

Client	Ministerie van Landbouw, Visserij, Voedselzekerheid en Natuur
Contact	Sonja Fortuin
Projectreference	
Keywords	Bivalve reefs; habitat suitability; DEB modelling; ecosystem restoration; Nature Restoration Regulation

Document control	
Version	1.0
Date	18-11-2026
Project nr.	11212288-003
Document ID	11212288-003-ZKS-0001
Pages	77
Classification	
Status	Final

Author(s)

	Sebastiaan Mestdagh Floris van Rees Devanshi Pathak Lauriane Vilmin Loreta Cornacchia Jelle Rienstra	

Samenvatting

Deze studie beoordeelt het herstelpotentieel voor de rifvormende Europese platte oester (*Ostrea edulis*), gewone mossel (*Mytilus edulis*) en paardenmossel (*Modiolus modiolus*) in de Noordzee, Waddenzee en Zuidwestelijke Delta (Westerschelde, Oosterschelde, Grevelingenmeer). Het werk ondersteunt het Nationaal Herstelplan (in Nederland: Natuurplan) onder de Europese Natuurherstelverordening en levert een ruimtelijk expliciete analyse van waar herstel van biogene riffen ecologisch haalbaar is.
Abiotische habitatgeschiktheidsmodellen worden gecombineerd met Dynamic Energy Budget- (DEB-)modellen. Habitatgeschiktheidsmodellen identificeren waar de omgevingscondities overeenkomen met de ecologische niches van de soorten, terwijl DEB-modellen evalueren of individuen voldoende kunnen groeien en reproduceren om duurzame populaties te vormen. Samen bieden deze methoden een robuuste beoordeling van het herstelpotentieel onder huidige milieuomstandigheden.

Verspreidingsgegevens van soorten werden verzameld uit biodiversiteitsdatabases, historische bronnen en monitoringprogramma's. Omgevingsvariabelen zijn afkomstig uit hydrodynamische modellen van Deltares, nieuwe predicties, sedimentdata van TNO en literatuurbronnen. Voor de Noordzee zijn zowel Generalized Additive Models (GAM) als Random Forests (RF) gebruikt om habitatgeschiktheid te voorspellen; in de Waddenzee en Zuidwestelijke Delta zijn Random Forest en ruimtelijke Integrated Nested Laplace Approximation (INLA) modellen toegepast.
DEB-modellen zijn ontwikkeld voor *O. edulis* en *M. edulis* op basis van hydrodynamische waterkwaliteitsmodellen voor de Noordzee en het Grevelingenmeer. Groei werd over meerdere jaren gesimuleerd om een lengte-gebaseerde geschiktheidsindex te bepalen. Statistische relaties tussen DEB-uitkomsten en omgevingsvariabelen maakten extrapolatie over volledige bekkens mogelijk.

Belangrijkste bevindingen:

- *O. edulis*
  - Noordzee: Grootste potentieel in de Voordelta en delen van het Friese Front.
  - Waddenzee: Geschiktheid is over het algemeen laag door zeer beperkte recente waarnemingen; meest kansrijke gebieden zijn de geulsystemen van het Eierlandse Gat en Vlie. De betrouwbaarheid van de modelresultaten is echter laag omwille van het zeer lage aantal waarnemingen.
  - Zuidwestelijke Delta: Hoog potentieel in de Oosterschelde (nabij Neeltje Jans) en in ondiepe, relatief zuurstofrijke delen van het Grevelingenmeer.
- *M. edulis*
  - Noordzee: Brede geschiktheid in de kustzone, vooral de Voordelta en kustnabije gebieden langs de Waddeneilanden.
  - Waddenzee: Grote delen van het gebied zijn geschikt; intergetijden-hotspots bevinden zich op het wantij bij Ameland en Schiermonnikoog, en subtidale geschiktheid is het hoogst nabij de Afsluitdijk.
  - Zuidwestelijke Delta: Hoog potentieel in ondiepe delen van het Grevelingenmeer en verschillende intergetijdengebieden in de Oosterschelde. In de Westerschelde neemt de geschiktheid sterk af stroomopwaarts.
- *M. modiolus*
  - Consequent lage geschiktheid in Nederlandse wateren. Deze soort lijkt daarom geen realistische kandidaat voor herstel in Nederland.

De resultaten tonen aan dat de omgevingscondities gunstig blijven voor het herstel van *O. edulis*- en *M. edulis*-riffen een schaal waarbij deze substantieel kunnen bijdragen aan ecosysteemfuncties in alle onderzochte bekkens, met uitzondering van de Westerschelde (voor *O. edulis*). Herstelstrategieën dienen zich op basis daarvan te richten op:

- Het versterken en uitbreiden van bestaande populaties van *O. edulis*- en *M. edulis* in de Voordelta.
- Herstel in de geulsystemen van de Waddenzee (*O. edulis*) en op het wantij (*M. edulis*).
- Strategische locatiekeuze in de Oosterschelde en het Grevelingenmeer, met expliciete aandacht voor zuurstofdynamiek in dat laatste.

Hoewel er onzekerheden blijven als gevolg van databeperkingen, modelaannames en milieuvariabiliteit, biedt de studie een wetenschappelijk onderbouwde basis voor het prioriteren van herstelmaatregelen binnen het Nederlandse Nationaal Herstelplan.

Summary

This study assesses the restoration potential of the reef-forming European flat oyster (*Ostrea edulis*), blue mussel (*Mytilus edulis*), and horse mussel (*Modiolus modiolus*) in the North Sea, Wadden Sea, and Southwestern Delta (Westerschelde, Oosterschelde, Lake Grevelingen). The work supports the Netherlands' National Restoration Plan under the EU Nature Restoration Regulation and provides a spatially explicit analysis of where biogenic reef restoration is ecologically feasible.

Abiotic habitat suitability modelling is combined with Dynamic Energy Budget (DEB) modelling. Habitat suitability modelling identifies where environmental conditions align with species' ecological niches, while DEB modelling evaluates whether individuals can grow and reproduce sufficiently to form sustainable populations. Together, these methods offer a robust assessment of restoration potential under present-day environmental conditions.

Species distribution data were compiled from biodiversity databases, historical records, and monitoring programmes, while environmental layers were extracted from Deltares hydrodynamic models, custom-made predictions, TNO sediment data and literature. For the North Sea, both Generalized Additive Models (GAM) and Random Forests (RF) were used to predict habitat suitability; in the Wadden Sea and Southwestern Delta, Random Forest and spatial Integrated Nested Laplace Approximation (INLA) models were applied.
DEB models were developed for *O. edulis* and *M. edulis* using hydrodynamic water quality models for the North Sea and Lake Grevelingen. Growth was simulated over multi-year periods to derive a length-based suitability index. Statistical relationships between DEB outputs and environmental variables enabled extrapolation across full basins.

Key Findings:

- *O. edulis*
  - North Sea: Highest potential in the Voordelta and parts of the Frisian Front.
  - Wadden Sea: Suitability is low overall due to very limited recent observations; most promising areas are the Eierlandse Gat and Vlie tidal inlet systems. However, reliability of the model results is low due to the low number of observations.
  - Southwestern Delta: Strong potential in the Oosterschelde (near Neeltje Jans) and where shallow, relatively well-oxygenated areas of Lake Grevelingen.
- *M. edulis*
  - North Sea: Coastal zone shows broad suitability, particularly the Voordelta and nearshore areas along the Wadden Islands.
  - Wadden Sea: Large parts of the basin are suitable; intertidal hotspots occur on tidal divides near Ameland and Schiermonnikoog, and subtidal suitability is highest near the closure dam.
  - Southwestern Delta: High potential in shallow areas of Lake Grevelingen and various intertidal areas in the Oosterschelde. Suitability in the Westerschelde declines strongly upriver.
- *M. modiolus*
  - Consistently low suitability across Dutch waters. This species therefore does not seem to be a realistic candidate for restoration in the Netherlands.

The results demonstrate that habitat conditions remain favourable for *O. edulis* and *M. edulis* reef restoration at a scale at which they can make a substantial contribution to ecosystem

functioning in all basins except the Westerschelde (for *O. edulis*). Restoration strategies should focus on:

- Enhancing and expanding existing *O. edulis* and *M. edulis* populations in the Voordelta.
- Restoration in Wadden Sea tidal inlet systems (*O. edulis*) and on tidal divides (*M. edulis*).
- Strategic site selection in the Oosterschelde and Lake Grevelingen, with explicit attention to oxygen dynamics in the latter.

While uncertainties remain due to data gaps, model assumptions, and environmental variability, the study provides a science-based foundation for prioritising restoration actions under the Dutch National Restoration Plan.

Contents

	Samenvatting	**4**
	Summary	**6**
	Contents	**8**
1	**Introduction**	**10**
2	**Methods**	**12**
2.1	Data collection	12
2.1.1	Species distribution data	12
2.1.1.1	North Sea	12
2.1.1.2	Wadden Sea	13
2.1.1.3	Southwestern Delta	13
2.1.2	Environmental data	14
2.1.2.1	North Sea	14
2.1.2.2	Wadden Sea	16
2.1.2.3	Southwestern Delta	16
2.1.2.4	Southwestern Delta – Sediment maps	16
2.2	Abiotic habitat suitability modelling	18
2.2.1	North Sea	18
2.2.2	Wadden Sea	19
2.2.2.1	*O. edulis*	19
2.2.2.2	*M. edulis*	19
2.2.3	Southwestern Delta	21
2.3	Bivalve growth potential	22
2.3.1	DEB Theory	22
2.3.2	D-HYDRO suite of models	23
2.3.2.1	North Sea: Hydrodynamic and water quality modelling	23
2.3.2.2	Lake Grevelingen: Hydrodynamic and water quality modelling	24
2.3.2.3	DEBGRZ	25
2.3.3	DEB model setup	26
2.3.3.1	Site selection	26
2.3.3.2	1D model setup	28
2.3.3.3	Statistical extrapolation of DEB results to a wider area	30
3	**Results**	**32**
3.1	Abiotic habitat suitability modelling	32
3.1.1	North Sea	32
3.1.1.1	Predicted habitat suitability for *O. edulis*	32
3.1.1.2	Predicted habitat suitability for *M. edulis*	34
3.1.1.3	Predicted habitat suitability for *M. modiolus*	36
3.1.2	Wadden Sea	38
3.1.2.1	Predicted habitat suitability for *O. edulis*	38
3.1.2.2	Predicted habitat suitability for *M. edulis*	39
3.1.3	Southwestern Delta	42
3.1.3.1	Sediment maps	42

3.1.3.2 Predicted habitat suitability for *O. edulis* 44
3.1.3.3 Predicted habitat suitability for *M. edulis* 45

3.2 Bivalve growth potential 49
3.2.1 North Sea 49
3.2.2 Lake Grevelingen 54

3.3 Integration 57
3.3.1 North Sea 57
3.3.2 Lake Grevelingen 59
3.3.3 Combined mapping across all study areas 60

4 Discussion 63

4.1 Implications for restoration opportunities 63
4.1.1 North Sea 63
4.1.2 Wadden Sea 64
4.1.3 Southwestern Delta 64

4.2 Ecological considerations of the model results 64

4.3 Additional elements to be considered for successful restoration 66

4.4 Methodological considerations and model uncertainty 67

4.5 Recommendations and conclusion 68
4.5.1 Recommendations on future modelling 68
4.5.2 Recommendations on management and restoration 69
4.5.3 Conclusion 70

References 71

Appendix 76

1 Introduction

The European regulation on nature restoration (or Nature Restoration Regulation - NRR, in Dutch: Natuurherstelverordening, NHV) obliges Member States to restore degraded ecosystems and enhance biodiversity and ecological resilience. In alignment with the EU Biodiversity Strategy for 2030, the NRR sets measurable restoration targets and emphasizes large-scale recovery of degraded marine habitats (article 5), including biogenic reefs, to reverse biodiversity loss and restore ecosystem functions. In this context, the Netherlands is developing a national restoration plan (Natuurplan) aimed at quantifying and mapping valuable and potentially valuable habitats, and identifying opportunities for the restoration of habitats that are not in favourable condition. In this process, it is important to consider current and future areas that have a conservation status or are planned or suggested for fishery restrictions.

Marine habitat types requiring protection and restoration have been grouped into seven broad categories under the NRR. These include group 1 (seagrass beds), group 2 (macroalgal forests), group 3 (shellfish beds), group 4 (maerl beds), group 5 (sponge, coral and coralligenous beds), group 6 (vents and seeps) and group 7 (soft sediments). Groups 4 and 6 do not occur within Dutch waters, but the other groups form an important focus for marine conservation and restoration efforts. The present study focuses specifically on group 3, which comprise habitat-forming assemblages created by reef-building species. Within Dutch coastal and marine waters, the principal reef-forming bivalves are the European flat oyster (*Ostrea edulis*), blue mussel (*Mytilus edulis*), and horse mussel (*Modiolus modiolus*). Deltares has been commissioned to produce habitat suitability maps for these species in the North Sea, Wadden Sea, and Southwestern Delta (Westerschelde, Oosterschelde, and Lake Grevelingen). This work is intended to provide quantitative insight into the current and future restoration potential of these biogenic reef systems. The three species can form extensive beds or reefs of high ecological value (Craeymeersch and Jansen, 2018), although it is uncertain whether *M. modiolus* can form reefs within the Dutch North Sea. As ecosystem engineers, reef-forming bivalves enhance habitat complexity, provide biogenic structure, increase local biodiversity and food availability, and modulate benthic-pelagic coupling through filtration, biodeposition, and nutrient cycling. As such, their reefs can facilitate associated communities, stabilise sediments, and improve water quality, thereby supporting wider ecological functioning and potentially delivering co-benefits for coastal protection (Ysebaert et al., 2018).

Historically, large flat oyster reefs occurred throughout the Dutch sector of the North Sea (Thurstan et al., 2024), most notably over a large area in what is now aptly called the Oyster Grounds. However, many of these reefs have largely disappeared due to overfishing and disease (Fey et al., 2010; Helmer et al., 2019).

Blue mussels are particularly associated with coastal environments that provide sufficient water movement and food supply, while avoiding excessive sediment burial (van der Meer, 2025). Extensive beds still occur in the Wadden Sea and Southwestern Delta (Troost et al., 2025a). Suitable habitat is therefore expected to be widespread in nearshore and estuarine areas, but more limited in offshore regions where substrate availability and recruitment conditions are less favourable.

The horse mussel occupies a boreal lower-intertidal to subtidal niche (to ~200 m depth) as a byssally attached suspension feeder in moderate- to high-energy environments, where it forms dense aggregations on mixed hard–soft substrates (Dinesen and Morton, 2014).

Consistent with these niche requirements, its predicted probability of occurrence was previously found to be highest in the northern parts of the North Sea (Herman and van Rees, 2022). Within Dutch waters, suitable conditions for *M. modiolus* are expected to be constrained relative to more northerly regions, although localised opportunities may exist where substrate heterogeneity and flow conditions align.

Based on species-specific niche requirements and spatial context, this study identifies current and future suitable areas in the North Sea and adjacent coastal waters for the restoration of biogenic bivalve reefs. While abiotic habitat suitability mapping provides an essential first indication of where environmental conditions align with the ecological needs of the three species, it does not fully capture the potential for long-term population persistence. To address this limitation, we complement habitat suitability mapping with dynamic energy budget (DEB) modelling in the North Sea and Lake Grevelingen. DEB models allow us to assess whether individuals in a given habitat can acquire sufficient energy to grow, reproduce, and maintain viable populations. This integration moves the assessment beyond abiotic benthic conditions alone, enabling us to distinguish areas where reef formation is theoretically possible, from those where it is ecologically sustainable. In the Wadden Sea and the Western and Oosterschelde, primary productivity is currently not thought to be a limiting factor for bivalve development (Beukema and Dekker, 2022; Craeymeersch et al., 2024), reducing the need for any additional analyses besides the habitat suitability mapping.

Together, the combined habitat suitability maps and DEB model outputs provide a spatially explicit and ecologically grounded estimate of restoration potential for *O. edulis*, *M. edulis* and *M. modiolus* across Dutch coastal and marine waters. Although factors such as larval connectivity and the hydrodynamic stability of introduced material can also influence the long-term establishment of biogenic reefs, these processes lie outside the scope of this assessment and should be considered in subsequent stages of restoration planning. The maps resulting from the analyses in this report will identify where restoration efforts for these reef-forming species makes ecological sense. In doing so, the work supports evidence-based prioritisation of restoration sites within the National Restoration Plan and contribute to a strategic, science-based approach to revitalising biogenic reef systems in the North Sea, Wadden Sea, and Southwestern Delta. The maps are made available through the IHM viewer (https://viewer.openearth.nl/ihm-viewer/?layers=TNwG8fEDSCWYYZ77hY6rJQ&folders=85223022,QkqWfw4ISFmthH1koe1OyQ,RGRP33bITV6NnUX9pyRMbw,HXYGvRdBSFaveDHP9JoDwQ&layerNames=Herstelpotentieel%20van%20O.%20edulis).

2 Methods

2.1 Data collection

2.1.1 Species distribution data

O. edulis and *M. edulis* have both been known to occur in all Dutch marine and coastal waters (North Sea, Wadden Sea and Southwestern Delta). *M. modiolus* is present in large parts of the greater North Sea, although it is relatively rare within the Dutch Exclusive Economic Zone (EEZ). In the Wadden Sea and Southwestern Delta, it is absent or too rare to be reliably modelled.

2.1.1.1 North Sea

O. edulis

Historical occurrences of *O. edulis* in the North Sea were derived from Bennema et al. (2020) and complemented with early-twentieth-century data from the Gilson dredge surveys digitized by Houziaux et al. (2008) The dataset from Bennema et al. (2020) combines digitized records from the nineteenth-century Huxley–Wodan and Poseidon expeditions with a reconstructed map of high historical oyster occurrence around the Oyster Grounds (Olsen, 1883).
This map was digitized in QGIS and used to generate pseudo-presence and pseudo-absence points for habitat modelling. Additional data from the Flemish Banks were included to cover the southern North Sea, which were digitized from the Gilson samples in figures from Houziaux et al., (2008). Contemporary observations from the DATRAS dataset provided by Wageningen Marine Research in the Voordelta, Rotterdam harbour, and Wadden Sea were excluded because the Delft3D model did not adequately resolve the hydrodynamic and water-quality conditions in these areas, preventing the derivation of reliable environmental predictors (see Herman and van Rees, 2022, for methodological details). Notably, the Voordelta supports a natural mixed-species oyster reef that includes the European flat oyster (Ostrea edulis), but this habitat could not be included in the present modelling framework. This dataset was supplemented by newly available historical data by Thurstan et al. (2024).

M. edulis and *M. modiolus*

Data for *M. edulis* and *M. modiolus* were obtained by extracting the derived macrobenthos presence/absence tables from EMODnet (downloaded 29-01-2026), filtering for surveys with complete taxonomic inventories, and constructing per-species presence/absence for all valid sampling events. The dataset was clipped to the extent of a Greater North Sea bounding box before exporting. Due to a lack of German data, additional presences (limited to datasets that, for other countries, were likely included in the EMODnet dataset) were extracted from OBIS and GBIF, filtered to the German EEZ, cleaned and limited to records only from 1990 onwards. Pseudo-absences were added inside the German EEZ to balance presence-only data. All data were then merged into a unified table.
Additional presence data were obtained from the ICES DATRAS dataset of standardized bottom-trawl fish surveys. Due to a low amount of usable data for *M. edulis*, this dataset was only used for *M. modiolus*.
Finally, for *M. edulis*, additional data were obtained from the annual shellfish monitoring surveys (WOT – Wettelijke Onderzoekstaken) along the Dutch coast by Wageningen Marine Research. For a full description of sampling design and data processing, see Troost et al. (2025a).

Before further analysis, the EMODnet dataset was merged with the WOT dataset (for *M. edulis*) or with the DATRAS dataset (for *M. modiolus*).

To avoid an underestimation of presence in the model due to high absence concentrations, all absence points within a radius of 3 km from any presence point were deleted.

2.1.1.2 Wadden Sea

O. edulis

Presence data for *O. edulis* were obtained from Wageningen Marine Research. We found five observations of *O. edulis* individuals in the annual WOT-MOSKOK surveys, in which stock size and time series are estimated for commercial bivalve species on the intertidal flats. One more observation was included, originating from the supplementary *Ensis* survey in 2017, in which *Ensis* sp. are targeted with a hydraulic grab in the Western Wadden Sea. All observations were found over the period from 2014 to 2021. Absence data were added by extracting the WOT-MOSKOK data points from Datahuis Wadden (downloaded 26-02-2026). To avoid an underestimation of presence in the model due to high absence concentrations, all absence points within a radius of 1 km from any presence point were deleted.

M. edulis

Polygons of *M. edulis*, Pacific oyster (*Magallana gigas*) and mixed *M. edulis* x *M. gigas* reefs were obtained from Wageningen Marine Research. In their WOT-MOSKOK surveys, sampling is stratified across intertidal and subtidal zones, with higher densities in areas known to contain shellfish reefs. Intertidal samples are collected manually at low tide, while subtidal areas are sampled from research vessels using bottom scrapers, suction dredges, or hydraulic grabs depending on depth and substrate. All collected material is sorted, counted, and weighed, with mussels and oysters assigned to standardised size classes. Intertidal reefs are mapped using GPS, and patches with ≥ 5 % cover of mussels or oysters are delineated as banks conform the definitions used by WMR (de Froe et al., 2025). Areas with lower cover are recorded as scattered shell material. Reefs are classified as:

- Pure mussel reef (≥ 5 % cover of *M. edulis*, < 5 % *M. gigas*)
- Pure oyster reef (< 5 % cover of *M. edulis*, ≥ 5 % *M. gigas*)
- Mixed mussel reef (≥ 5 % cover of both, *M. edulis* > 50 % of total cover)
- Mixed oyster reef (≥ 5 % cover of both, *M. gigas* > 50 % of total cover)

Biomass and density per station are extrapolated to total stock estimates using the representative area of each grid cell. Results are presented as total fresh biomass and bank area. When multiple gears are used, calibration factors (e.g. for suction dredge versus hydraulic grab) are applied to correct for differences in catch efficiency.

In addition to the WOT-MOSKOK surveys, we also added data from the sublittoral seed mussel survey of the Producentenorganisatie. This data was added to supplement the point data with additional location of blue mussel observations in the subtidal.

2.1.1.3 Southwestern Delta

Both point data with observations of *O. edulis* and *M. edulis* and polygons of *M. edulis*, *M. gigas* and mixed *M. edulis* x *M. gigas* reefs were obtained from Wageningen Marine Research and also originated from the annual WOT-MOSKOK surveys. The methodology of the surveys is consistent with that in the Wadden Sea.

2.1.2 Environmental data

2.1.2.1 North Sea

To characterise environmental conditions relevant for habitat suitability modelling, we mostly used the data layers described in Herman and van Rees (2022), who compiled a harmonised North Sea-wide dataset from multiple authoritative sources. Core variables include bathymetry, several scales of bathymetric position index (BPI5, 10, 30, 50, 75; each representing the relative depth of a map pixel compared to its surroundings at a length of, respectively, 5, 10, 30, 50 or 75 pixels; van der Reijden et al., 2021), bottom shear stress, temperature, salinity, and sediment composition (percentages of sand, mud and gravel). Continuous sediment fractions were preferred over categorical sediment classifications (e.g., FolkX), as they preserve compositional variability within sediment classes and allow habitat suitability models to capture gradual responses along sediment gradients.
Bathymetric data were obtained from the EMODnet Digital Terrain Model (DTM 2022), which integrates hydrographic surveys and existing bathymetric datasets from multiple providers into a harmonised grid. Sediment composition (percentages of sand, mud and gravel) was derived from the predictive maps developed by Stephens and Diesing (2015), who used random forest models trained on historical grain-size observations and environmental predictors. Temperature and salinity data were obtained from Copernicus Marine Service products. Bottom shear stress was derived from results of the Deltares 3D Dutch Continental Shelf Model - Flexible Mesh (3D DCSM-FM; Zijl et al., 2023a) hydrodynamic model.
In addition to these layers, we included maximum and time-averaged bottom chlorophyll a concentrations and temperature difference between surface and bottom (as a measure of temperature stratification), all from the 3D DCSM-FM hydrodynamics and water quality model (Vilmin et al., 2026).
An updated mud percentage map for the Dutch continental shelf was delivered by TNO in 2026 (Dabekaussen and Meijninger, 2026). This map was reprojected and resampled to match the spatial resolution, grid alignment, and extent of Stephens and Diesing (2015). Within the spatial domain covered by the TNO dataset, values of the Stephens and Diesing (2015) map were replaced by the new values. Figure 1 shows the difference between the old and new mud percentage values. By request of TNO, the significance of three different mud percentage maps was compared in the models: mud estimated with 25, 50 (the official mud percentage map), and 75 percent certainty. These layers can be found at https://viewer.openearth.nl/ihm-viewer/.

All raster layers were resampled to a common grid and projection to ensure consistent spatial analysis. For each observation point within each species' dataset, values from all environmental layers were extracted to create a unified species-environment table used in subsequent modelling steps.

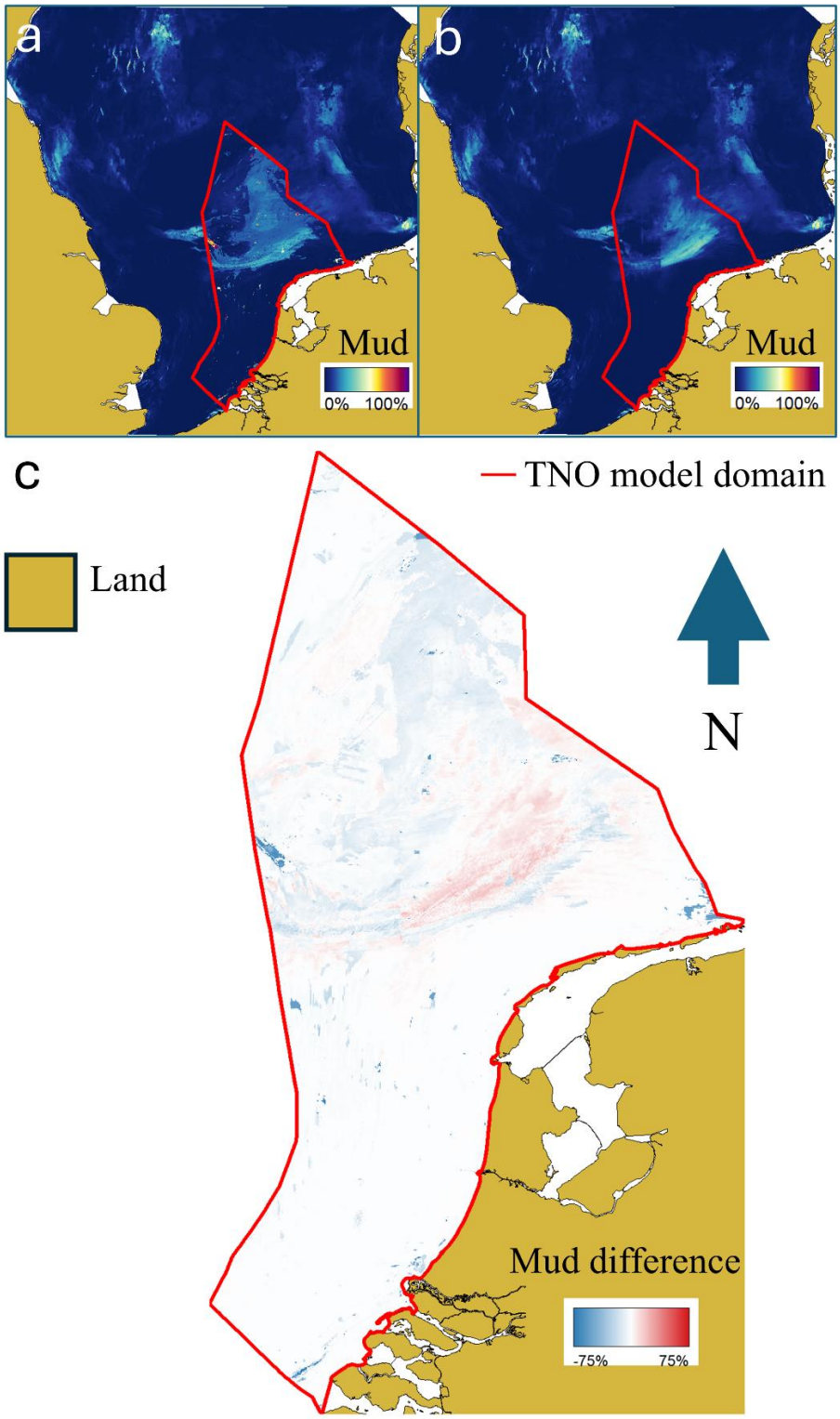


Figure 1: Mud fraction (%) maps derived from (a) Dabekaussen and Meijninger (2026), and (b) Stephens and Diesing (2015). The Dabekaussen and Meijninger (2026) product was reprojected and resampled to match the spatial resolution, grid alignment, and extent of Stephens and Diesing (2015). Within the spatial domain covered by the TNO dataset, values from Dabekaussen and Meijninger (2026) replace those of Stephens and Diesing (2015); outside this domain, the original Stephens and Diesing (2015) values are retained. Panel (c) shows the difference map computed as Stephens and Diesing (2015) minus Dabekaussen and Meijninger (2026) within the TNO domain.

2.1.2.2 Wadden Sea

For the Wadden Sea, orbital velocity, salinity (mean, maximum, minimum, standard deviation and variance) and water velocity (5th and 99th percentile) were derived from results of the Dutch Wadden Sea Model (DWSM; Zijl et al., 2023b). Median grain size and mud percentage were obtained by interpolation via kriging of samples taken during the Synoptic Intertidal Benthic Survey (SIBES) and its extension to subtidal areas (Franken et al. *i.p.*). Mean bottom chlorophyll a concentrations were extracted from the coarser-resolution 3D DCSM-FM model covering the entire Dutch continental shelf, including the Wadden Sea, rather than from a higher-resolution model specifically developed for the Wadden Sea. Exposure time and elevation were downloaded from the saltwater ecotope base layers, hosted by Rijkswaterstaat (https://downloads.rijkswaterstaatdata.nl/ecotopen_zout_raster/).

2.1.2.3 Southwestern Delta

For the Westerschelde, mean bed shear stress, mean salinity at the bottom and surface, mean water velocity at the bottom and surface, and depth-averaged salinity and water velocity were derived from the results of the Westerschelde Delft3D-Flexible Mesh hydrodynamic model (Westerschelde-DFM). Exposure time, maximum current velocity and elevation were downloaded from the saltwater ecotope base layers. For chlorophyll a concentration, point data were obtained from the annual monitoring of surface water quality (https://scheldemonitor.github.io/Eerstelijnsrapportage/fysisch-oppwater.html), filtered to the years 2015 to 2024 and interpolated via IDW interpolation.

For the Oosterschelde, bed level, depth-averaged water velocity and means and maxima of bed shear stress, surface chlorophyll a concentration, surface extinction coefficient, surface oxygen concentration, surface salinity, sea floor depth, surface temperature and total suspended solids were derived from the results of the Oosterschelde Delft3D-Flexible Mesh hydrodynamic model (Oosterschelde-DFM). Exposure time, maximum current velocity and elevation were downloaded from the saltwater ecotope base layers.

For Lake Grevelingen, bed level, standard deviation of surface and bottom oxygen concentration and means, minima and maxima at the surface and bottom of chlorophyll a concentration, primary productivity, oxygen concentration, phytoplankton concentration, salinity, temperature and water level, along with the temperature difference between surface and bottom and bed shear stress, were derived from the results of the Grevelingen Delft3D-Flexible Mesh hydrodynamic model (Grevelingen-DFM).

2.1.2.4 Southwestern Delta – Sediment maps

Because no full-coverage sediment raster layers were available, predictive models were used to generate continuous spatial maps from point observations. Sediment data were obtained from the MWTL (Monitoring Waterstaatkundige Toestand des Lands; the Dutch environmental monitoring programme on aquatic systems) monitoring programme (2023) and comprised measurements of median grain size (also referred to as D50) and mud content (<63 µm; KGF63) for the three basins in the Southwestern Delta. All sediment observations were projected to the Dutch national grid (RD New: EPSG:28992) to match the coordinate reference system of the environmental raster datasets. The observations were visually inspected for spatial coverage and outliers. For each system, sediment data were treated independently to account for system-specific hydrodynamics, morphology and sedimentary processes.

System-specific environmental predictors describing hydrodynamic forcing and morphology were compiled from the available model output rasters (see section 2.1.2.3). For the Oosterschelde and Westerschelde, predictors included maximum current velocity, emersion time and bed level, with mean water velocity additionally available for the Oosterschelde. These predictors reflect the relatively dynamic and tidally dominated nature of these systems.

For Lake Grevelingen, a more enclosed and low-energy basin, predictor selection was restricted to long-term mean variables only: bed level, mean total bed shear stress, mean water level, and mean water velocity. This selection was motivated by the limited temporal variability in hydrodynamic forcing and the relatively small number of sediment observations for this system.
All rasters were reprojected to EPSG:28992 and resampled to a common grid within each system using bilinear sampling. To avoid artefacts caused by incomplete spatial coverage, a mask was applied so that raster cells were retained only where valid data were available for all predictor layers.

Environmental predictor values were extracted from the raster stacks at each sediment sampling location. The extracted raster values were combined with the sediment observations to form system-specific modelling datasets, which served as input for the subsequent statistical modelling.

Random Forest was used to predict continuous spatial distribution of median grain size (D50) and mud content (KGF63) for the Eastern and Westerschelde. Models were fitted separately for each system and response variable. The choice of Random Forest was motivated by its ability to capture complex, non-linear relationships between sediment properties and environmental drivers and its robustness to multicollinearity among predictors. All Random Forest models were fitted with 500 trees and variable importance calculation enabled. Model performance was evaluated using root mean square error (RMSE), mean absolute error (MAE), the coefficient of determination (R^2), and a normalised RMSE (nRMSE). These metrics were derived from out-of-bag predictions and were used to assess the general predictive skill of the models and to compare performance between systems and response variables.

For Lake Grevelingen, Random Forest models showed little predictive skill, reflecting both the limited number of available sediment observations and the relatively weak coupling between local sediment variability and the available environmental predictors. Therefore, Generalized Additive Models (GAMs) were used for Lake Grevelingen to characterise large-scale sediment gradients in a more constrained and interpretable manner. Separate GAMs were fitted for median grain size and mud content. Median grain size was modelled on a log scale assuming a Gaussian error distribution to ensure strictly positive predictions, while mud content was modelled using a beta regression with a logit link to respect the bounded nature of proportional data. Spatial structure was represented by a bivariate smooth of the spatial coordinates, complemented by smooth terms for the selected environmental predictors. Model fitting was performed using restricted maximum likelihood (REML).
Predictions for Lake Grevelingen were restricted to permanently submerged areas by applying a polygon-based land mask to exclude islands, followed by an additional mask excluding cells with negligible mean water velocity. This two-step masking procedure prevented extrapolation beyond the sediment domain and ensured physically meaningful predictions.
Model performance for the GAMs was assessed using RMSE, MAE, R^2 and nRMSE derived from penalised in-sample predictions. These metrics were interpreted as indicators of the strength of large-scale sediment trends rather than precise point-level predictive accuracy.

Trained models were applied to the corresponding environmental raster stacks to generate continuous spatial predictions of median grain size and mud content for each system. Predictions were restricted to areas with complete predictor coverage and valid sediment domain. Resulting rasters were exported as GeoTIFF files and visually inspected for spatial coherence and physical plausibility.

2.2 Abiotic habitat suitability modelling

2.2.1 North Sea

For the habitat suitability modelling, both Generalized Additive Modelling (GAM) and Random Forest (RF) were used. GAM allows for an easy ecological interpretation by addressing relationships between predictors and presence or absence of species. Random Forest is better able to capture interactions or to handle collinearity and noisy predictors. Especially in heterogeneous environments, combining the two methods can improve predictive accuracy.

Environmental predictor rasters were loaded and transformed to UTM zone 31N (EPSG:32631), before creating a multi-layer raster stack. The species observation data points were reprojected to match the coordinate reference system of the environmental raster stack. Environmental values were extracted at each sampling point. Pearson correlation coefficients between the environmental predictors were then calculated, and a correlation matrix was generated to evaluate potential collinearity among predictors. A set of predictors with minimal collinearity was retained for each species.

A GAM with binomial error structure and logit link was fitted to the selected predictors. Only predictors that showed statistical significance ($p < 0.05$) were retained in the model (Table 1). The model can be written as:

$$Y_i \sim \text{Bernoulli}(p_i)$$

$$\text{logit}(p_i) = \beta_0 + \sum_j \beta_j x_{ij} + \sum_k s_k (x_{ik})$$

where Y_i denotes species presence or absence at location i ($Y_i = 1$ for presence and $Y_i = 0$ for absence), p_i is the probability of occurrence, β_0 is the intercept, $\beta_j x_{ij}$ represent predictors included as linear terms, and $s_k(\cdot)$ are spline smoothers used to capture nonlinear relationships. Smooth terms were applied where exploratory analysis indicated deviations from linearity in the predictor–response relationships. Under a Bernouilli distribution, each observation is treated as a single trial with probability p_i of presence, making it a natural choice for presence/absence data. In a GAM framework, this allows the probability of occurrence to be modelled as a smooth, potentially nonlinear function of environmental predictors (Wood, 2017).

*Table 1: Environmental predictors used in the predictive models for O. edulis, M. edulis, and M. modiolus in the North Sea that were retained after checks on collinearity between predictors. Predictors marked with * were fitted using spline smoothers with basis dimension k = 10 to account for nonlinear effects in the GAM; variables marked with ** were modelled using spline smoothers with k = 5.*

O. edulis	*M. edulis*	*M. modiolus*
BPI30	BPI30*	BPI30*
Mean bottom shear stress	Mean bottom shear stress	Mean bottom shear stress
Maximum bottom chlorophyll a*	Mean bottom chlorophyll a	Mud content
Mud content**	Mud content	Maximum temperature stratification
Maximum temperature stratification*	Salinity	Salinity
Mean temperature	Depth	Mean temperature
Gravel content		Gravel content
Depth		Depth

The environmental raster stack was subset to match the predictors used in the GAM. A spatial prediction was generated across the full North Sea environmental grid, producing a continuous raster of predicted probability of occurrence for each of the three species.

The Random Forest models were fitted with 500 trees and variable importance calculation enabled. The same predictor sets were used as for GAM. Model fitting used out-of-bag sampling internal to Random Forest to reduce overfitting. Continuous rasters of predicted probability of occurrence were created by extracting the probability of presence.

The final habitat suitability map for each species was constructed by calculating the mean raster value at every pixel between GAM and Random Forest. To assess the sensitivity of habitat suitability predictions to uncertainty in sediment composition, we incorporated multiple mud content scenarios derived from TNO mud percentage maps derived by Dabekaussen and Meijninger (2026). In addition to the baseline model using the median (50th percentile) mud map, alternative models were fitted and predicted using the 25th and 75th percentile mud scenarios. This approach was applied consistently for all species and both modelling frameworks (GAM and Random Forest). By comparing predictions across these scenarios, we quantified how variation in estimated mud content influences the spatial distribution of suitable habitat.

2.2.2 Wadden Sea

2.2.2.1 *O. edulis*

With only six presences, a GAM cannot fit stable smooth terms and is dominated by the much larger absence class, leading to unstable, uninterpretable, or meaningless response curves. Even with standard Random Forest, the risk of misclassifying presence as absence can lead to a significant underrepresentation of high probability of occurrence in the prediction. In addition, INLA is likely to overfit the spatial field and give unstable parameter estimates. To overcome this issue, a class-weighted Random Forest was applied, in which class imbalance is dealt with by applying class weights that increase the misclassification cost for the presence class (Valavi et al., 2021).

Environmental predictor rasters were loaded and transformed to UTM zone 31N (EPSG:32631), before creating a multi-layer raster stack. The species observation data points were reprojected to match the coordinate reference system of the environmental raster stack. Environmental values were extracted at each sampling point.

Following the methodology suggested in Valavi et al. (2021), the weight for the presence class was calculated as the ratio of the number of absences over the number of presences, while the weight for the absence class was set to 1. A Random Forest was then fitted with 1000 trees, variable importance calculation enabled and class weights applied. Probability of occurrence was predicted on the raster stack and exported as a GeoTIFF.

2.2.2.2 *M. edulis*

As a first step toward constructing a spatial presence–absence map of *M. edulis* in the Wadden Sea, we produced cumulative rasters representing the number of years in which mussels were recorded between 2015 and 2024. These rasters identify grid cells with recurring mussel presence and form the basis for defining mussel habitat occurrence in subsequent analyses.

For the intertidal zone, we constructed a yearly presence raster based on the annual WMR survey polygons of intertidal mussel beds. For each survey year, polygons delineating mussel banks were rasterized onto a 200 × 200 m grid covering the Wadden Sea. A cell was assigned a value of 1 if it was touched by a mussel-bed polygon each year, and yearly rasters were summed to obtain a cumulative map indicating in how many years (0–10) mussel beds were present at that location. Reefs that included both mussels and the pacific oyster within one bed were also included, since both species can co-occur in a reef.

For the subtidal zone, we applied the same yearly counting procedure to WOT survey point observations and, additionally, observation from mussel spat of the Producentenorganisatie "*mosselzaad sublittorale survey WZ*" were also included. Confirmed *M. edulis* presences within the Wadden Sea domain (4.7–7° E, 52.8–53.6° N) were buffered by 200 m before rasterization. This buffer size reflects the approximate sampling footprint of the towed dredges and suction dredges used in the subtidal surveys, which typically sample along 100–200 m transects and disturb sediment across a track width of 1–2 m (van der Meer et al., 2025). The buffer therefore represents the effective area covered by a single dredge tow rather than a fixed-point location. Buffered polygons were merged per year and rasterized on the same 200 × 200 m grid as the intertidal dataset. Grid cells intersecting buffered areas were assigned a value of 1 per year, and these were summed across 2015–2024 to produce a cumulative subtidal occurrence raster.

To assess the sensitivity of habitat classification to the definition of mussel presence, we converted the cumulative occurrence raster into binary presence–absence layers using cutoff values ranging from 0 to 9. For each grid cell, presence was assigned if the number of years with observed *M. edulis* occurrence exceeded the cutoff, and absence otherwise. For example, a cutoff of 0 classified cells as presence if mussels were recorded in at least one year, whereas a cutoff of 4 required presence in at least five years, and a cutoff of 9 required presence in all ten years. Increasing cutoff values therefore resulted in progressively more conservative habitat definitions, distinguishing locations with occasional mussel occurrence from those with persistent presence. For each cutoff, a Random Forest model was trained on a balanced dataset of 1000 presence and 1000 absence samples.

We first used Random Forest classification models to evaluate the effect of cutoff choice on predicted habitat suitability. For each cutoff, we related the binary response to four environmental predictors representing major abiotic gradients in the Wadden Sea: mean salinity, wave orbital velocity, drying duration, and mud fraction. Other salinity metrics and chlorophyll *a* concentration were excluded due to strong correlations with mean salinity, while additional hydrodynamic variables were omitted to reduce multicollinearity and retain a parsimonious set of ecologically relevant predictors. To reduce class imbalance, equal numbers of presence and absence cells were randomly sampled for model fitting. Models were fitted with 500 trees and evaluated using out-of-bag (OOB) error, while probability maps were predicted across the full model domain. This step served as a sensitivity analysis to determine how strongly model outcomes depended on the strictness of the presence definition.

Based on this analysis, we selected cutoff values of 7 and 9 for spatial modelling with INLA, as these provide conservative definitions of persistent mussel habitat. In contrast to the North Sea models, where broad-scale environmental gradients explained much of the spatial variation in habitat suitability, mussel occurrence in the Wadden Sea exhibited substantial residual spatial autocorrelation after accounting for abiotic predictors. This remaining spatial dependence may reflect ecological processes such as reef expansion, local recruitment, and dispersal, as well as environmental heterogeneity not fully captured by the selected predictors (van der Meer et al., 2025). To explicitly account for this spatial dependence, we therefore applied a spatial modelling framework using Integrated Nested Laplace Approximation (INLA; Rue et al., 2009).

For each selected cutoff, we fitted a binomial spatial model with logit link:

$$Y_i \sim \text{Bernoulli}(p_i), \text{logit}(p_i)$$

$$= \beta_0 + \beta_1 sal_i + \beta_2 u_{orbital,i} + \beta_3 drydur_i + \beta_4 Mud_i + w(s_i)$$

where Y_i is the binary presence–absence response for grid cell i, and $p_i$is the probability of mussel presence. The intercept β_0 represents the baseline log-odds of mussel occurrence, while coefficients β_1–β_4 represent the effects of environmental predictors: mean salinity (sal_i), near-bed wave orbital velocity ($u_{orbital,i}$), drying duration ($drydur_i$), and sediment mud fraction (Mud_i). In this formulation, relationships with the environmental predictors were assumed to be linear, while any remaining nonlinear or spatially structured variation was captured by the spatial random field.

The term $w(s_i)$ represents a spatial random field at location s_i, capturing residual spatial autocorrelation in mussel occurrence not explained by the environmental predictors. This spatial field was modelled using the stochastic partial differential equation (SPDE) approach with a Matérn covariance structure. The fitted models were then used to predict the probability of recurrent mussel presence across the Wadden Sea on the 200 × 200 m grid.

2.2.3 Southwestern Delta

We applied the same general workflow as described for the Wadden Sea to construct cumulative occurrence rasters, define binary presence–absence layers, and fit both Random Forest (RF) and spatial INLA models. Here, we describe only the key differences for the southwestern Dutch Delta.

First, analyses were conducted separately for each basin (Lake Grevelingen, Oosterschelde, and Westerschelde) to account for strong environmental heterogeneity. Models were trained on basin-specific data and predictions were generated per basin, after which results were mosaiced to obtain continuous habitat maps for the full delta for each modelling approach (RF and INLA).

For *O. edulis*, only point observations were available and treated as in the Wadden Sea workflow. The Westerschelde basin was excluded from the *O. edulis* analysis due to absence of observed occurrences. For *M. edulis*, both point observations and mapped reef polygons were included in the presence data. Polygon data were rasterized directly and therefore represent observed reef extent, in contrast to the Wadden Sea subtidal data where buffered point observations were used.
Environmental predictors were largely identical to those used in the Wadden Sea (salinity, hydrodynamic forcing, and sediment characteristics). Random Forest (RF) models related presence–absence to these predictors as:

$$Y_i \sim \mathrm{RF}(sal_i,\ bss_i,\ flow_i,\ [chlor_i,\ mud_i]^*)$$

where $Y_i$denotes species presence in grid cell i, and predictors include salinity (sal_i), suspended sediment concentration (bss_i), near-bed flow velocity ($flow_i$), chlorophyll-a concentration ($chlor_i$), and mud fraction (mud_i).

Spatial INLA models were formulated as:

$$Y_i \sim \text{Bernoulli}(p_i), \text{logit}(p_i)$$

$$= \beta_0 + f_1(sal_i) + f_2(bss_i) + f_3(flow_i) + [f_4(chlor_i) + f_5(mud_i)]^* + w(s_i)$$

where p_i is the probability of occurrence, $\beta_0$is the intercept, and $f_k(\cdot)$are non-linear smooth functions (RW2) of the environmental predictors. The spatial random field $w(s_i)$captures residual spatial autocorrelation and was implemented using the SPDE approach with a Matérn covariance structure. In contrast to the Wadden Sea models, smooth functions were included here because exploratory analyses indicated stronger nonlinear relationships between environmental predictors and species occurrence, necessitating a more flexible functional form.
$*$Terms in brackets were excluded for *M. edulis* in the Westerschelde basin due to reduced reliability of chlorophyll-a and mud fraction layers in this system.

Finally, model evaluation and prediction followed the same approach as for the Wadden Sea. Basin-specific predictions were mosaiced per method, allowing direct comparison between RF and INLA outputs. As in the Wadden Sea, RF models capture general environmental suitability but tend to overpredict presence, whereas INLA explicitly accounts for spatial autocorrelation and produces more spatially constrained predictions.

2.3 Bivalve growth potential

2.3.1 DEB Theory

Dynamic Energy Budget (DEB) theory provides a mechanistic modelling framework grounded in first principles and simple physiological rules that describe how organisms acquire and allocate energy and nutrients, and how these processes shape physiological organization throughout the life cycle (Kooijman, 2010). As a generic modelling approach, DEB represents individual organisms in terms of their energy acquisition and utilization for growth, reproduction, and maintenance, making the framework broadly applicable across species and life stages.

Figure 2 describes the common DEB structure. The model includes food ingestion from the environment, where intake is proportional to the organism's surface area. A portion of the ingested food is assimilated into a reserve pool, while the remainder is lost as faeces. Energy stored in the reserve is mobilized and allocated according to the κ-rule: a fixed fraction supports somatic maintenance and growth, while the remaining fraction is used for development and reproduction. If the energy allocated to somatic maintenance and growth is insufficient to meet maintenance requirements, the deficit is compensated by utilizing

structural biomass, causing the organism to shrink. Energy allocated to reproduction supports maturation in juveniles and reproductive output in adults (Boerman, 2025).

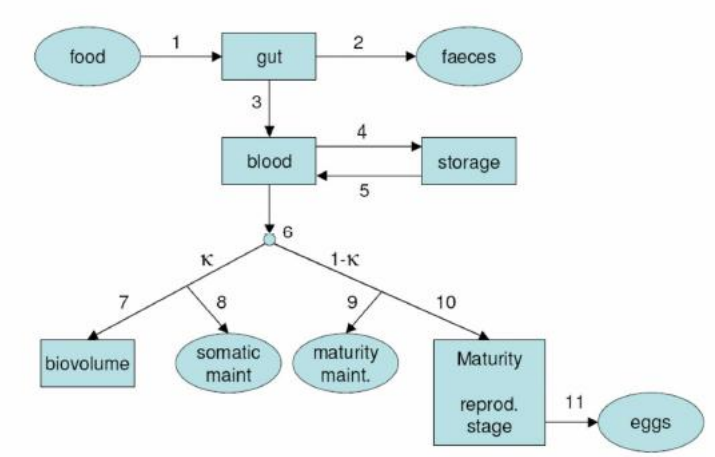


Figure 2: General structure of a DEB model with (1) ingestion, (2) defecation, (3) assimilation, (4 and 5) storage or reserve dynamics, (6) utilization, (7) growth, (8) maintenance, (9) maturation, (10) reproduction, and (11) spawning (from Troost, 2013)

Two main approaches exist for modelling organism growth in DEB theory: isomorphs and V1-morphs. In the isomorph framework, isomorphs are organisms that maintain a constant body shape throughout their life cycle and as they grow, their surface-to-volume ratio changes with body size (Kooijman, 2010). A population of organisms can be modelled using the isomorph approach by grouping individuals into various cohorts (age classes) of equal individuals following the same growth trajectory. Additionally, the number of individuals within each cohort is included as an additional state variable along with the information about recruitment and mortality rates (Troost, 2013).

The other DEB approach, called V1-morph approach, is used to scale the individual growth model up to population level. When organism size no longer affects physiology, a population can be modelled as a single large individual, simplifying the model by removing the need for a density state variable. This is useful when population size or age distribution data are limited, or when the focus is on system-level dynamics rather than individuals. The approach assumes a constant size distribution over the year (Troost, 2013), with a fixed average length as an input parameter that strongly influences population physiology. Larval settlement is treated as an increase in total population size, allowing settlement and mortality to be combined into a net mortality rate.

2.3.2 D-HYDRO suite of models

The D-HYDRO Modelling Suite, developed by Deltares, provides an integrated modelling framework for simulating key processes in water systems. It represents hydrodynamics to describe water flow, levels, and currents, which provide the basis for coupled simulations of sediment transport. The suite also includes water quality modelling (D-Water Quality module) to simulate the transport and transformation of substances such as nutrients and pollutants, and supports ecological assessments by linking physical and chemical conditions to habitat suitability and ecosystem response.

2.3.2.1 North Sea: Hydrodynamic and water quality modelling

The 3D Dutch Continental Shelf Model - Flexible Mesh (3D DCSM-FM), developed by Deltares, simulates hydrodynamics across the Northwest European Continental Shelf, including the North Sea and adjacent shallow areas such as the Wadden Sea, spanning 15°W–13°E and 43°N–64°N (Figure 3; Zijl et al., 2021). Its flexible mesh grid uses coarser

resolution in deep waters and near open boundaries, with finer resolution in shallow areas and the Southern North Sea, enhancing the representation of local physical processes compared to fixed-grid models. The model simulates both water levels (tide and surge) and residual transport, the latter being essential for water quality and ecological applications.

In the coupled hydrodynamics - water quality version of 3D DCSM-FM (Vilmin et al., 2026), biogeochemical processes are simulated using the D-Water Quality module, which models key nutrient cycles including nitrogen (N), phosphorus (P), silica (Si), organic carbon (C), and dissolved oxygen (O_2). Processes include phytoplankton growth, respiration, and mortality, organic matter mineralization and settling, biogenic silica dissolution, nitrification and denitrification, atmospheric nutrient deposition, oxygen re-aeration and dynamics of bottom *M. edulis* and *Ensis* populations in coastal areas. Phytoplankton dynamics are handled by the BLOOM module, allowing multiple functional groups. In this study, marine diatoms, flagellates, dinoflagellates, and *Phaeocystis* are included.

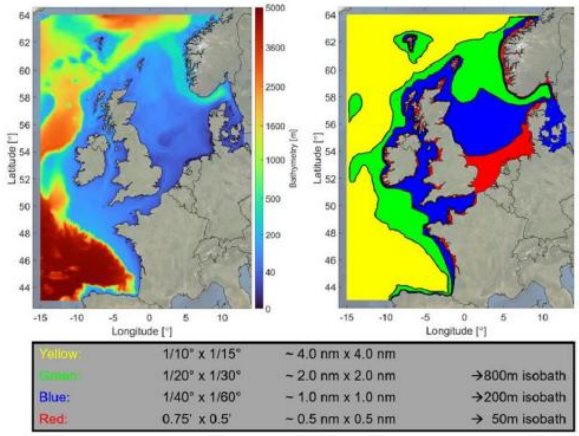


Figure 3: Bathymetry and grid cell sizes in 3D DCSM-FM (Zijl et al., 2021)

2.3.2.2 Lake Grevelingen: Hydrodynamic and water quality modelling

To represent hydrodynamics and water quality in Lake Grevelingen, a three-dimensional hydrodynamic D-HYDRO model developed as part of the sixth-generation Rijkswaterstaat model framework was used (Groeneboom et al., 2020). Building on earlier applications for the 2000 and 2008 periods, as well as a tidal scenario, the model was subsequently extended to include a water quality module for the year 2017 (van der Heijden and Nolte 2022).

The model domain (see Figure 4) includes Lake Grevelingen and is bound by the surrounding dikes of Goeree-Overflakkee and Schouwen-Duiveland (to the north and south, respectively), the Grevelingen Dam (to the east), and the Brouwersdam (in the west). Because Lake Grevelingen is a former estuary of the North Sea, the system consists of sandbanks and channels. The average depth in the channels is about 15 to 20 m with the deepest point in the model seabed is at -45.3 m NAP. The interior of the computational grid is filled with completely uniform triangular computational cells with a resolution of 100 m and the boundary of the model domain consists of triangular cells with a resolution of 50 m. The model schematization is a 3D representation of the system and describes the processes as depth-dependent.

The water quality model calculates the concentrations of nutrients (nitrate, ammonium, orthophosphate, silicate), dissolved oxygen, phytoplankton (diatoms, flagellates, dinoflagellates, and *Phaeocystis*), and detritus in the water column. In the sediment, only the stock of organic matter is calculated, but detailed sediment processes and pore water

concentrations are not modelled. The grazing of detritus and algae by shellfish and zooplankton, and the water-bottom exchange of phosphate, are modelled.

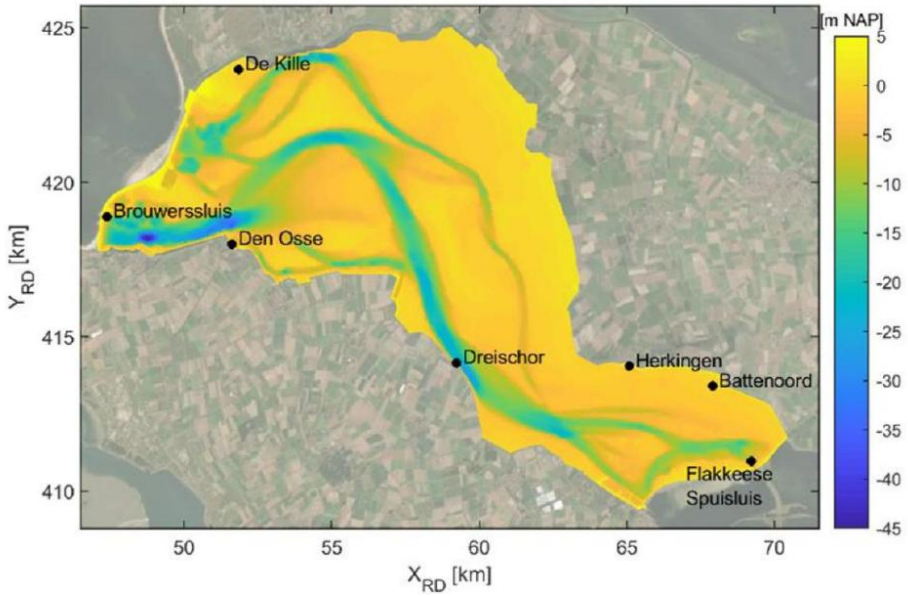


Figure 4: Overview of locks (Brouwerssluis and Flakkeese Spuisluis) and polder discharges (Battenoord, Den Osse, Dreischor, De Kille and Herkingen pumping stations). (from van der Heijden and Nolte 2022)

2.3.2.3 DEBGRZ

DEBGRZ is a module within D-Water Quality that simulates the grazing (phytoplankton consumption) of zooplankton and/ or zoobenthos, based on DEB theory (Kooijman, 2010). D-Water Quality is an environmental modelling module from the D-HYDRO (Delft3D FM) suite that can be used to simulate water quality processes.

The DEBGRZ module simulates grazer dynamics driven by hydrodynamic conditions and can represent a wide range of marine grazer species, requiring the input of species-specific parameters. Originally, the DEBGRZ module was set up for (passive) shellfish, but it can also be used to model other benthic or (active) pelagic filter feeders (Deltares, 2025). A full overview of the DEBGRZ module and its equations can be found in the D-Water Quality Technical Reference Manual (Deltares, 2025).

When modelling isomorphs, the model considers four state variables: structural biomass (V), energy biomass (E), gonadal biomass (R), and the number of individuals (N). Initial values for all state variables need to be specified in units per surface area (m^{-2}) (for benthic organisms). When modelling V1-morphs, the population is treated as a single large individual, eliminating the need for the state variable N. An additional parameter, the reference length (Lref), represents the population's average length and sets the constant surface-to-volume ratio, strongly influencing population physiology.

2.3.3 DEB model setup

2.3.3.1 Site selection

North Sea

Site selection for DEB modelling in the North Sea was based on three main categories of criteria: abiotic factors (e.g., temperature, hydrodynamics), biotic factors (e.g., food availability), and logistical constraints. As a first step, areas unsuitable for restoration such as designated sand extraction zones, shipping lanes, and locations of oil and gas platforms were excluded from consideration. Candidate DEB modelling sites were then identified using information on current and planned Marine Strategy Framework Directive (MSFD) areas, existing and proposed restoration sites, offshore wind farm locations, and areas where bottom trawling is currently restricted or expected to be restricted in the future. To ensure broad environmental representation, additional sites were included to expand the range of abiotic conditions and bottom-food availability captured by the DCSM model (see Figure 6). Thresholds for suitable abiotic and biotic conditions for *O. edulis* survival were defined following Kamermans et al. (2018). The spatial suitability map developed in this study was also utilised to ensure that selected sites represented the full gradient of habitat suitability. Ensuring a wide coverage of environmental conditions is essential for enabling robust extrapolation of DEB model results in subsequent analyses. Figure 5 shows the site locations selected for DEB modelling. Note that DEB modelling was not performed for the Wadden Sea because food availability is not a limiting factor for bivalve growth in this region (Beukema and Dekker, 2022).

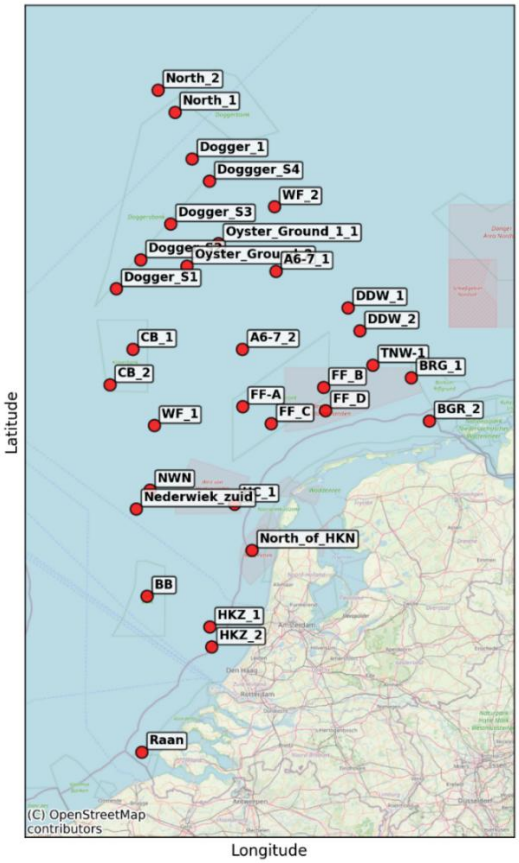


Figure 5: DEB modelling sites in the Dutch North Sea region. (A6-7: Offshore wind area 6-7; BB: Brown Bank; BRG: Borkum Reef Ground; CB: Cleaver Bank (Klaverbank); DDW: Doordewind; FF: Frisian Front; HKZ: Hollandse Kust Zuid; NWN: Nederwiek Noord; TNW: Ten Noorden van de Waddeneilanden; WF: Potential future offshore wind areas).

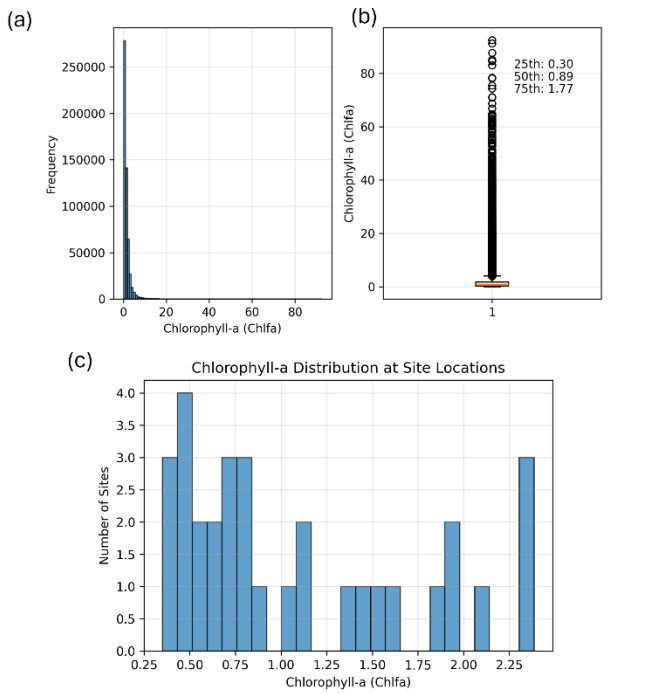


Figure 6: Distribution of bottom chlorophyll-a coverage (a) and boxplot of chlorophyll-a values (b) in the North Sea (DCSM domain- average of 2015-2017 model run) and the distribution of chlorophyll-a values (extracted from the DCSM model) at the DEB modelling sites (c).

Lake Grevelingen

Since information on planned restoration activities in Lake Grevelingen was not available, DEB modelling sites in the lake were selected using a systematic K-means clustering approach (Lloyd, 1957; MacQueen, 1967). K-means is an unsupervised algorithm that groups data into clusters based on similarity, iteratively assigning points to the nearest centroid until stable clusters are formed. This allowed the environmental variation in the lake to be captured efficiently without requiring prior assumptions.

The clustering was based on average bottom chlorophyll-a concentrations, temperature, and bed level, combined with the spatial distribution of natural shellfish beds and commercial shellfish plots. The optimal number of clusters (k = 4) was determined using the elbow method, where the point of diminishing improvement in the Within-Cluster Sum of Squares (WCSS) indicates the most appropriate cluster number. Environmental clusters were then integrated with shellfish distribution data to classify lake areas into four types: zones with only wild shellfish, only cultured shellfish, both wild and cultured shellfish, and reference zones without shellfish. A stratified sampling strategy was used so that the selected sites represented all combinations of environmental clusters (1-4) and site types, while also maintaining broad geographical coverage. This process resulted in the selection of 11 DEB modelling sites for Lake Grevelingen (Figure 7, Figure 8).

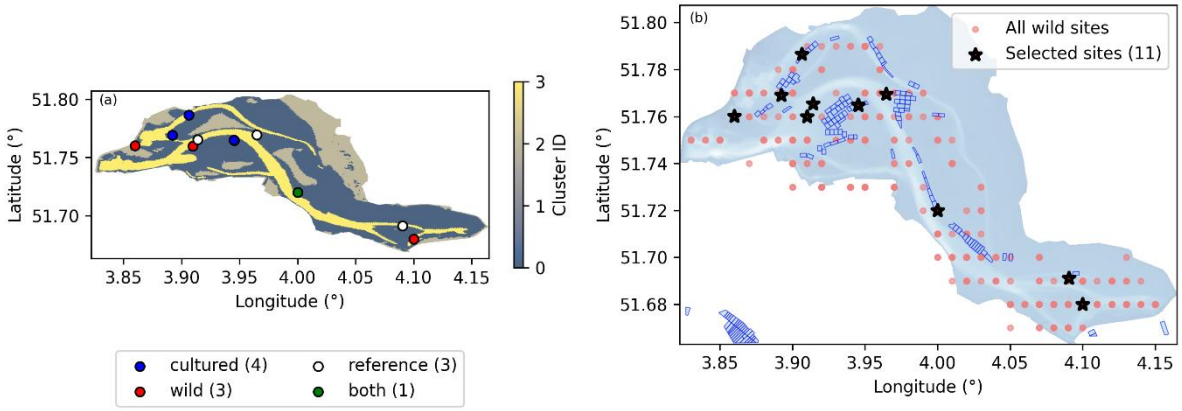


Figure 7: Lake Grevelingen study area (a) showing environmental clusters with the selected sites and (b) showing study area with wild shellfish (O. edulis) locations and cultured plots of shellfish (blue polygons). Figures are not to scale.

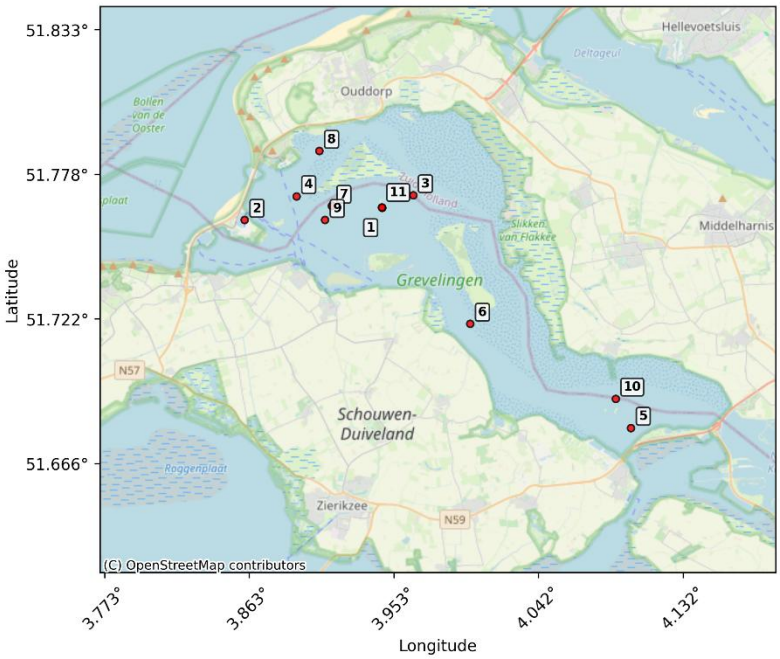


Figure 8: Lake Grevelingen study area with the locations of DEB modelling sites.

2.3.3.2 1D model setup

The 1D column models were forced using outputs from the corresponding 3D water quality models for each study area. Extracted 3D model results were converted into 1D-compatible input formats that provided initial conditions for all water quality state variables at each depth layer, as well as time-varying hydrodynamic and biogeochemical inputs at 5-day and 1-day intervals for the North Sea and Lake Grevelingen models, respectively. Meteorological forcing at the surface was likewise taken from the 3D model. The 1D model structure, processes, and substances correspond to those in the 3D model, with the addition of grazer-specific state variables.

Initial conditions for grazers were supplied only for the bottom layer to simulate benthic growth. Initial grazer wet weights (wet weight at birth, gC) were derived from literature values. For *O. edulis*, a wet weight at birth of 3.89×10^{-7} g was used (Walne, 1964; Stechele,

2022a), while for *M. edulis* a value of 2.36 × 10^{-7} g was applied (Van Haren and Kooijman, 1993; Stechele, 2022b). Wet weights were converted to carbon units following species-specific conversion factors from Troost (2013). These values were used to initialise the structural grazer biomass (V) for both species. The energy biomass reserve (E) was set to one-tenth of the initial structural biomass. All isomorph 1D model runs were initiated with five grazer individuals per km^2 (i.e. for oysters this is defined as the minimum density for a reef structure (Bennema et al., 2020)).

The models for *O. edulis* and *M. edulis* were run separately, each using its own DEB parameter set. For *O. edulis*, parameters were adopted from earlier work in the North Sea (Boerman, 2025) within the ULTFARMS project (https://ultfarms.eu; Grant Agreement n. 101093888). Core parameters were sourced from Stechele et al. (2022a), supplemented with values from FutureMARES project reports (Vilmin et al., 2024). Additional DEBGRZ parameters not published by Stechele et al. (2022a) were taken from Troost (2013). An overview of the full parameter set is available in Boerman (2025).

The parameter set for the DEBGRZ module for mussels (*M. edulis*) was based on multiple sources. Earlier Deltares studies initially used values calibrated to simulate blue mussels in the Oosterschelde (Troost et al., 2010; van Kessel et al., 2022). This parameter set was updated within the ULTFARMS project using more recent values from Stechele et al. (2022b), which has been found to better represent offshore mussel growth (Table 2). Additional parameters that were not reported in the paper were obtained or recalculated through personal communication with the first author (B. Stechele), to account for differences in DEB model versions and implementation in DEBGRZ. Additional DEBGRZ-specific parameters based on Troost et al. (2010) and van Kessel et al. (2022) are reported in Table 5. Species-specific conversion factors (described below) were retrieved from the Add-my-Pet (AmP, https://bio.vu.nl/thb/deb/deblab/add_my_pet/) database.

Recalculated parameters

Several parameters had to be recalculated because they were not directly reported in Stechele et al. (2022b). Moreover, the DEBGRZ implementation uses an earlier DEB formulation that does not include acceleration (i.e., incorporating metabolic changes during the mussel's life cycle). Therefore, some parameters were recalculated assuming an acceleration factor $s_M = 1$. The half-saturation constant for food uptake (X_k) was recalculated due to different units between the DEBGRZ and Stechele model. The value reported in Stechele et al. (2022b) is 0.56 µg chl L^{-1}, which was multiplied by 0.12 to convert from µg chl L^{-1} to gC m^{-3}. However, the chlorophyll to carbon ratio can vary considerably in space and time.

Conversion factors

Two conversion factors required by DEBGRZ were calculated using values from the AmP database. For the conversion coefficient from volume to carbon (cVC), the density of dry weight for *M. edulis* (0.09 g cm^{-3}) was multiplied by the carbon weight per body dry weight (0.45 gC g^{-1}). For the conversion coefficient from energy to carbon (cEC), the molecular mass of carbon (12.011 u) was divided by the chemical potential of the reserves (550000 J $molC^{-1}$).

*Table 2 Parameters sourced from Stechele et al. (2022). Parameters adapted or recalculated are marked with **.

Parameter	Units	Value	Description
T_A	K	7022	Arrhenius temperature
T_H	K	296	Upper boundary temperature optimum
T_L	K	275	Lower boundary temperature optimum
T_{AL}	K	45430	Arrhenius temperature at lower boundary
T_{AH}	K	31380	Arrhenius temperature at upper boundary
E_g	J cm^{-3}	2348	Volume specific cost for structure
shape	-	0.3188	Shape coefficient
k_R	-	0.95	Reproduction efficiency
Kappa	-	0.9495	Allocation fraction to soma
p_M	J d^{-1} cm^{-3}	43.79	Volume-specific somatic maintenance at 20 °C
Xk*	gC m^{-3}	0.066	Half saturation constant for food uptake
JXm*	J cm^2 d^{-1}	108.454	Maximum surface area-specific ingestion rate
Em*	J cm^{-3}	197.481	Maximum energy density

For the North Sea, model setups included boundary conditions and initial profiles for 32 sites. All North Sea sites used a fixed number of depth layers (n = 20), with layer thickness varying according to local bed level. In Lake Grevelingen, 11 sites were modelled, with depth-layer numbers ranging from 6 to 30 and a fixed layer thickness of 0.5 m. These configurations were based directly on the corresponding 3D water quality models and thus reflect area-specific bathymetry and model structure.

For both study areas, an isomorph approach was used to simulate individual growth and enable spatial extrapolation of DEB outputs from point locations. The model run period was set to 30 years for *O. edulis* (North Sea: 2015-2044; Lake Grevelingen: 2017-2046) and 10 years for *M. edulis* (North Sea: 2015-2024; Lake Grevelingen: 2017-2026). For the North Sea, the reference 3D water-quality model was available for the years 2015-2017, which determined 2015 as the starting year for the 1D model. The 1D model repeatedly applied this 3-year forcing period (including intra-annual dynamics) throughout the full model run. For Lake Grevelingen, the 2017 model setup was used to define the 1D model structure and forcings. This single-year forcing was repeated annually for the entire 1D model simulation period. The selection of the 1D model time periods for each species was based on multiple test simulations using different durations. The final periods were chosen once yearly bivalve growth had stabilized, meaning no additional growth occurred between successive years. Repeating the same forcing over multiple years was sufficient to represent the system's internal dynamics. However, this approach does not account for potential climate-change effects.

2.3.3.3 Statistical extrapolation of DEB results to a wider area

To extrapolate the DEB modelled growth outcomes across the entire study area, the relationship between the final species length obtained from the 1D column models and relevant environmental variables (e.g., mean bottom chlorophyll-a, temperature, oxygen) were examined. The final length in the DEB simulations represents the local growth potential at each site. Mean bottom values of each environmental variable were extracted from the corresponding 3D water-quality model outputs and paired with the final lengths from each site.

Based on these relationships, single or multivariate linear regression models were developed to predict final bivalve lengths using site-specific environmental conditions. Prior to fitting multivariate models, potential collinearity among predictor variables was assessed using Pearson correlation coefficients and by calculating variance inflation factors (VIF). All predictors were standardised (mean = 0, SD = 1). The dataset was then split into 70% training and 30% testing subsets. Model performance was evaluated for both subsets using the coefficient of determination (R^2), root mean squared error (RMSE), and mean absolute error (MAE). The final regression model was subsequently used to extrapolate bivalve growth potential (final lengths) across the full study area.

From the resulting continuous length maps, values below the minimum length required for reproduction were removed. The remaining extrapolated lengths were converted into a length suitability index (0-1), using the reproductive minimum length as the lower bound (index = 0) and the typical adult shell length as the upper bound (index = 1).

For *O. edulis*, the minimum reproductive length was set to 2.5 cm (based on observations and communication from Pauline Kamermans, WMR). For *M. edulis*, the minimum reproductive length was taken as the length at puberty (1.2 cm) from the Add-my-Pet (AmP) database. The upper bound of the DEB-length index for each species was defined using the typical adult sizes observed in the North Sea: 10-12 cm for *Ostrea edulis* (Gercken & Schmidt, 2014) and approximately 4 cm for *Mytilus edulis* (Larsen & Riisgård, 2016; University of Michigan Museum of Zoology, n.d.). Assuming that individuals of both bivalve species are capable of reaching reproductive maturity and producing substantial numbers of larvae at these adult sizes, the index value of 1 was assigned to all shell lengths greater than or equal to these maximum reference lengths.

The maximum possible final length for each species in the DEB model was also determined by running an optimum-condition DEB scenario at the site where the largest DEB length had been obtained under isomorphic model runs. This optimum scenario assumed a constant temperature of 20 °C and surplus food availability at the model boundary, reflecting the assumption that oysters and mussels reach their physiological maximum size under high-temperature, high-food conditions.

3 Results

3.1 Abiotic habitat suitability modelling

3.1.1 North Sea

3.1.1.1 Predicted habitat suitability for *O. edulis*

Predicted habitat suitability for *O. edulis* in the Dutch part of the North Sea was found to be highest in the Oyster Grounds, in line with earlier studies. Random Forest (RF) and GAM largely showed similar patterns (Figure 9). Different mud percentage scenarios did not reveal large differences. The final map, calculating the mean values between the RF and GAM models, used the 50th percentile mud percentage map (Figure 10).

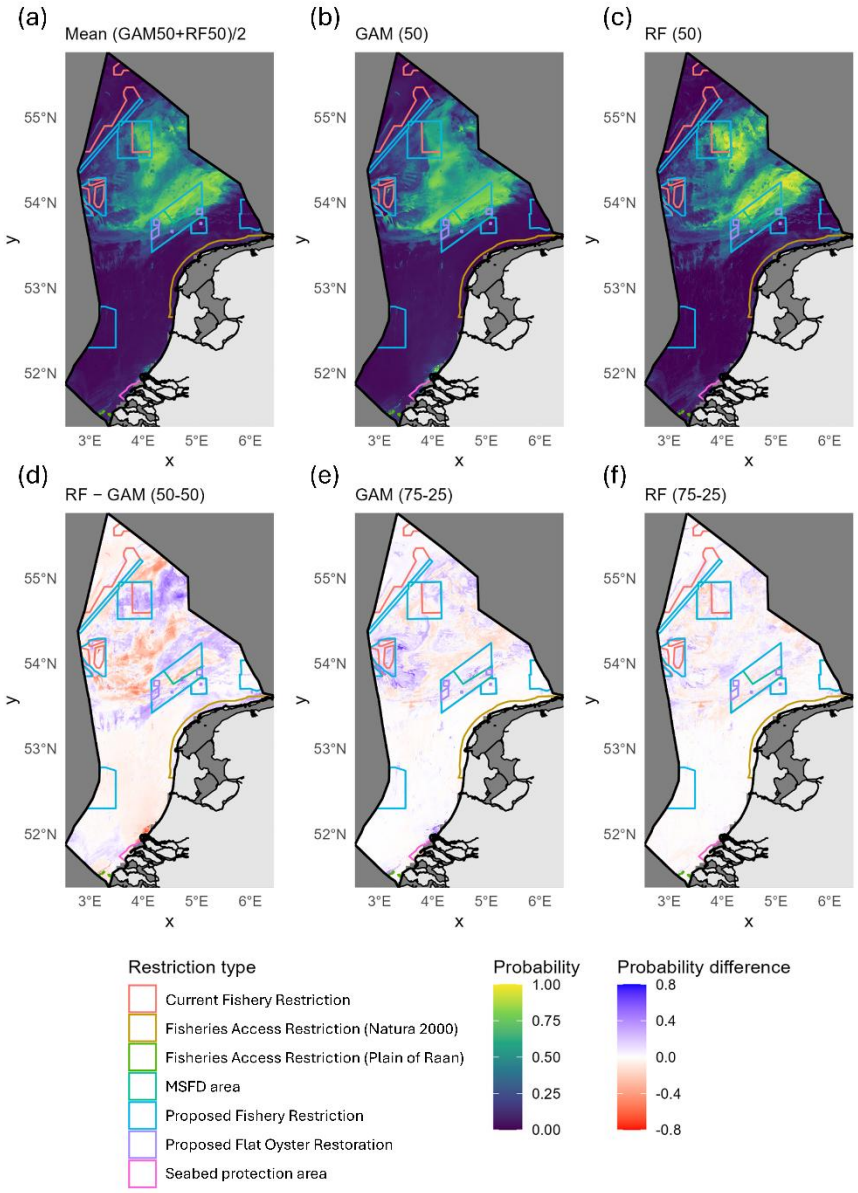


Figure 9: Predicted habitat suitability for O. edulis in the North Sea based on different modelling approaches and mud percentile scenarios compiled by TNO. Panels show (top row, left to right): (a) mean probability of occurrence from an equal-weight ensemble of GAM and Random Forest models, and (b) individual GAM and (c) Random Forest predictions trained and predicted using the 50th percentile mud map; (bottom row, left to right): (d) the difference between Random Forest and GAM predictions (RF − GAM), and model predictions based on alternative mud scenarios using the 75th and 25th percentiles of the mud percentage maps using a GAM (e) and RF (f). The 75th and 25th percentile scenarios represent, for each grid cell, the mud percentages below which 75% and 25% of the Random Forest predictions fall, respectively. Compared with the median (50th percentile), these reflect muddier and less muddy conditions, allowing us to assess how uncertainty in sediment composition affects predicted habitat suitability. The map is clipped to the Dutch Exclusive Economic Zone (EEZ; black outline), with areas outside the EEZ masked. Overlaid vector layers represent spatial policy and management constraints, providing spatial context on existing, historic, and future management regimes and are shown to indicate where predicted oyster habitat coincides with regulated or protected marine areas.

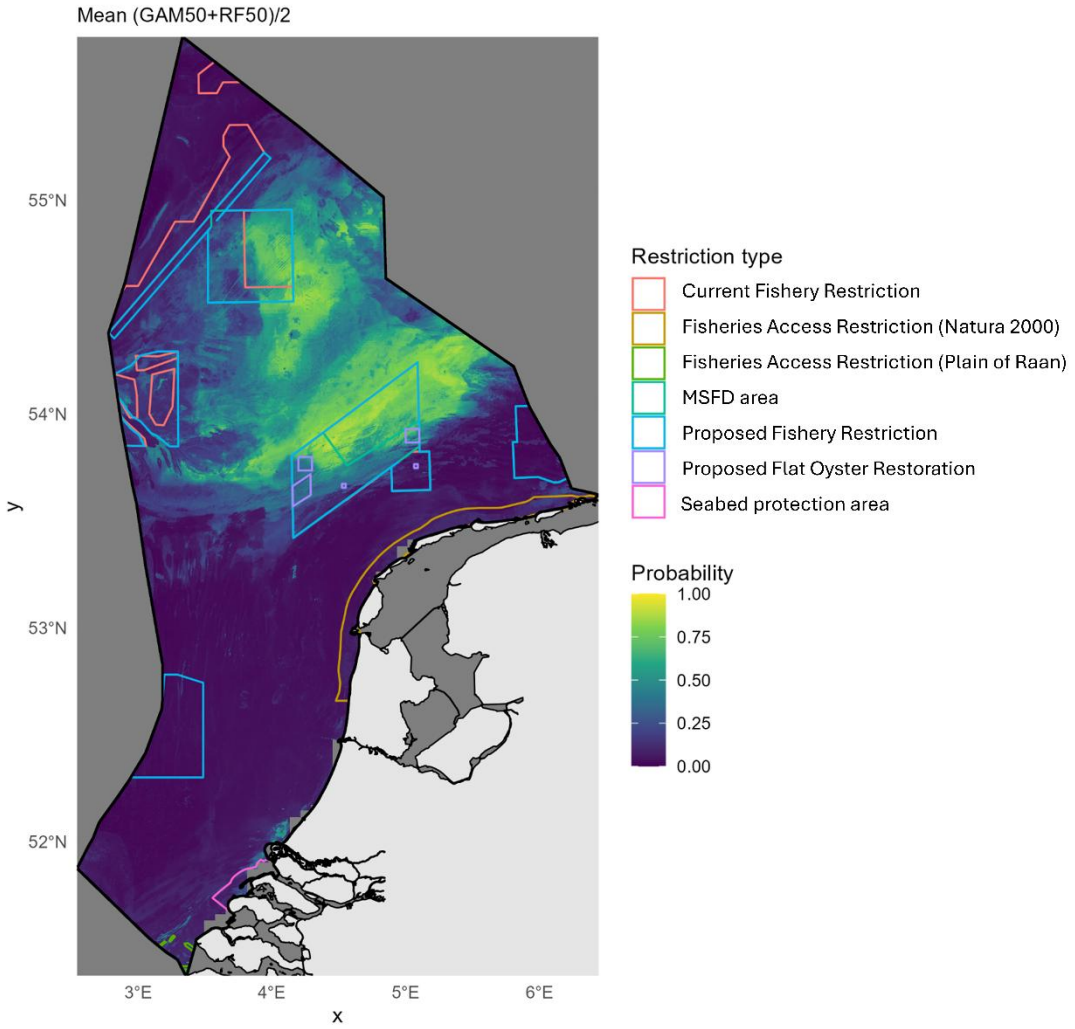


Figure 10: Mean predicted habitat suitability for the European flat oyster (O. edulis) in the North Sea, based on an equal-weight ensemble of Generalized Additive Models (GAM) and Random Forest (RF) models trained using the 50th percentile mud percentage map from TNO. Suitability is shown as probability of occurrence. The map is clipped to the Dutch Exclusive Economic Zone (EEZ; black outline), with areas outside the EEZ masked. Overlaid vector layers represent spatial policy and management constraints: Natura 2000 protected areas, Marine Strategy Framework Directive (MSFD) areas, and fisheries restriction zones. These shapefiles provide spatial context on existing, historic, and future management regimes and are shown to indicate where predicted oyster habitat coincides with regulated or protected marine areas.

3.1.1.2 Predicted habitat suitability for *M. edulis*

Predicted habitat suitability for *M. edulis* in the Dutch part of the North Sea was mostly concentrated along the coast. Random Forest (RF) and GAM largely showed similar patterns, although RF predicted notably higher probabilities in suitable areas (Figure 11). This difference may reflect the greater flexibility of RF in capturing nonlinear relationships and interactions among environmental predictors, potentially resulting in more extreme predictions. Different mud percentage scenarios did not reveal large differences. The final map, calculating the mean values between the RF and GAM models, used the 50th percentile mud percentage map (Figure 12).

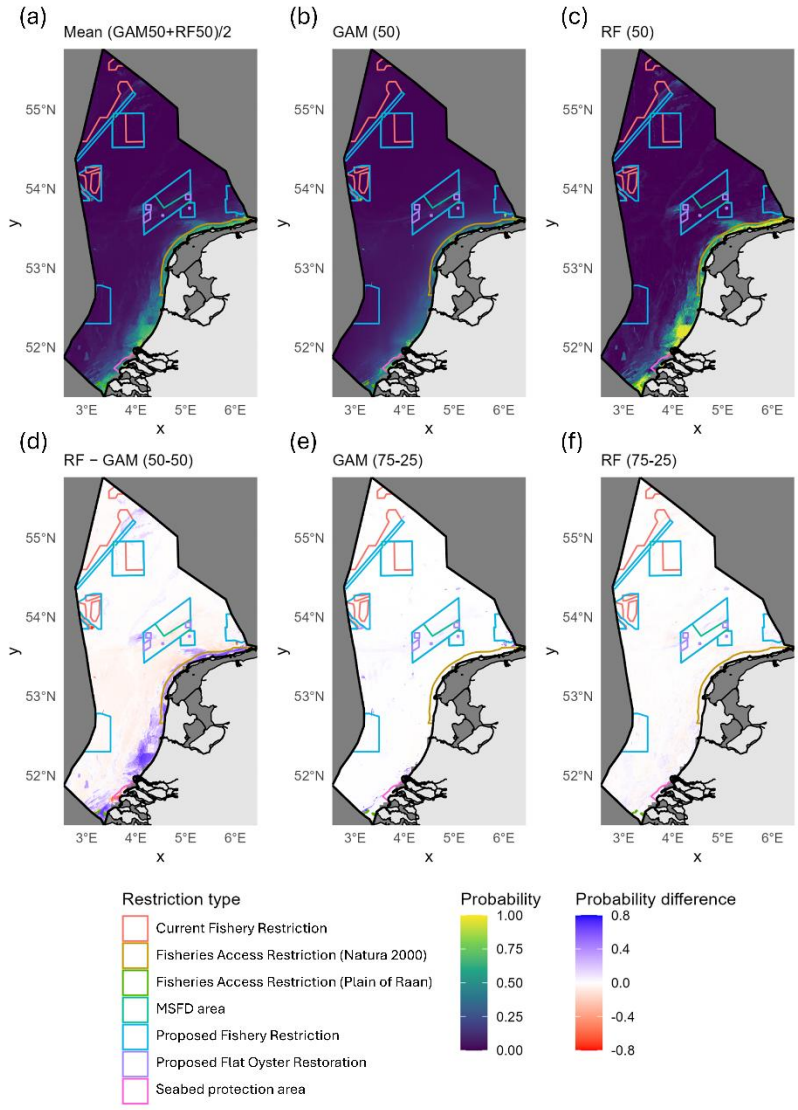


Figure 11: Predicted habitat suitability for M. edulis in the North Sea based on different modelling approaches and mud percentile scenarios compiled by TNO. Panels show (top row, left to right): (a) mean probability of occurrence from an equal-weight ensemble of GAM and Random Forest models, and (b) individual GAM and (c) Random Forest predictions trained and predicted using the 50th percentile mud map; (bottom row, left to right): (d) the difference between Random Forest and GAM predictions (RF − GAM), and model predictions based on alternative mud scenarios using the 75th and 25th percentiles of the mud percentage maps using a GAM (e) and RF (f). The 75th and 25th percentile scenarios represent, for each grid cell, the mud percentages below which 75% and 25% of the Random Forest predictions fall, respectively. Compared with the median (50th percentile), these reflect muddier and less muddy conditions, allowing us to assess how

uncertainty in sediment composition affects predicted habitat suitability. The map is clipped to the Dutch Exclusive Economic Zone (EEZ; black outline), with areas outside the EEZ masked. Overlaid vector layers represent spatial policy and management constraints, providing spatial context on existing, historic, and future management regimes and are shown to indicate where predicted oyster habitat coincides with regulated or protected marine areas.

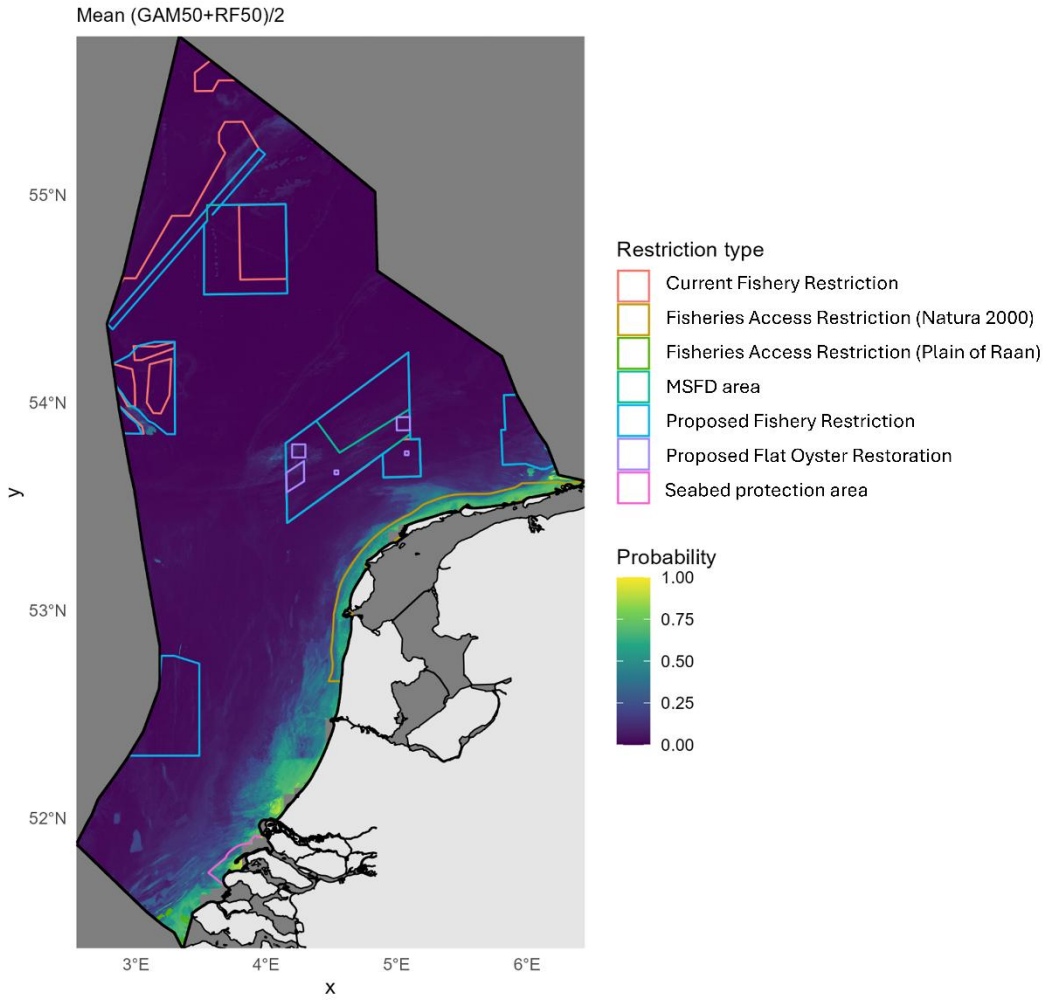


Figure 12: Mean predicted habitat suitability for the blue mussel (M. edulis) in the North Sea, based on an equal-weight ensemble of Generalized Additive Models (GAM) and Random Forest (RF) models trained using the 50th percentile mud percentage map from TNO. Suitability is shown as probability of occurrence. The map is clipped to the Dutch Exclusive Economic Zone (EEZ; black outline), with areas outside the EEZ masked. Overlaid vector layers represent spatial policy and management constraints: Natura 2000 protected areas, Marine Strategy Framework Directive (MSFD) areas, and fisheries restriction zones. These shapefiles provide spatial context on existing, historic, and future management regimes and are shown to indicate where predicted oyster habitat coincides with regulated or protected marine areas.

3.1.1.3 Predicted habitat suitability for *M. modiolus*

The models provided no indication of suitable habitat for *M. modiolus* within the Dutch Exclusive Economic Zone (EEZ) (Figure 13). Different mud percentage scenarios did not reveal large differences. The final map, calculating the mean values between the RF and GAM models, used the 50th percentile mud percentage map (Figure 14).

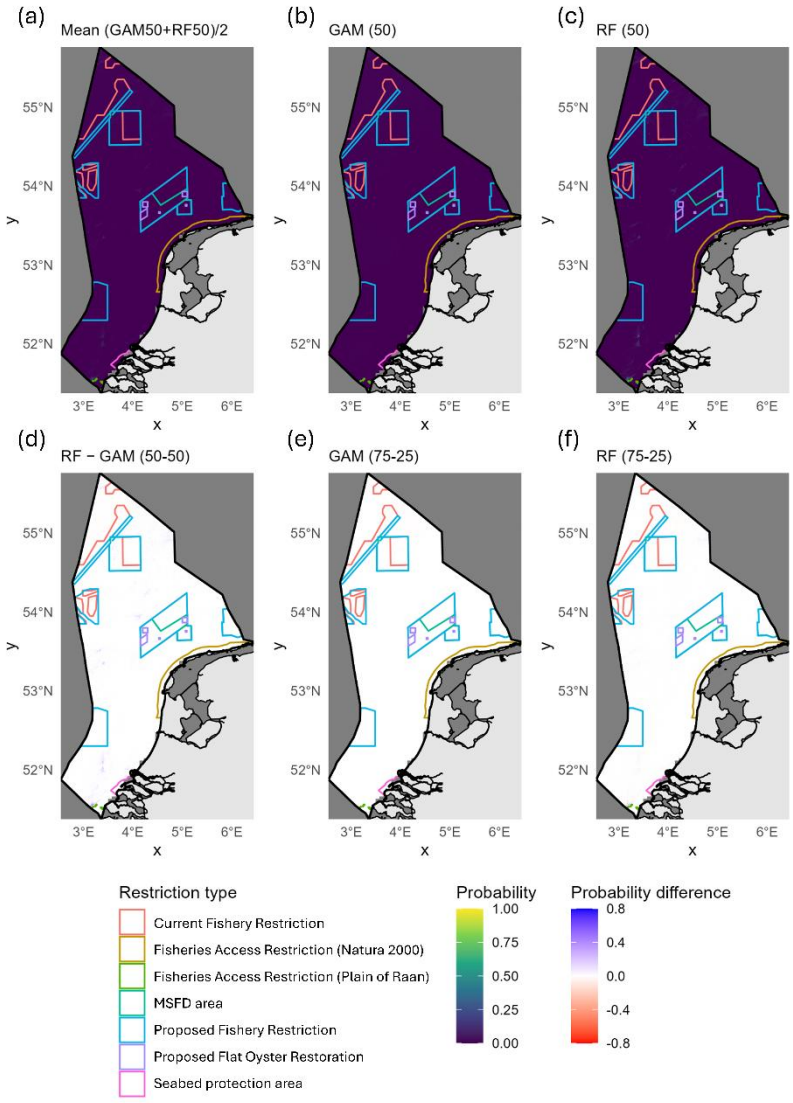


Figure 13: Predicted habitat suitability for M. modiolus in the North Sea based on different modelling approaches and mud percentile scenarios compiled by TNO. Panels show (top row, left to right): (a) mean probability of occurrence from an equal-weight ensemble of GAM and Random Forest models, and (b) individual GAM and (c) Random Forest predictions trained and predicted using the 50th percentile mud map; (bottom row, left to right): (d) the difference between Random Forest and GAM predictions (RF − GAM), and model predictions based on alternative mud scenarios using the 75th and 25th percentiles of the mud percentage maps using a GAM (e) and RF (f). The 75th and 25th percentile scenarios represent, for each grid cell, the mud percentages below which 75% and 25% of the Random Forest predictions fall, respectively. Compared with the median (50th percentile), these reflect muddier and less muddy conditions, allowing us to assess how uncertainty in sediment composition affects predicted habitat suitability. The map is clipped to the Dutch Exclusive Economic Zone (EEZ; black outline), with areas outside the EEZ masked. Overlaid vector layers represent spatial policy and management constraints, providing spatial context on existing, historic, and

future management regimes and are shown to indicate where predicted oyster habitat coincides with regulated or protected marine areas.

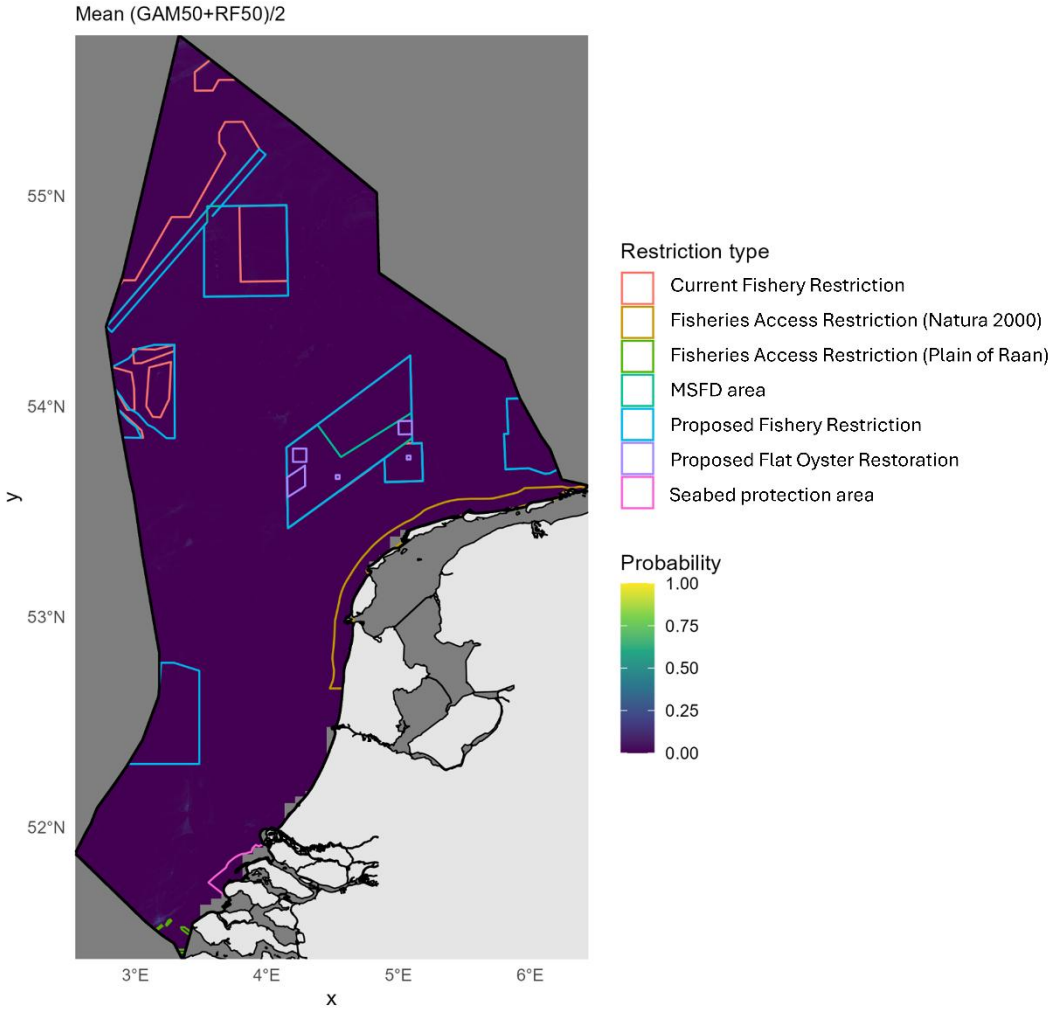


Figure 14: Mean predicted habitat suitability for the horse mussel (M. modiolus) in the North Sea, based on an equal-weight ensemble of Generalized Additive Models (GAM) and Random Forest (RF) models trained using the 50th percentile mud percentage map from TNO. Suitability is shown as probability of occurrence. The map is clipped to the Dutch Exclusive Economic Zone (EEZ; black outline), with areas outside the EEZ masked. Overlaid vector layers represent spatial policy and management constraints: Natura 2000 protected areas, Marine Strategy Framework Directive (MSFD) areas, and fisheries restriction zones. These shapefiles provide spatial context on existing, historic, and future management regimes and are shown to indicate where predicted oyster habitat coincides with regulated or protected marine areas.

3.1.2 Wadden Sea

3.1.2.1 Predicted habitat suitability for *O. edulis*

Predicted habitat suitability based on class-weighted Random Forest can be seen in Figure 15. Due to the small number of presence points, predicted suitability is generally low. The highest predictions can be seen near Vlieland (in the tidal inlet systems of Eierlandse Gat and Vlie), where presence was confirmed through observations, and to a lesser extent in tidal inlets further to the east (e.g. Pinkegat/Zoutkamperlaag between Ameland and Schiermonnikoog).

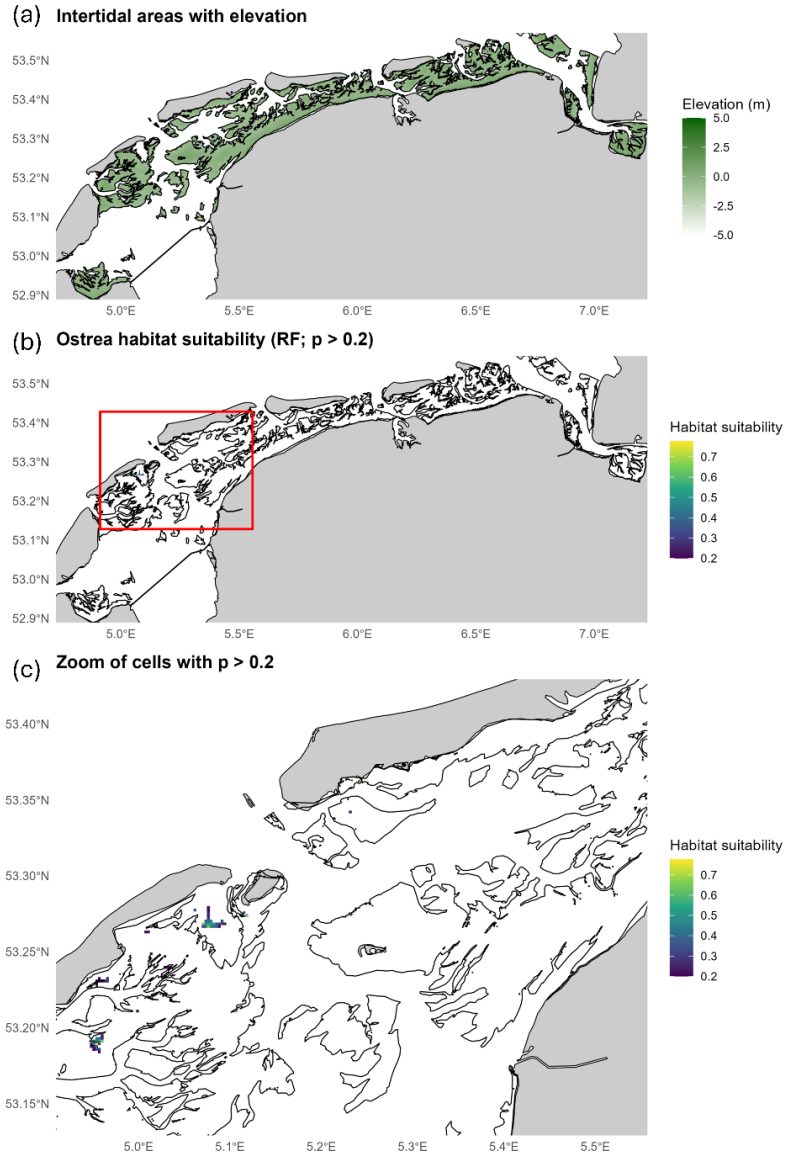


Figure 15: Panel (a): distribution of intertidal areas, with elevation indicated by the colour scale, as context for Panel (b): the predicted probability of flat oysters (O. edulis) presence in the Wadden Sea based on random forest (RF) prediction, probability lower than 0.2 removed for clarity. Colours indicate predicted probability (0.2–0.7). Contours display transitions between tidal flats and channels. Panel (c) shows the zoomed in extent displayed in the red square in panel (b).

3.1.2.2 Predicted habitat suitability for *M. edulis*

The prediction of mussel presence based on abiotic variables using a Random Forest, under different definitions of “presence,” is shown in Figure 16. Higher cutoff thresholds are increasingly conservative, with values of >9 indicating locations where mussels were observed consistently across years (10 out 10). However, intertidal and subtidal surveys differ substantially in detectability. Intertidal reefs are reliably observed during annual surveys as they are directly visible, whereas subtidal reefs are more difficult to detect and may be missed due to limitations of sampling methods (e.g. just missed by a bottom scrapers, suction dredges, or hydraulic grab).

As a result, higher cutoff thresholds disproportionately exclude subtidal occurrences, leading to a decline in predicted suitable area that reflects both stricter classification and under-detection. Consequently, the out-of-bag (OOB) error primarily reflects numerical classification accuracy, but does not capture this observational bias in the data.

Because presence data aggregate both intertidal and subtidal observations, and subtidal reefs are more likely to be missed in individual years despite being present, we avoid focusing solely on the most conservative threshold (10 out of 10 years). Instead, we adopt a cutoff of 7 years as well, which balances confidence in persistence with a more realistic inclusion of subtidal reefs. At this threshold, consistent subtidal suitability begins to emerge, particularly near closure dams, ensuring that the most reliable subtidal habitats are retained in the analysis.

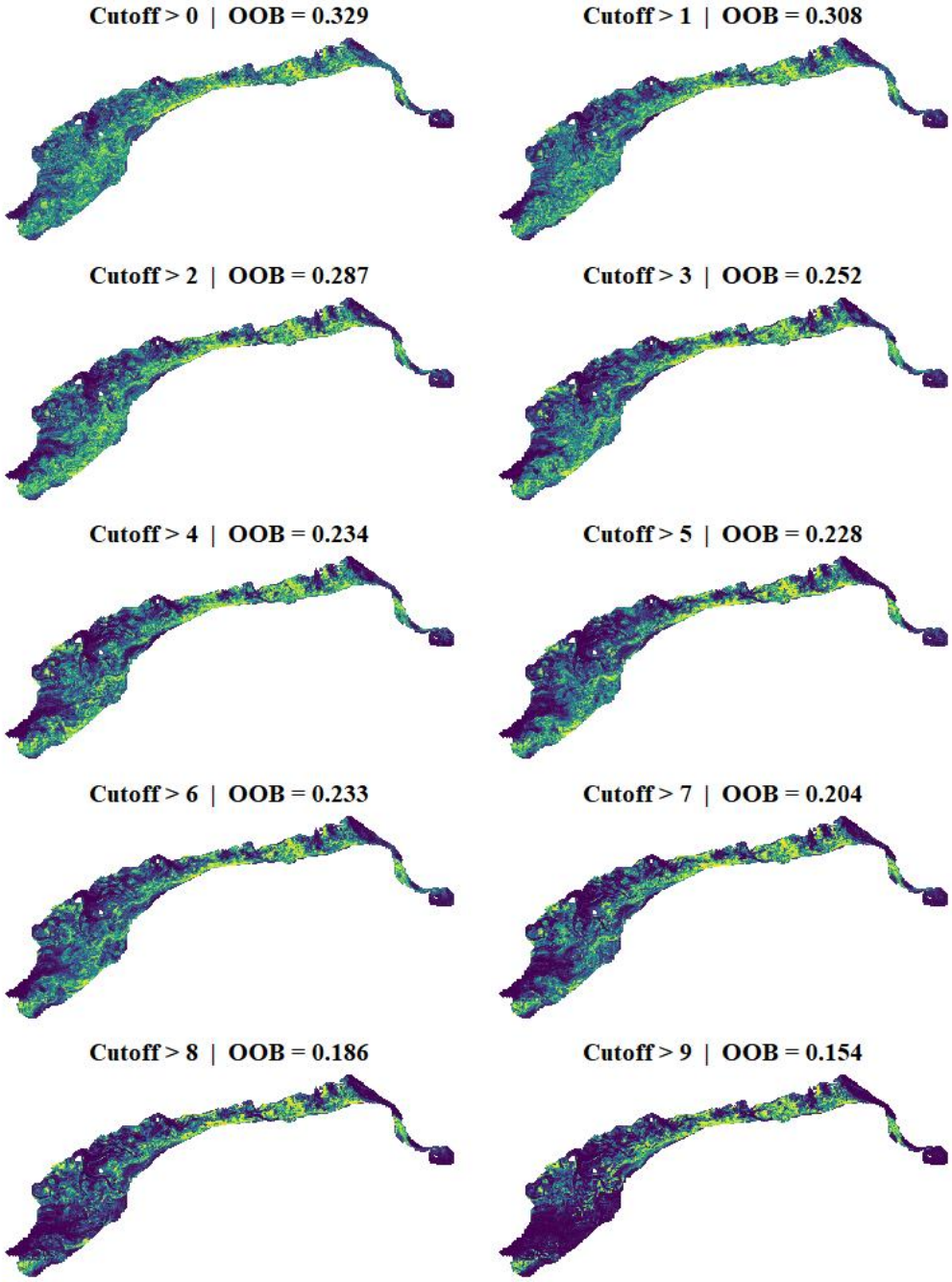


Figure 16: Predicted probability of Mytilus presence for increasing occurrence thresholds (cutoff > 0 – > 9) in the Wadden Sea. Each panel shows the spatial probability (0–1) of exceeding the corresponding occurrence threshold. Reported OOB (out-of-bag) errors indicate model uncertainty, with lower values representing higher predictive performance.

Observations INLA models

While the Random Forest models using presence thresholds of ≥7 out of 10 years and 10 out of 10 years achieve classification accuracies of 80% (OOB = 0.20) and 85% (OOB = 0.15), respectively (Figure 16), these metrics primarily reflect the model's ability to reproduce observed patterns rather than to infer underlying ecological processes. In particular, the RF predictions appear strongly influenced by spatial clustering in the data (i.e. spatial confounding), with high suitability concentrated around observed mussel locations, without explicitly accounting for spatial autocorrelation.

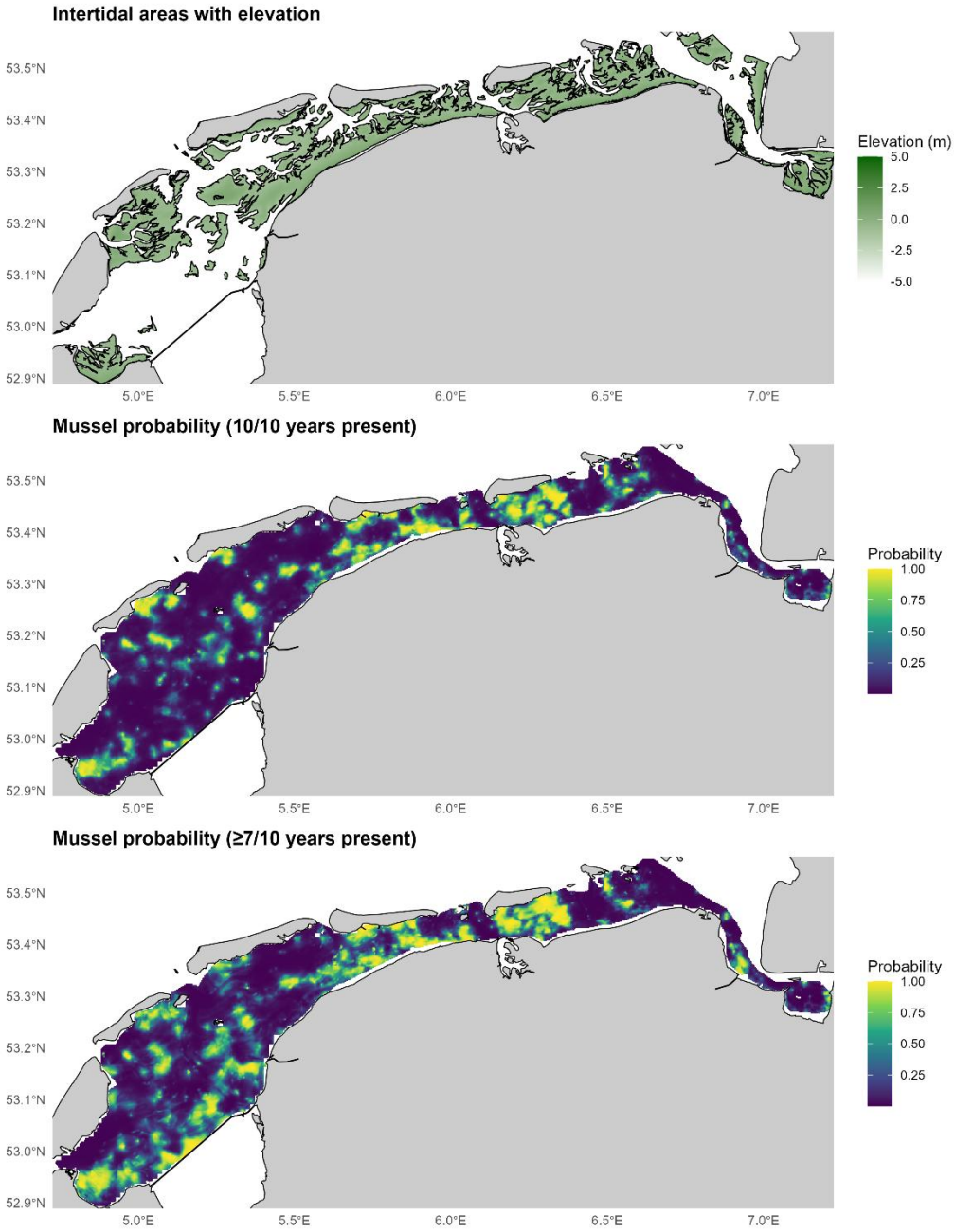


Figure 17: Predicted probability of persistent blue mussel (M. edulis) presence in the Wadden Sea based on the spatial INLA model. The top panel shows distribution of intertidal areas, with elevation indicated by the colour scale. The middle and bottom panels show the probability that mussels were present in all 10 out of 10 years, and the probability of presence in at least 7 out of 10 years. Colours of the middle and bottom panels indicate predicted probability (0–1).

Because Random Forest does not separate environmental effects from spatial structure, these predictions may overfit localized patterns and limit ecological interpretability. We therefore use the same presence thresholds (≥7/10 and 10/10) within the INLA framework, which explicitly accounts for spatial autocorrelation through the spatial random field (Figure 17). This allows us to distinguish between environmentally driven suitability and spatially structured residual variation, and to evaluate how sensitive the results are to the definition of presence. As a result, the predicted suitable area decreases slightly compared to the RF models, while retaining the main regions identified as suitable. Using the more conservative cutoff (≥9/10), we can state with greater confidence that suitable areas include the tidal flats in front of the Kooihoeksschor, the tidal flats northeast of Vlieland fringing the island, the tidal flats along the Frisian coast between Zwarte Haan and Holwerd, and the tidal divides between Schiermonnikoog and Ameland. When the cutoff is lowered to ≥7/10, additional suitable areas emerge in subtidal zones adjacent to the closure dam, consistent with observations reported by van der Meer et al. (2025).

3.1.3 Southwestern Delta

3.1.3.1 Sediment maps

Model performance varied across systems and responses. In the Oosterschelde, Random Forest models for D50 and mud content were moderately able to model observed values, but sufficient to support broad scale habitat suitability patterns (Table 3, Figure 18). In the Westerschelde, predictive skill was very low for D50 and absent for mud, reflecting the high dynamics and unmodelled variability of this estuary. For Lake Grevelingen, Generalized Additive Models produced a moderate skill mud layer that is suitable as a predictor, while the D50 layer captured only weak basin scale trends and should be interpreted cautiously.

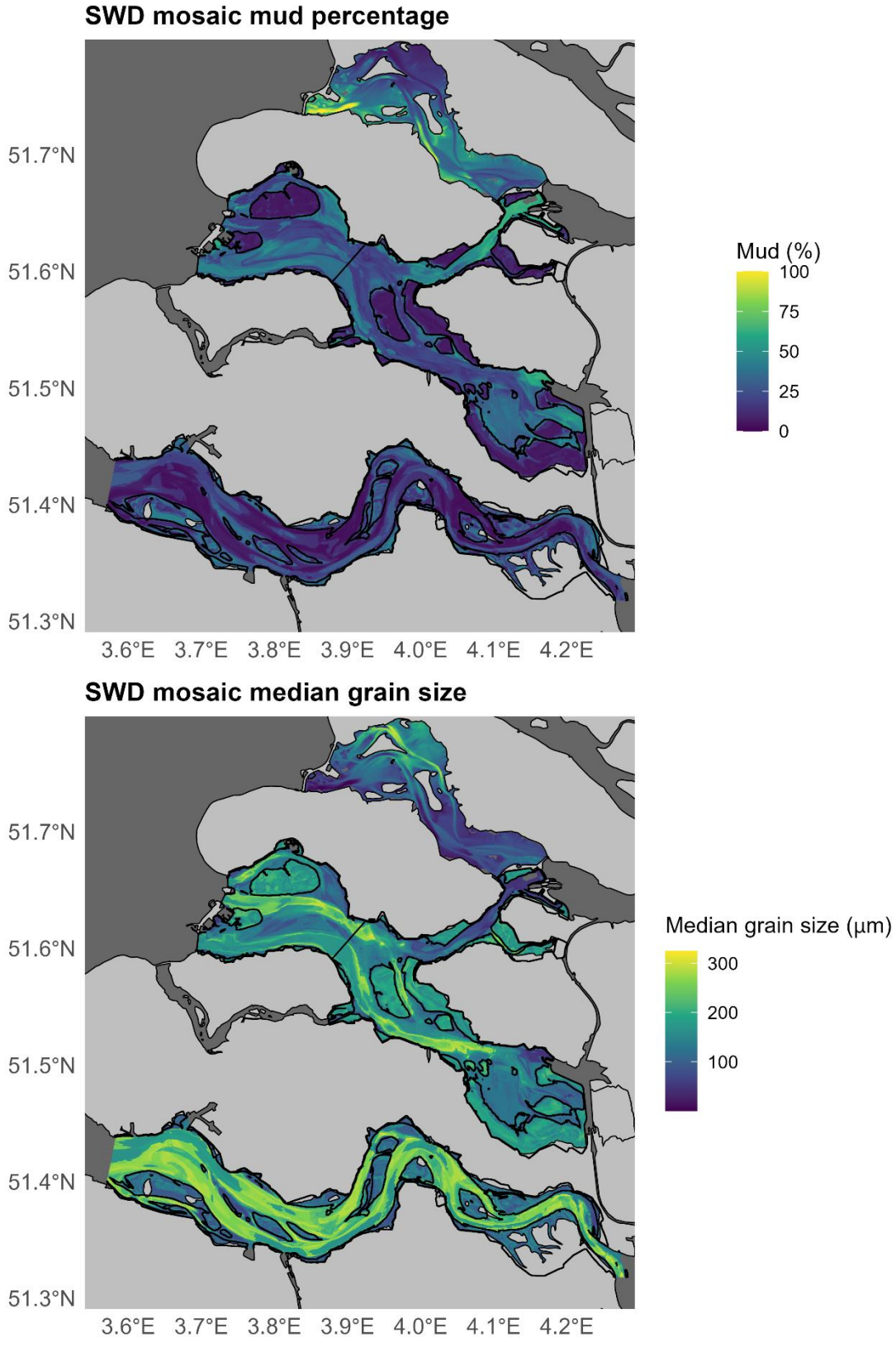


Figure 18: Predicted sediment composition across the Southwestern Delta, showing (top) mud content (%) and (bottom) median grain size (D50; µm) for the Oosterschelde, Westerschelde, and Lake Grevelingen. Predictions were generated using Random Forest (RF) models for the Oosterschelde and Westerschelde and Generalized Additive Models (GAMs) for Lake Grevelingen. Land is shown in grey. Black outlines depict the

intertidal areas. Dark grey indicates waterbodies without data. Model performance varied among basins, with generally lower predictive skill in the Westerschelde, particularly for mud content (Table 3). Predictions should therefore be interpreted as broad-scale sediment patterns rather than precise local estimates.

Table 3: Model performance metrics for Random Forest (RF) and Generalized Additive Models (GAM) used to predict median grain size (D50) and mud content (%mud) across the three studied basins in the Southwestern Delta. N represents the number of sampling points, RMSE the Root Mean Square Error, MAE the Mean Absolute Error, R^2 the coefficient of determination, and nRMSE the normalized Root Mean Square Error (expressed as a percentage). Lower RMSE, MAE and nRMSE values indicate better predictive accuracy, whereas higher R^2 values indicate better model performance. Negative R^2 values indicate that the model performs worse than a baseline prediction using the mean observed value.

System	N (points)	Model	RMSE	MAE	R^2	nRMSE
Oosterschelde	64	RF – D50	65.58	22.81	0.25	85.92
	60	RF - %mud	17.64	5.70	0.31	82.55
Westerschelde	92	RF – D50	76.22	27.79	0.04	97.62
	90	RF - %mud	27.04	9.97	-0.34	115.03
Lake Grevelingen	53	GAM – D50	70.14	53.13	0.16	96.16
	53	GAM - %mud	21.02	18.68	0.39	79.20

3.1.3.2 Predicted habitat suitability for *O. edulis*

Lake Grevelingen appears more suitable for *O. edulis* than the Oosterschelde. In the INLA predictions, areas of higher suitability closely follow the locations where flat oysters were observed, with little extrapolation to areas where oysters were not recorded (Figure 19). This suggests that the abiotic predictors used in the model do not consistently define a shared environmental niche across all presence locations. Instead, the model largely reproduces the spatial pattern of the observations through the spatial random field.

A similar pattern emerges in the Random Forest (RF) predictions. Rather than identifying broader areas with comparable environmental conditions, the RF model mainly predicts suitability in locations with almost identical abiotic conditions to the observed presence points. As a result, the predicted suitable areas remain limited and closely aligned with the observation locations. This indicates that the model does not detect a clear common abiotic niche for flat oysters. The apparent environmental signal may therefore partly reflect spatial

confounding, where environmental variables correlate with location, rather than a strong ecological driver of oyster presence.

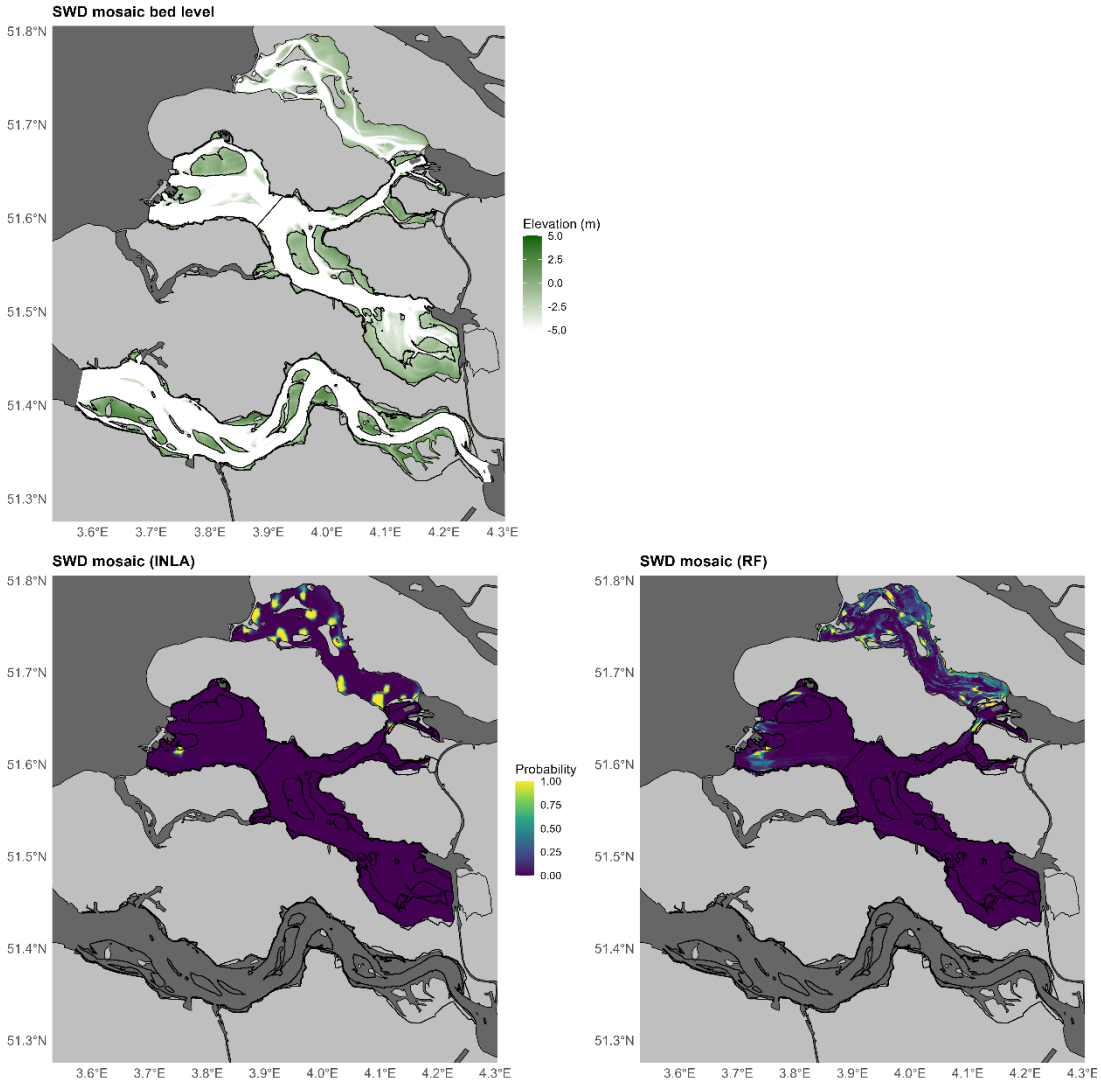


Figure 19: Predicted probability of O. edulis occurrence in the southwestern delta.
The top panel shows distribution of intertidal areas, with elevation indicated by the colour scale. Bottom left panel: INLA spatial model. Bottom right panel: Random Forest (RF). Colours indicate predicted probability of presence (0–1); land is shown in grey. Black outlines depict the intertidal areas. Dark grey indicates waterbodies without data.

3.1.3.3 Predicted habitat suitability for *M. edulis*

Both models, INLA and RF, identify broadly similar regions of potential *M. edulis* habitat in the southwestern Dutch Delta, but they differ in the spatial extent of the predicted suitable areas (Figure 20). The INLA model indicates that the probability of *M. edulis* presence is only weakly explained by the non-linear relationships with the environmental predictors. Instead, much of the spatial pattern is captured by the spatial random field, which appears as localized, patchy areas centered around the observed mussel locations. Consequently, the predicted suitable habitat remains relatively small and spatially clustered.
In contrast, the Random Forest (RF) model identifies complex patterns in the abiotic predictors, including non-linear responses and interactions among variables. Because RF does not explicitly account for spatial structure, it instead predicts suitability based on environmental similarity to locations where mussels were observed. This results in larger contiguous areas being classified as suitable habitat. Notably, the RF model also predicts

suitability in locations where *M. edulis* was not observed, effectively extrapolating the environmental niche inferred from the presence data.
Overall, both approaches highlight similar environmental settings for *M. edulis* occurrence, but differ in how strongly they extrapolate these conditions across space. The INLA model yields a more spatially constrained prediction driven by observed occurrences, whereas the RF model delineates broader areas with comparable abiotic conditions that may represent potential restoration opportunities.
It is important to note that the prediction for *M. edulis* in the Westerschelde is biased by a low number of presences. This is likely to have caused the RF prediction to be dominated by overfitting.

To synthesize the spatial predictions from both modelling approaches, we combined the INLA and RF outputs into an ensemble suitability map by taking their mean (Figure 21). This integration highlights areas where both models consistently predict suitable conditions, while reducing model-specific biases in spatial extrapolation. By thresholding low suitability values (< 0.05), the resulting maps emphasize locations with stronger agreement between models and more robust habitat potential.

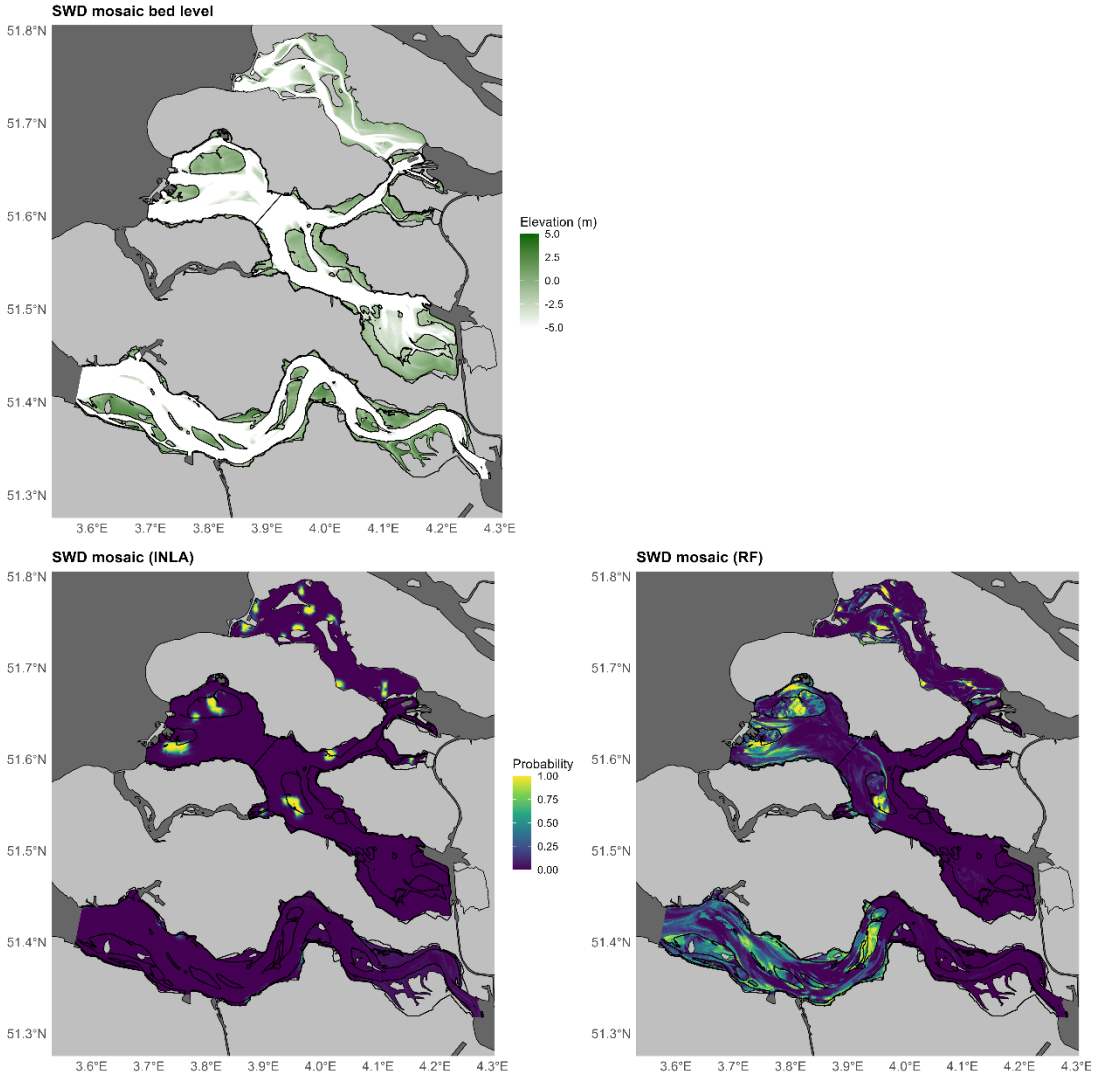


Figure 20: Predicted probability of M. edulis occurrence in the southwestern delta.
The top panel shows distribution of intertidal areas, with elevation indicated by the colour scale. Bottom left panel: INLA spatial model. Bottom right panel: Random Forest (RF). Colours indicate predicted probability of presence (0–1); land is shown in grey. Black outlines depict the intertidal areas. Dark grey indicates waterbodies without data.

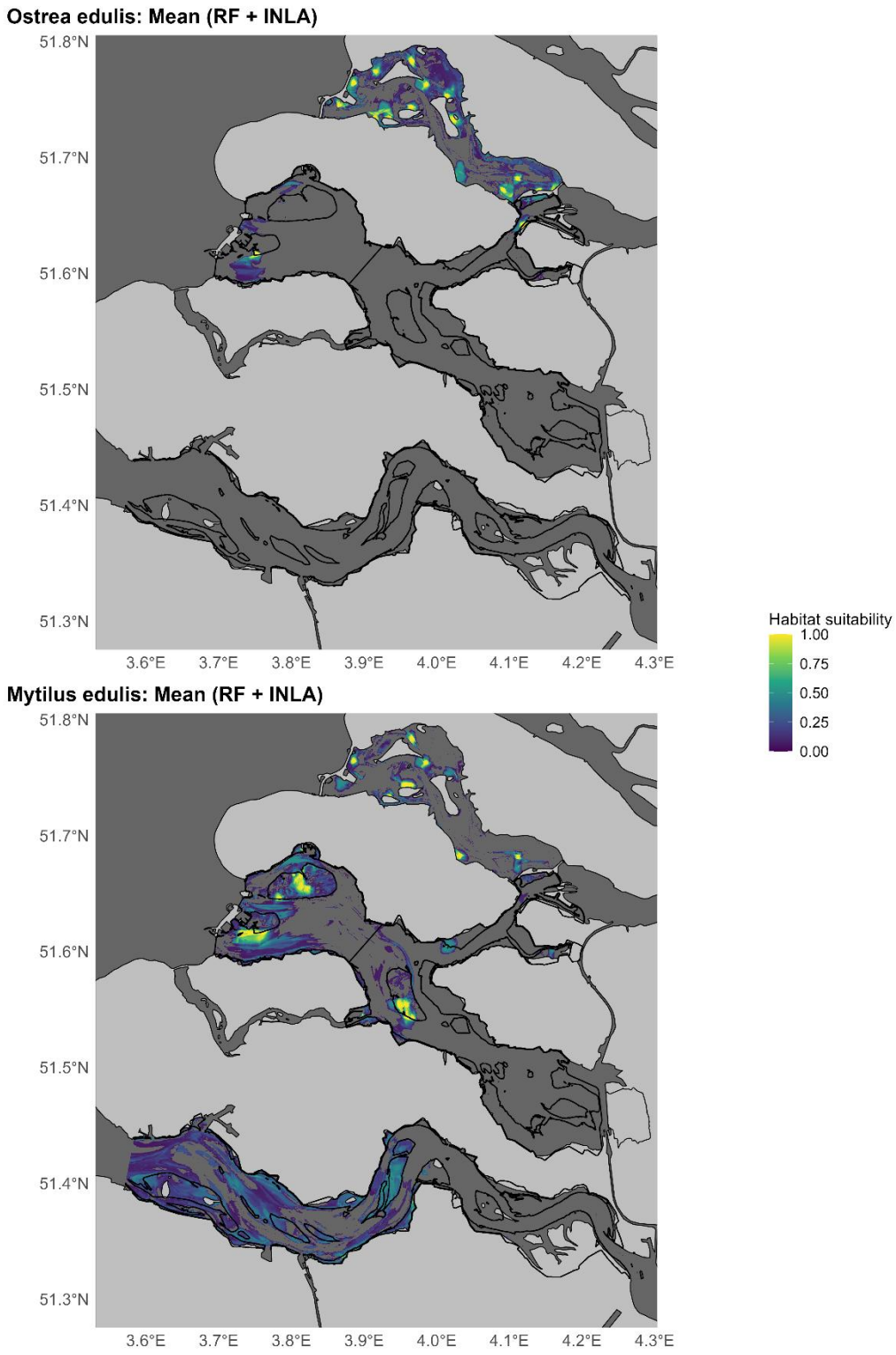


Figure 21: Mean habitat suitability for O. edulis (top) and M. edulis (bottom) across the southwestern Dutch delta (SWD), derived from an ensemble of INLA and Random Forest models.
Suitability values represent predicted occurrence probabilities (0–1). To emphasize areas of meaningful habitat potential and suppress marginal predictions, all values below 0.05 are set to NA. Black outlines depict the intertidal areas. Dark grey indicates waterbodies without data.

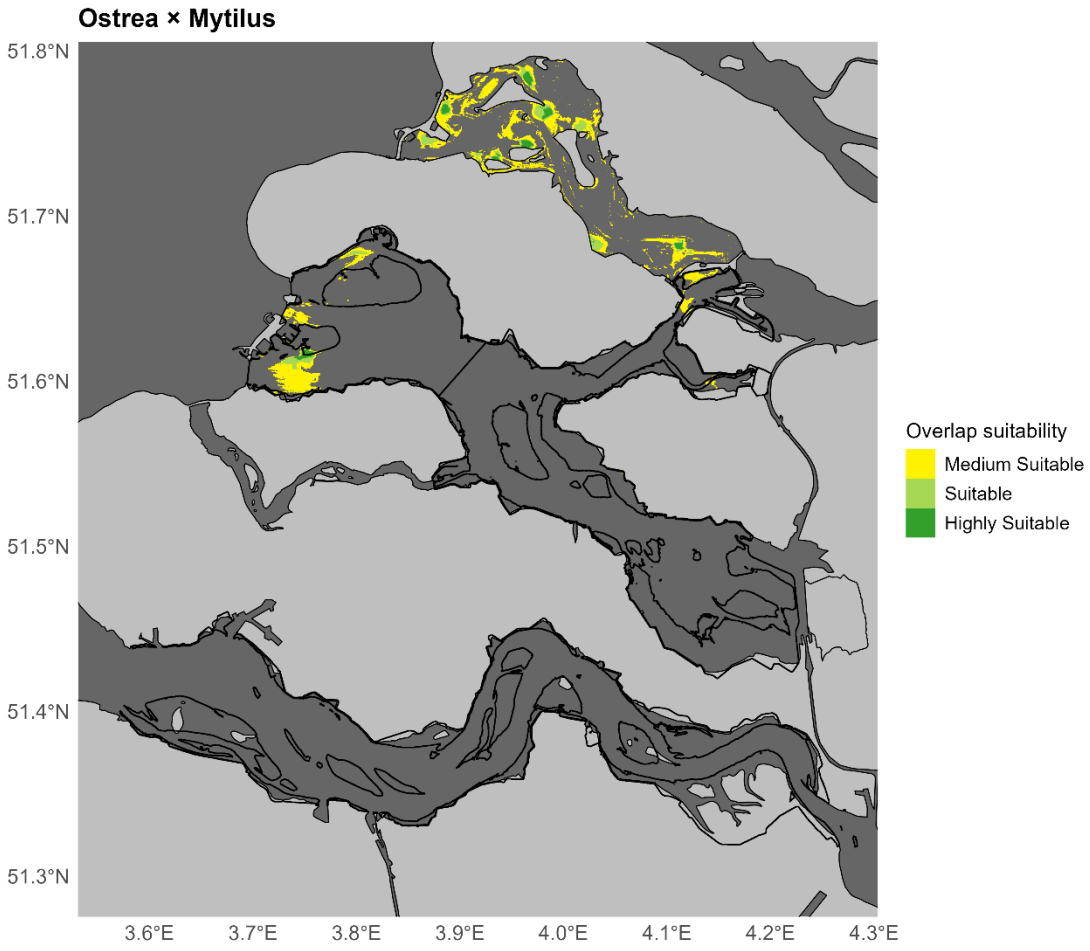


Figure 22: Spatial overlap in predicted habitat suitability for Ostrea edulis and Mytilus edulis in the Southwestern Delta. Overlap was calculated by multiplying the mean Random Forest (RF) and INLA suitability predictions for both species, excluding values below 0.05. The resulting product was rescaled to 0–1 using min-max normalization and classified into three categories: medium suitability (0–0.20), suitable (0.20–0.50), and highly suitable (≥0.50). Higher values indicate locations where both species show relatively high predicted habitat suitability.

3.2 Bivalve growth potential

3.2.1 North Sea

Both *O. edulis* and *M. edulis* exhibit rapid growth during their early life stages, after which growth rates stabilise, approximately after 15 years for *O. edulis* and after about 3 years for *M. edulis* (Figure 23). By the end of the 30-year simulation period, *O. edulis* reaches final shell lengths ranging from 0.35 cm at Dogger_S4 to 9.2 cm at BGR_2 (Figure 24). Dogger_S4 also shows the lowest final shell length for *M. edulis* (0.12 cm) at the end of the 10-year simulation (Figure 25). The maximum simulated growth for *M. edulis* in the North Sea (2.6 cm) occurs at the North_of_HKN site. Overall, coastal sites exhibit higher shell growth for both species, with reduced growth observed at more offshore locations (Figure 24, Figure 25). This spatial pattern aligns with known gradients in bottom environmental conditions such as food availability and temperature. These environmental variables generally decrease with increasing distance from the coast, resulting in less favourable growth conditions offshore.

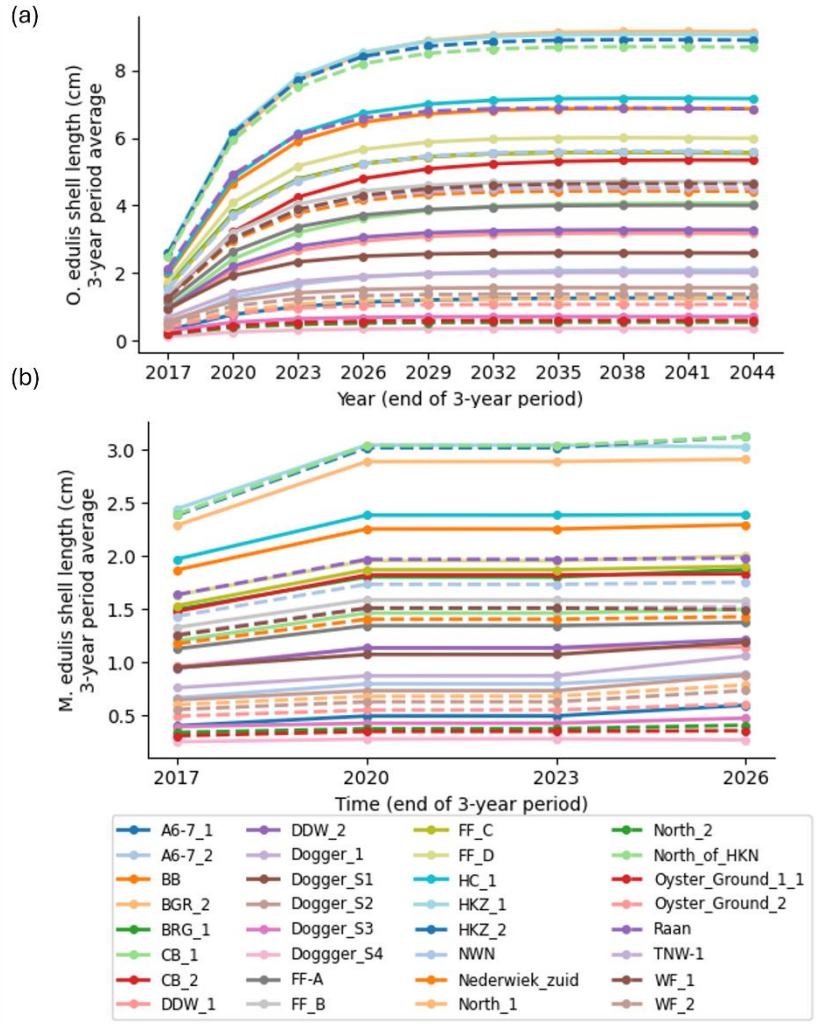


Figure 23: Time-series of modelled (a) O. edulis and (b) M. edulis shell lengths in the North Sea.

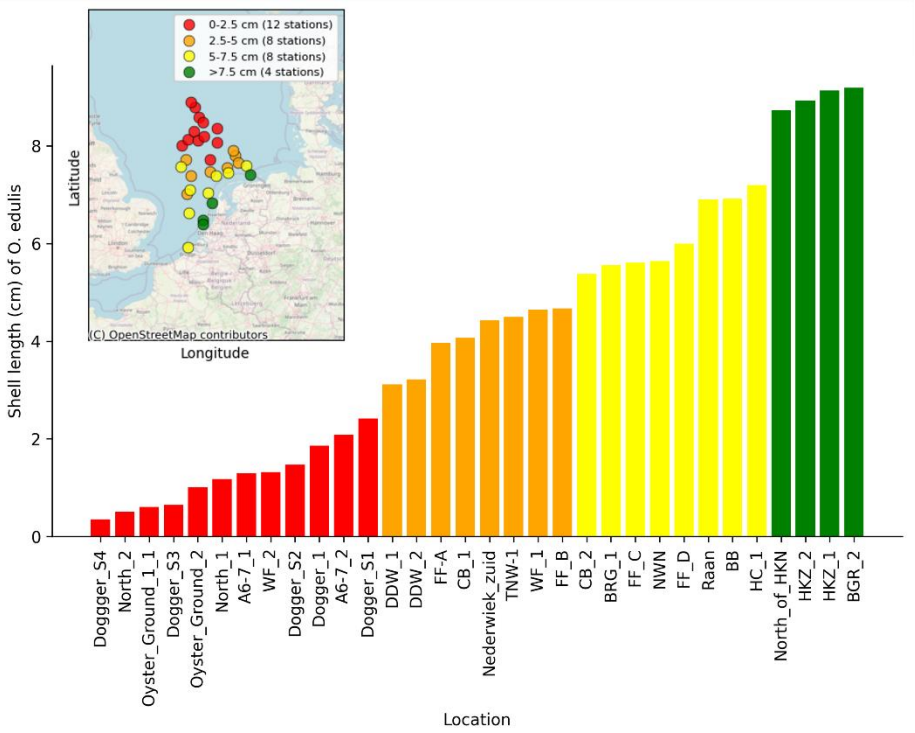


Figure 24: Bar plot of modelled shell lengths attained by O. edulis at the end of simulation at each site in the North Sea with the map (inset figure) showing shell length categories of O. edulis in the North Sea derived from 1D DEB models. The colours of the bar represent the categories shown in the inset figure.

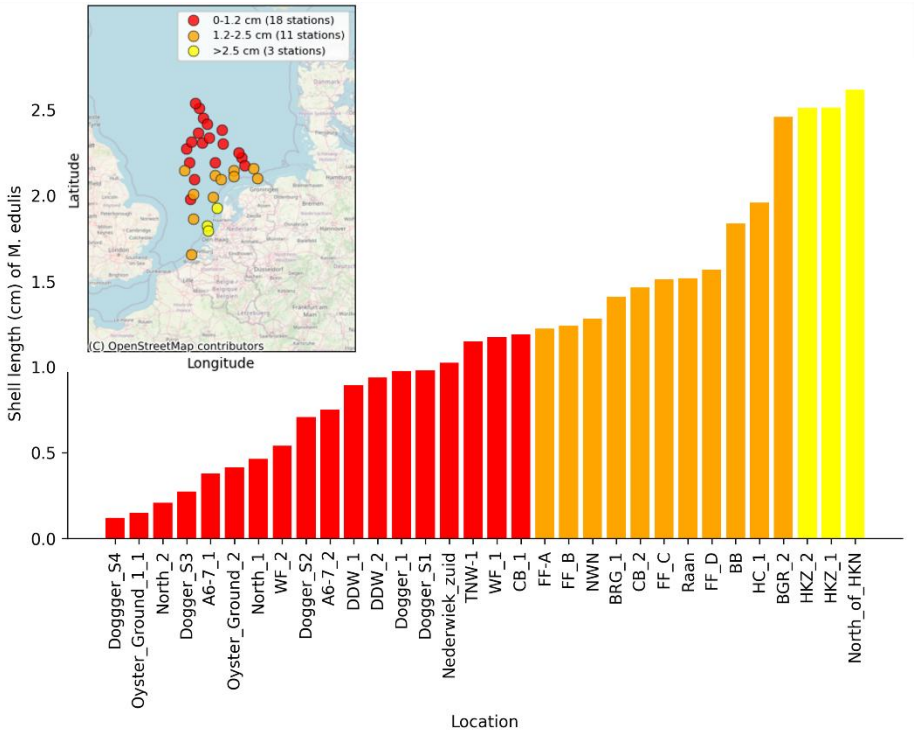


Figure 25: Bar plot of modelled shell lengths attained by M. edulis at the end of simulation at each site in the North Sea with the map (inset figure) showing shell length categories of M. edulis in the North Sea derived from 1D DEB models. The colours of the bar represent the categories shown in the inset figure.

To quantify the influence of environmental drivers, statistical relationships between final shell lengths and average bottom environmental conditions were assessed. Environmental data for 2015-2017 were extracted from the 3D water quality model of the North Sea. Bottom chlorophyll-a (R^2 = 0.82, R = 0.90) and bottom temperature (R^2 = 0.78, R = 0.88) show strong correlations with *O. edulis* final shell lengths across the 32 DEB model sites. Similarly, *M. edulis* shows robust correlations with chlorophyll-a (R^2 = 0.76, R = 0.87) and temperature (R^2 = 0.69, R = 0.83). Based on these relationships, bivariate statistical models were developed for both species using bottom chlorophyll-a and temperature as predictors.

The relationship between bottom chlorophyll-*a* and bottom temperature across the 32 DEB model sites showed moderate to good association (R^2 = 0.58, R = 0.76), indicating that both variables provide complementary environmental information. Similarly, VIF scores of 5 for each predictor reflect moderate but acceptable collinearity for use in combined analyses.

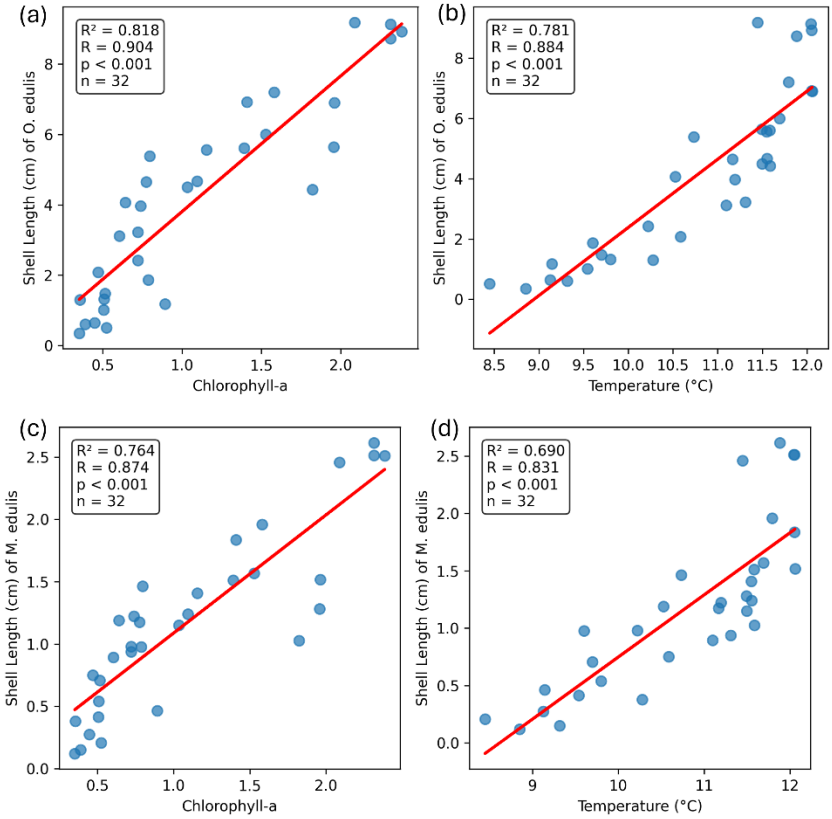


Figure 26: Plots showing coefficient of determination (R^2), Pearson correlation (R) and p value for linear relationships between O. edulis and environmental variables (a, b) and between M. edulis and environmental variables (c, d) in the North Sea.

The bivariate regression models developed for *O. edulis* and *M. edulis* performed consistently well when evaluated against independent datasets (Figure 26). For *O. edulis*, model performance remained high in both the training (R^2 = 0.92) and test datasets (R^2 = 0.87). *M. edulis* showed a similar pattern, with only minor differences between the training (R^2 = 0.82) and test datasets (R^2 = 0.80). Residual patterns were largely random for both species, with only one isolated deviation, indicating that the models captured the dominant environmental drivers of growth without major bias. These outcomes support the use of the bivariate models for spatial extrapolation across the Dutch EEZ (Figure 27).

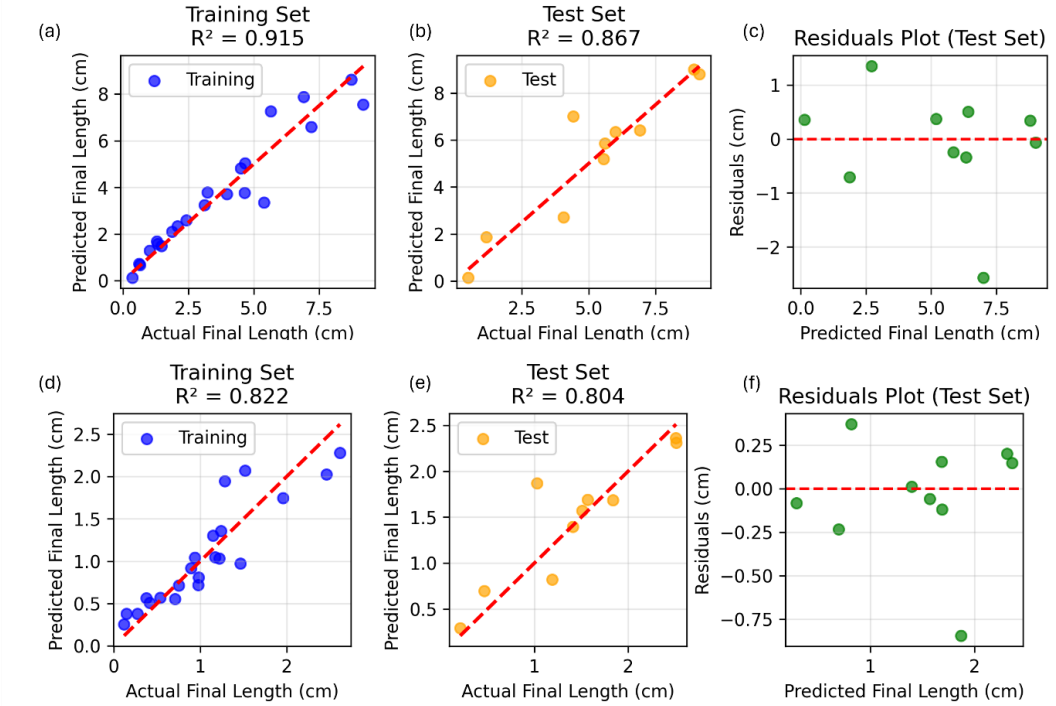


Figure 27: Performance of multivariate linear regression model for test dataset, training data and the figures showing distribution of residuals for O. edulis (a, b ,c) and M. edulis (d, e, f) in the North Sea.

Predicted shell lengths for *O. edulis* across the Dutch EEZ ranged from 0 to >40 cm (Figure 28). Coastal areas exhibit the highest predicted lengths, generally >10 cm, with the largest values concentrated in small coastal pockets, particularly along the southwestern delta region. Farther offshore, predicted lengths were predominantly <2.5 cm, although several offshore patches reached 2.5-5 cm, indicating that suitable conditions for *O. edulis* survival may still occur at these locations. Assuming that *O. edulis* may reproduce at shell lengths ≥2.5 cm, these offshore patches may represent environmentally marginal but viable areas.

Observed biological limits informed the interpretation of these length distributions. *O. edulis* can reach maximum lengths of ~22-23 cm (Cole, 1941; Hermans et al., 2020) under high-food, high-temperature conditions and may live for up to ~35 years (Richardson and Saurel, 2003). Within the DEB simulations, an optimum-condition run at the BGR_2 site yielded a maximum shell length of 16.6 cm. Based on the observed biological limits for reproductive capability in the species, predicted lengths were rescaled to a 0-1 suitability index, with values <2.5 cm assigned a suitability of 0 and values >10 cm assigned a suitability of 1 (Figure 34e). This scaling highlights clear gradients in suitable growth conditions across the Dutch EEZ, with optimal areas concentrated nearshore and progressively less suitable habitats occurring offshore.

Predicted shell lengths for *M. edulis* across the Dutch EEZ ranged from 0 to 12 cm (Figure 28). The spatial pattern closely resembled that of *O. edulis*, with the largest shell lengths occurring along the coastal strip and substantially smaller lengths in offshore areas. However, unlike *O. edulis*, *M. edulis* does not reach biologically meaningful sizes for reproduction in the offshore region. As a result, the overall spatial extent of suitable habitat for *M. edulis* is considerably smaller than that predicted for *O. edulis*.

Biological limits for interpreting *M. edulis* growth were defined using observed reproductive thresholds. The lower boundary for reproductive viability was set at 1.2 cm, corresponding to

the shell length at puberty reported in the Add-my-Pet database. The upper boundary was defined based on the literature as 4 cm based on the reproductive capability of *M. edulis*.

An optimum-condition DEB simulation at the North_of_HKN site, the location that produced the largest *M. edulis* individuals in the baseline runs, yielded a maximum attainable shell length of 6.6 cm.

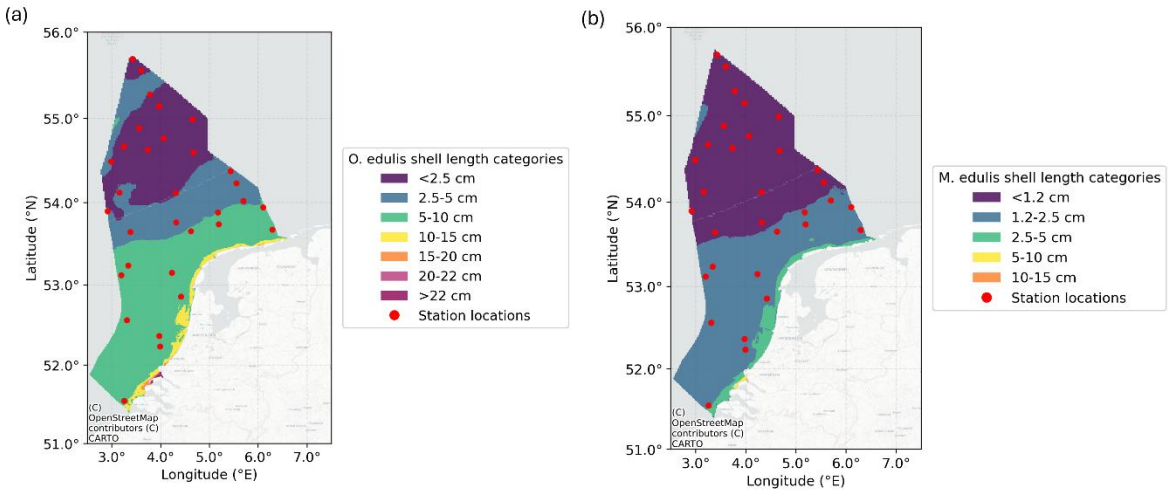


Figure 28: Maps showing extrapolated shell lengths of (a) O. edulis and (b) M. edulis in the Dutch North Sea region based on the multivariate linear regression model in the North Sea.

3.2.2 Lake Grevelingen

Lake Grevelingen shows consistently high growth potential for both *O. edulis* (Figure 29) and *M. edulis* (Figure 30) across all DEB modelling sites. At the end of the simulation period, predicted shell lengths at every site exceed the minimum thresholds assumed for survival in this study (2.5 cm for *O. edulis* and 1.2 cm for *M. edulis*). Growth potential is generally highest at sites located within zones characterized by either cultured shellfish, wild shellfish, or a combination of both. In contrast, sites in the reference zones (sites 3, 7, and 10), where neither wild nor cultured shellfish are present, show the lowest predicted growth for both species. The four sites with the greatest growth potential fall within zones containing cultured shellfish (sites 1, 11, and 4) or zones hosting both wild and cultured shellfish (site 6). Furthermore, the ranking of sites from lowest to highest predicted shell length is identical for *O. edulis* and *M. edulis*, indicating that both species respond similarly to the environmental conditions within Lake Grevelingen.

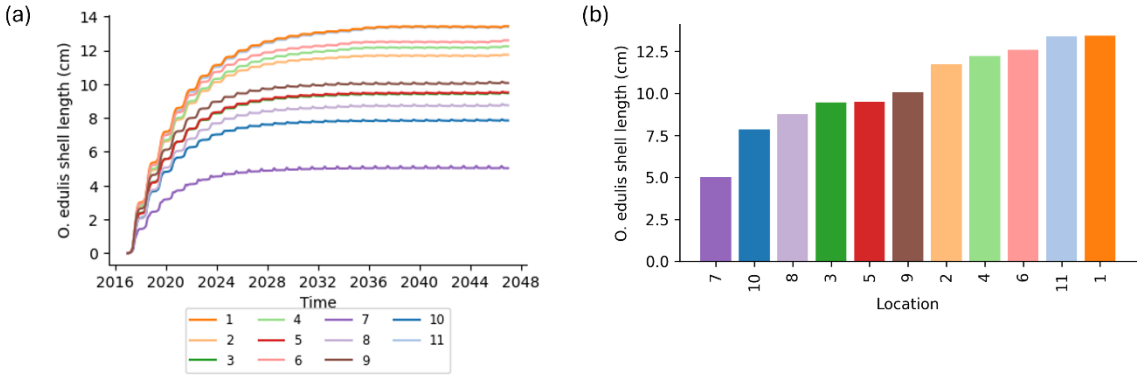


Figure 29: Time-series of O. edulis shell length growth with time in DEB models in the Lake Grevelingen (a) and bar plot of final shell lengths attained by O. edulis in DEB models at the end of simulation period at sites in the Lake Grevelingen (b).

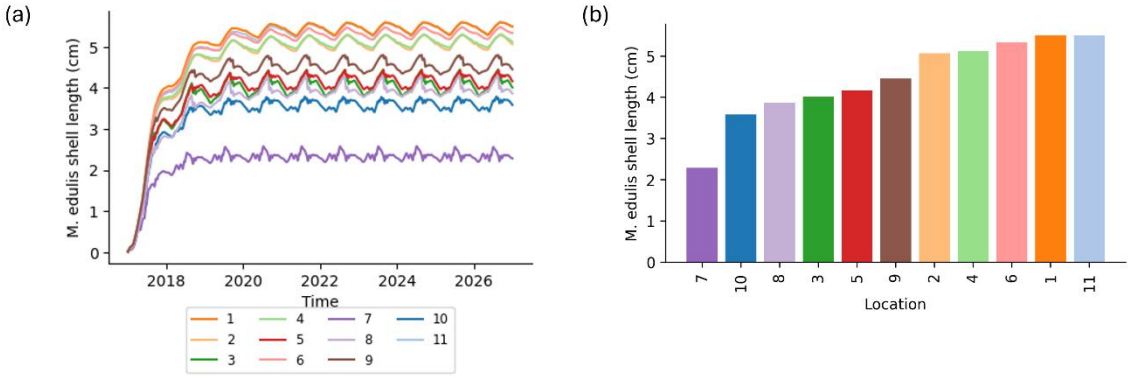


Figure 30: Time-series of M. edulis shell length growth with time in DEB models in the Lake Grevelingen (a) and bar plot of final shell lengths attained by M. edulis in DEB models at the end of simulation period at sites in the Lake Grevelingen (b).

For extrapolation of DEB results to the entire lake area, statistical relationships were examined between final shell lengths and multiple environmental variables, including mean and minimum bottom chlorophyll-*a*, temperature, dissolved oxygen, salinity, and temperature stratification. Among these variables, only mean bottom dissolved oxygen shows a meaningful relationship with final shell length. *O. edulis* exhibits a strong linear relationship (R^2 = 0.68, R = 0.83), and *M. edulis* shows a similarly strong relationship (R^2 = 0.73, R = 0.85) with mean bottom oxygen (Figure 31). On this basis, mean bottom dissolved oxygen is used to extrapolate bivalve growth potential across Lake Grevelingen (Figure 32).

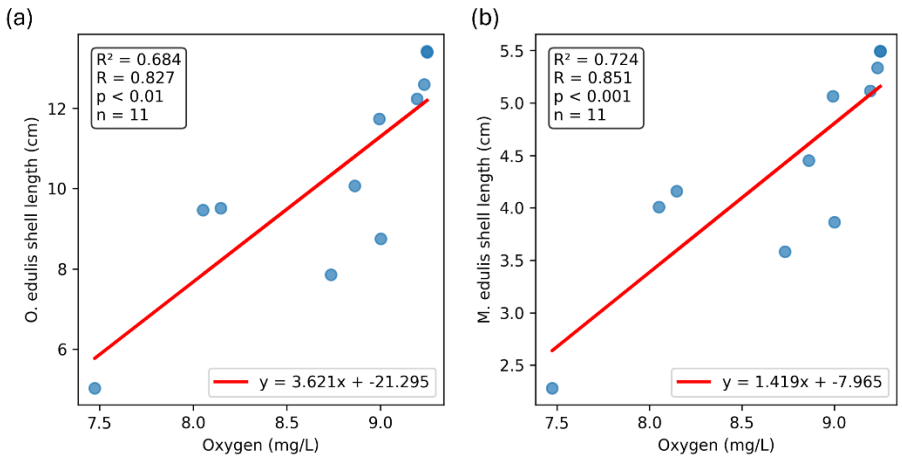


Figure 31: Plots showing coefficient of determination (R^2), Pearson correlation (R) and p value for linear relationships between O. edulis and mean bottom dissolved oxygen (a) and between M. edulis and mean bottom dissolved oxygen (b) in the Lake Grevelingen.

The extrapolated *O. edulis* shell lengths range from negative values to approximately 15 cm, while *M. edulis* lengths range from negative values up to around 6 cm (Figure 33). Negative values occur in areas where dissolved oxygen approaches zero in the 3D water quality model outputs, primarily shallow flats and island zones, indicating environments where growth is not possible. The extrapolated negative values are an artefact of the model. Relatively shallow and well-oxygenated parts of the lake show the highest predicted growth potential for both species. In the deeper areas, bivalves do not reach the minimum shell lengths required for survival due to low oxygen availability.

Final lengths are scaled to a DEB-based suitability index using species-specific biological limits. Minimum and maximum thresholds remain the same as that of the North Sea scaling for *O. edulis* (2.5 - 10 cm) and *M. edulis* (1.2 – 4 cm), as described in section 2.3.3.3. Maximum attainable lengths derived from optimum-condition DEB simulations, conducted at the sites with the highest baseline growth, yielded the same values of 16.6 cm for *O. edulis* and 6.6 cm for *M. edulis* as that of the North Sea optimum-condition runs.

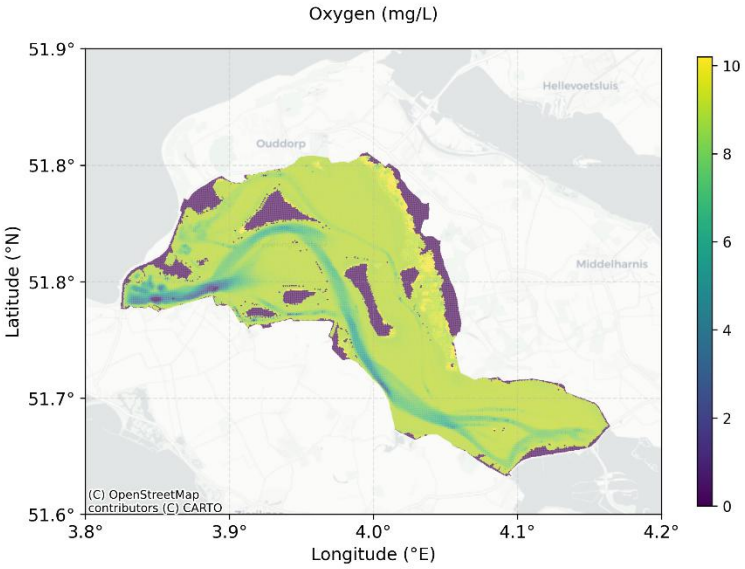


Figure 32: Map showing modelled mean bottom oxygen during 2017 in the 3D water quality model of the Lake Grevelingen.

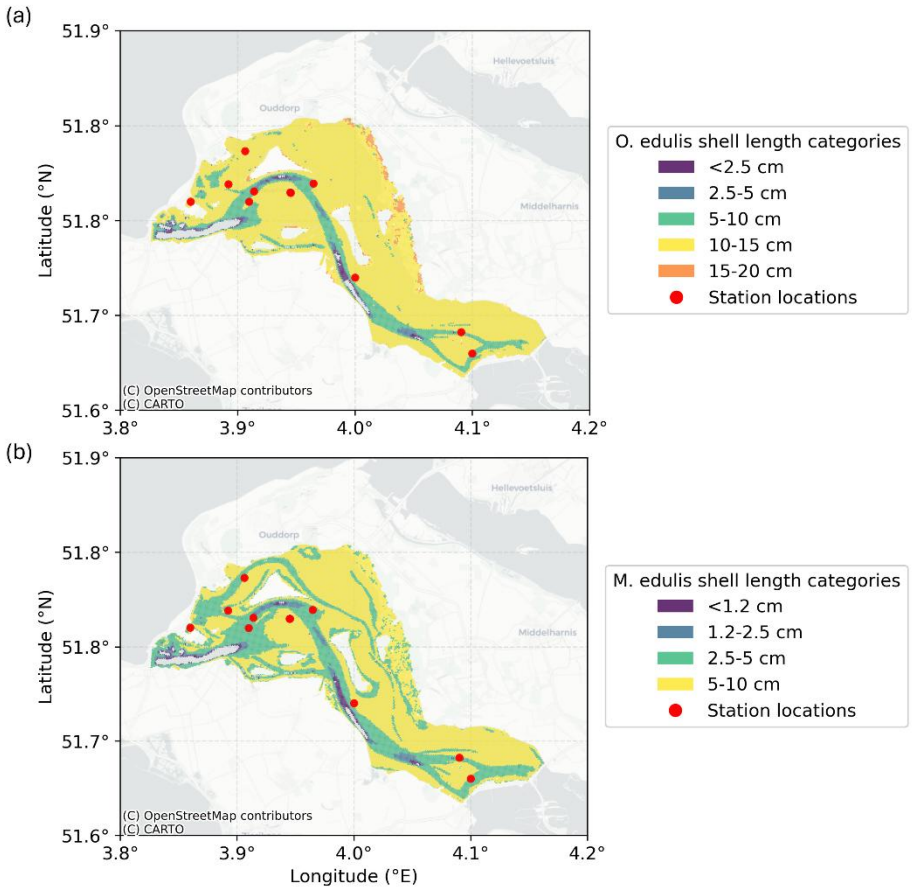


Figure 33: Maps showing extrapolated shell lengths of (a) O. edulis and (b) M. edulis based on the multivariate linear regression model in the Lake Grevelingen.

3.3 Integration

3.3.1 North Sea

The integrated maps show species-specific differences between suitability using machine learning and statistical techniques (RF+GAM mean) and DEB-derived growth potential (Figure 34). For *O. edulis*, the two approaches diverge spatially. The DEB index indicates higher growth potential near the Dutch coastline, whereas the SDM mean identifies higher suitability near historic offshore oyster grounds. Despite this contrast, two areas consistently emerge as favorable under both methods: (1) the Frisian Front and (2) the Voordelta in front of the southwestern delta, near the Port of Rotterdam. These overlap zones represent locations where environmental suitability and energetic performance coincide. However, the high predicted suitability near the Port of Rotterdam should be interpreted with caution, as dredging and sediment disposal activities are not explicitly accounted for in the models and may locally constrain reef establishment. However, some findings of flat oysters have been established near the Port of Rotterdam, which are recorded in the DATRAS dataset (Herman & van Rees, 2022). For *M. edulis*, SDM and DEB patterns are more aligned. Both indicate higher suitability near the coast, including along the southern North Sea coast and in Natura 2000 areas on the North Sea side of the Wadden Sea islands. As a result, the overlap surface largely follows the coastal gradient.

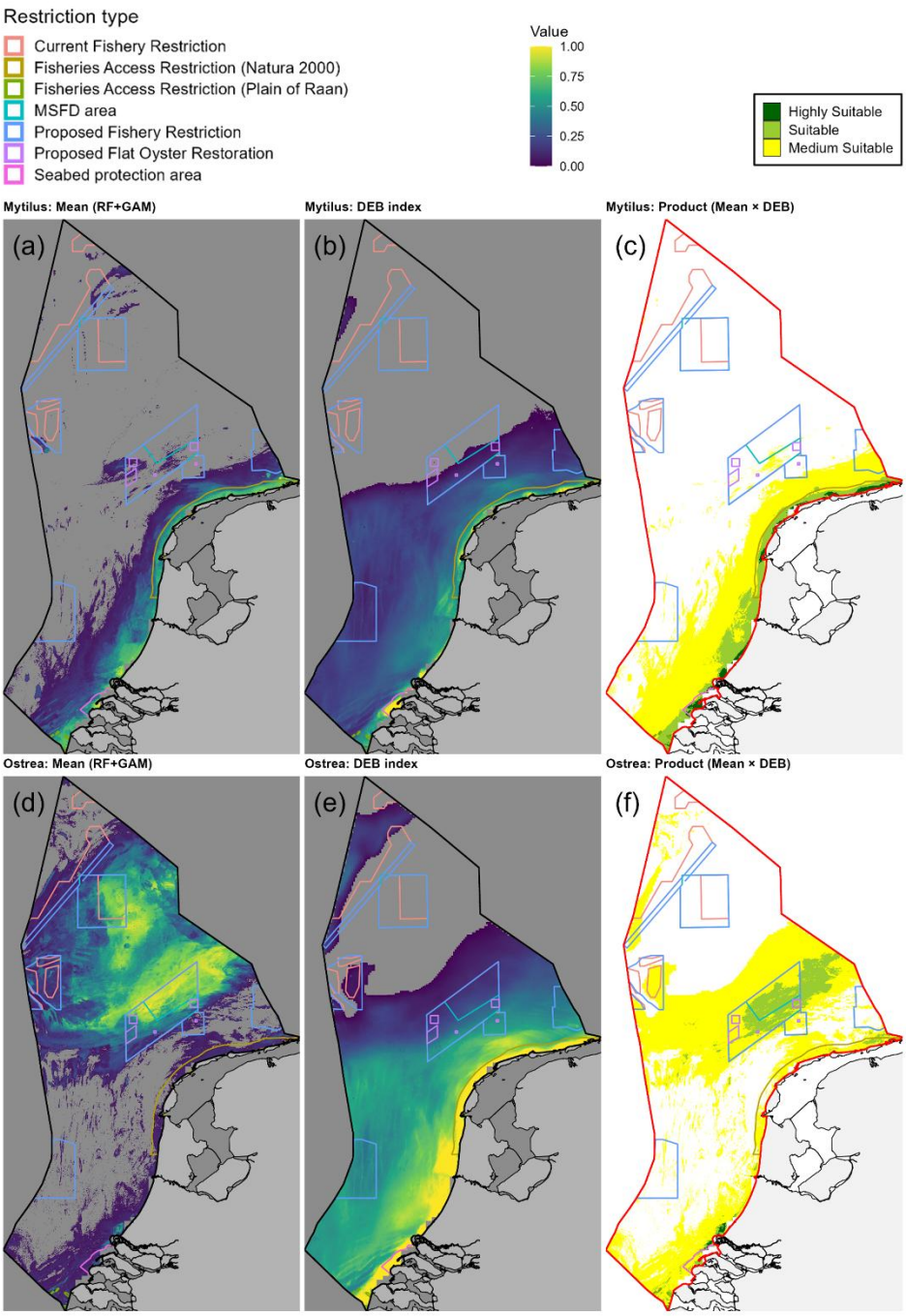


Figure 34: Integrated suitability maps combining species distribution models and DEB-based growth suitability for O. edulis (top row) and M. edulis (bottom row) in the Dutch North Sea.
Left column: normalized mean habitat suitability derived from RF and GAM models (values scaled to 0–1; SDM values < 0.05 set to NA to suppress marginal suitability). Middle column: normalized Dynamic Energy Budget (DEB) length suitability index (0–1). Right column: interaction surface calculated as the product of the normalized SDM mean and DEB index (Mean × DEB), subsequently rescaled to 0–1 to emphasize relative overlap intensity, and displayed as three suitability classes: medium (0.00–0.20), suitable (0.20–0.50), and highly suitable (≥ 0.50).

3.3.2 Lake Grevelingen

An integrative approach was also used for Lake Grevelingen, which shows the highest overall suitability within the southwestern delta. The DEB model was specifically applied here due to known stratification issues, which can constrain growth conditions. Notably, the ensemble prediction from RF and INLA aligns closely with the DEB results: areas with reduced DEB suitability under stratified conditions also correspond to low predicted habitat suitability. Both *M. edulis* and *O. edulis* display similar spatial patterns, with favourable conditions occurring in sheltered areas around 1) Hompelvoet, north of 2) Stampersplaat, adjacent to the 3) Brouwersdam, and near the 4) Slikken van Dijkwater (Figure 35). Existing commercial shellfish plots do not necessarily coincide with areas of high suitability for natural reef development, but are often located adjacent to them.

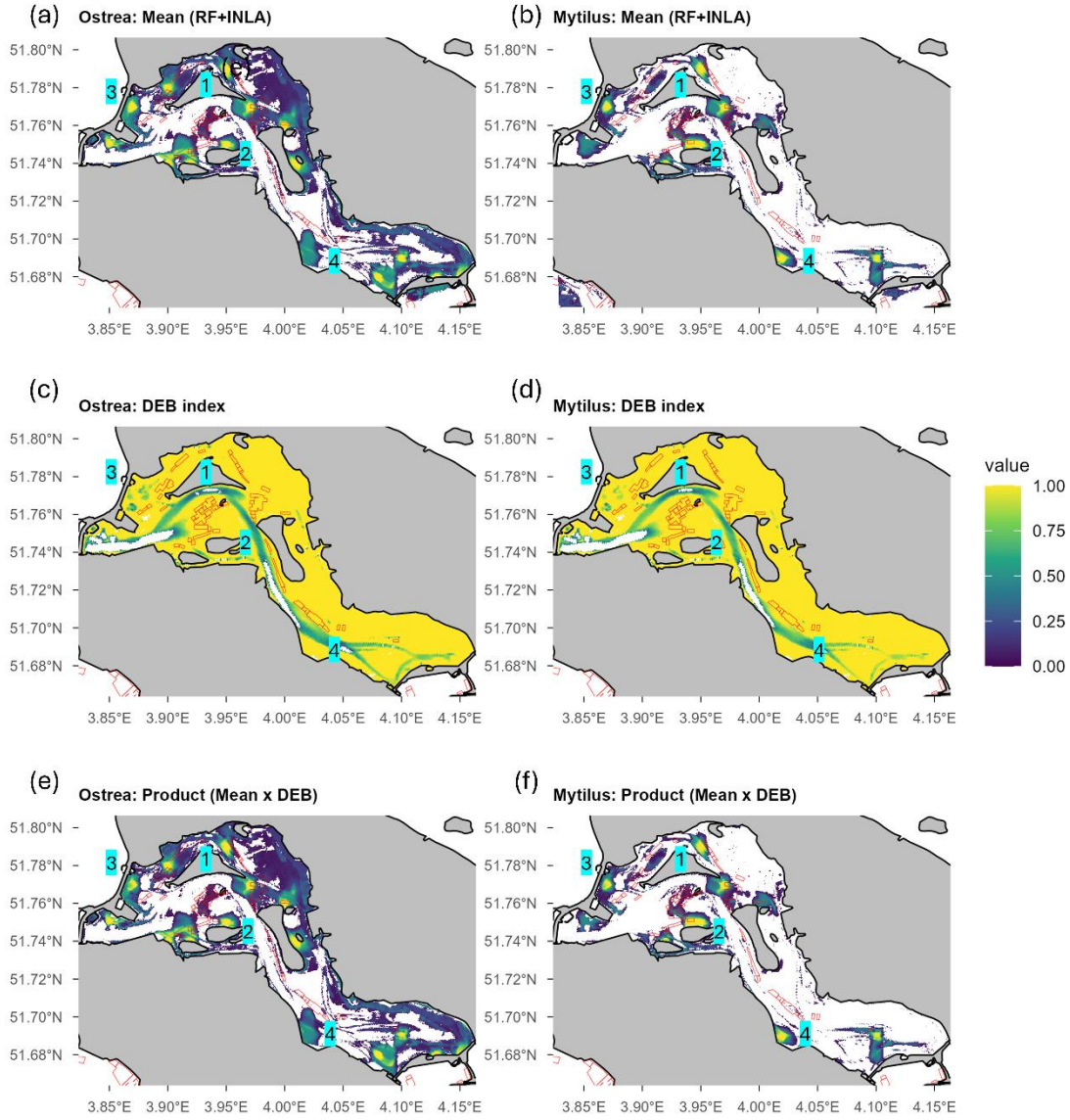


Figure 35: Integrated suitability maps combining species distribution models (SDMs) and Dynamic Energy Budget (DEB)-based growth suitability for O. edulis and M. edulis in Lake Grevelingen. Panels (a, b) show mean habitat suitability derived from RF and INLA models (scaled to 0–1; SDM values <0.05 set to NA to suppress marginal suitability). Panels (c, d) show the DEB length-based suitability index (0–1). Panels (e, f) show the integrated suitability, calculated as the product of the thresholded mean SDM suitability and DEB index (Mean × DEB), subsequently rescaled to 0–1 to emphasize relative overlap between habitat suitability and growth potential. Panels (a, c, e) represent O. edulis, while panels (b, d, f) represent M. edulis. Existing

commercial shellfish plots are outlined in red. Numbers indicate locations referred to in the text: (1) Hompelvoetplaat, (2) Stampersplaat, (3) Brouwersdam, and (4) Slikken van Dijkwater.

3.3.3 Combined mapping across all study areas

In this section, final maps for the restoration potential of *O. edulis* (Figure 36), *M. edulis* (Figure 37) and *M. modiolus* (Figure 38) are shown, combining abiotic habitat suitability modelling (for all basins) with DEB models (for North Sea and Lake Grevelingen).

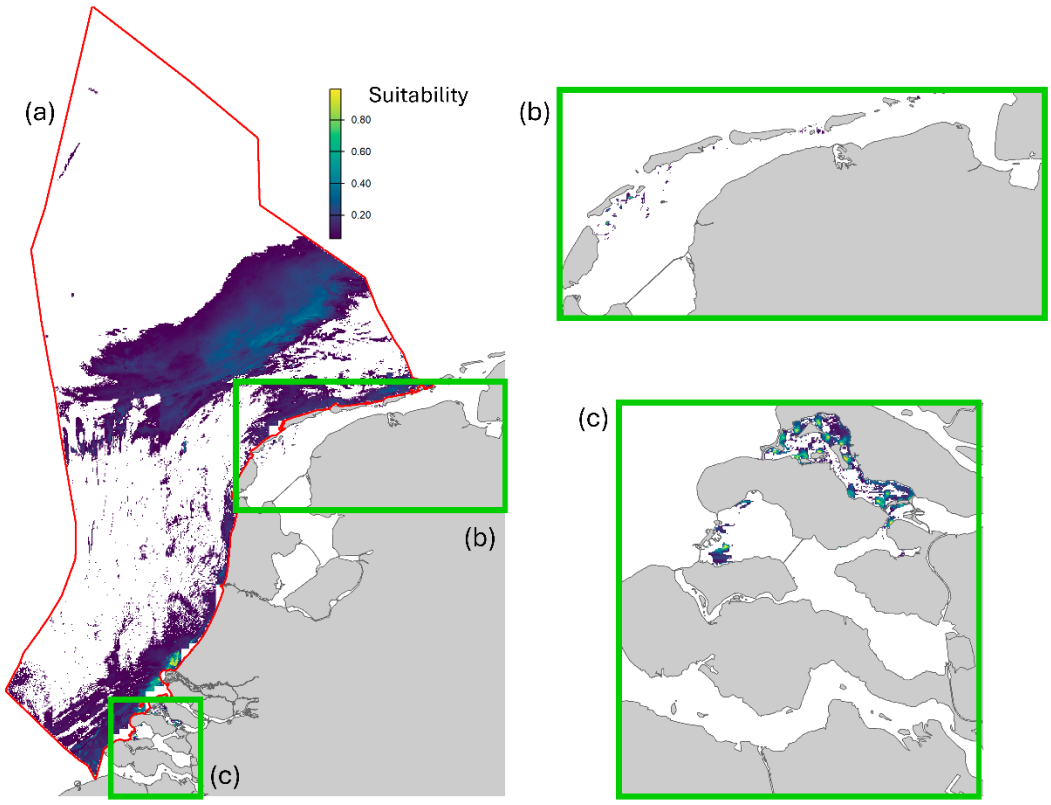


Figure 36: Spatial distribution of habitat suitability for O. edulis across the Dutch coastal basins. The mosaic panel combines basin-specific models: in the North Sea, suitability is calculated as the product of the normalized SDM mean (RF and GAM) and DEB index: (SDM Mean × DEB), subsequently rescaled to 0–1 (a). In the Wadden Sea, suitability is based on RF (b). In the Southwestern Delta, suitability is based on the mean of INLA and RF predictions, except for the Grevelingen for which suitability is the product of the thresholded SDM mean and DEB index (SDM Mean × DEB), subsequently rescaled to 0–1 (c). Green outlines in the mosaic denote the extent of the Southwestern Delta and Wadden Sea subdomains. The Dutch EEZ is shown in red and land as a grey polygon.

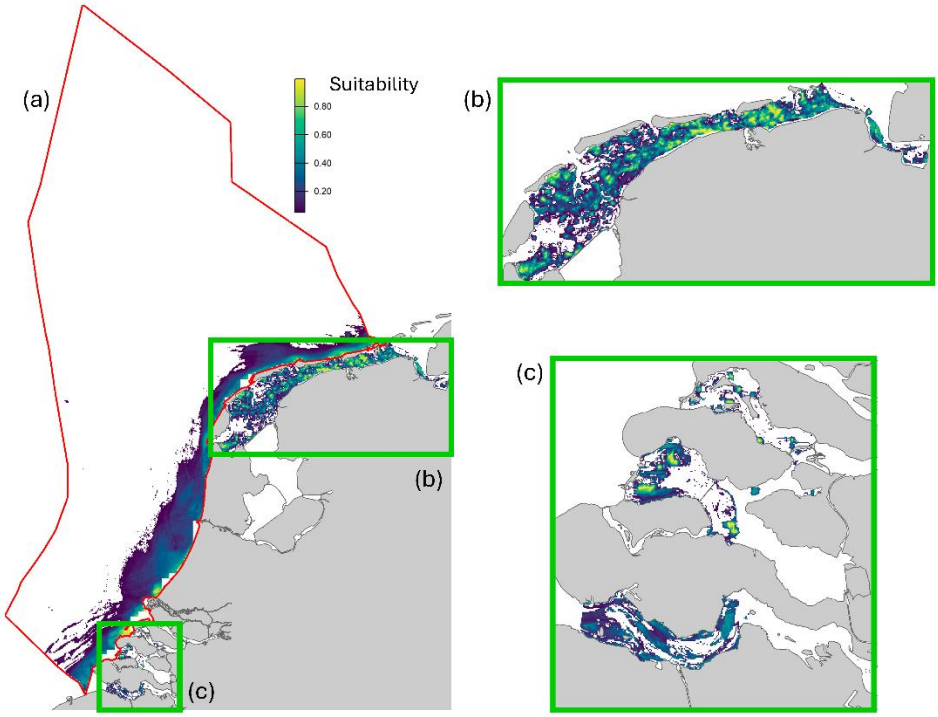


Figure 37: Spatial distribution of habitat suitability for M. edulis across the Dutch coastal basins. The mosaic panel combines basin-specific models: in the North Sea, suitability is calculated as the product of the normalized SDM mean and DEB index (SDM Mean × DEB), subsequently rescaled to 0–1 (a). In the Wadden Sea, suitability is based on the mean of RF and INLA predictions (b). In the Southwestern Delta, suitability is based on the mean of INLA and RF predictions, except for the Grevelingen for which suitability is the product of the thresholded SDM mean and DEB index (SDM Mean × DEB), subsequently rescaled to 0–1 (c). Green outlines in the mosaic indicate the spatial extent of the Southwestern Delta and Wadden Sea subdomains. The Dutch EEZ is shown in red and land as a grey polygon.

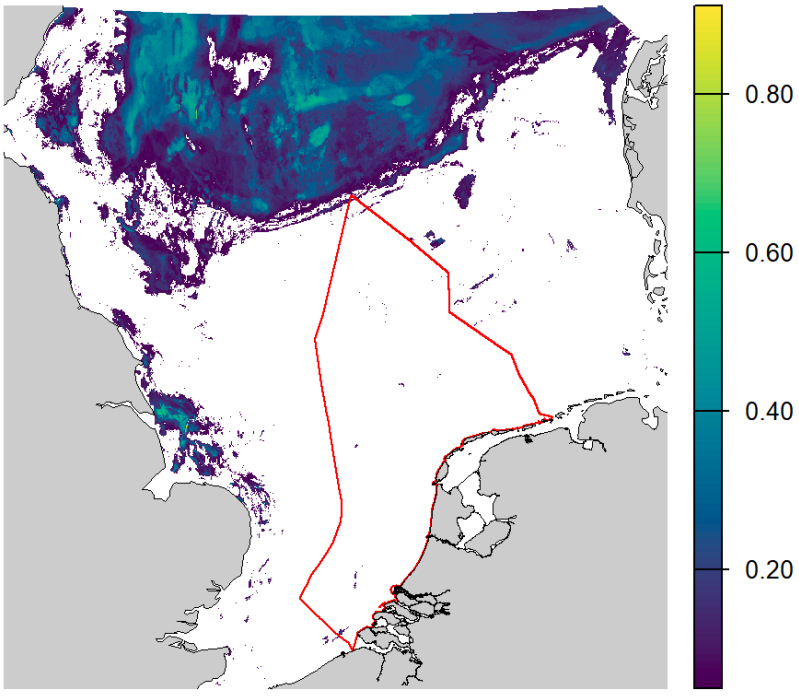


Figure 38: Spatial distribution of habitat suitability for M. modiolus in the Dutch North Sea. Suitability is based on the mean of GAM and RF predictions. No basin-specific subpanels are shown due to the absence of

comparable model outputs for the Wadden Sea and Southwestern Delta. The Dutch EEZ is shown in red and land in grey.

4 Discussion

4.1 Implications for restoration opportunities

The results described in this report indicate that several areas in the North Sea, Wadden Sea and Southwestern Delta are potentially suitable for the restoration of *O. edulis* and *M. edulis* reefs. Conversely, its low current and historical presence in Dutch waters (Bennema, 2022) make *M. modiolus* an unlikely candidate for ecosystem restoration, which is confirmed by our results (Table 4).

Table 4: Highest potential restoration locations for O. edulis, M. edulis and M. modiolus.

	North Sea	**Wadden Sea**	**Southwestern Delta**
O. edulis	Frisian Front, Voordelta	Tidal inlet systems of Eierlandse Gat and Vlie, potentially also Pinkegat/Zoutkamperlaag	**Lake Grevelingen**: mostly shallow-water areas **Oosterschelde**: near Neeltje Jans **Westerschelde**: no occurrence
M. edulis	Along the coastline, in particular Voordelta	For the intertidal: on the tidal divides of both Ameland and Schiermonnikoog. For the subtidal, in vicinity of the closure dam	**Lake Grevelingen**: shallow-water areas **Oosterschelde**: hotspots near Neeltje Jans and on the Roggeplaat and Galgeplaat **Westerschelde**: intertidal areas west of Hansweert
M. modiolus	*No indications that Dutch coastal and marine waters are suitable for restoration of M. modiolus reefs*		

4.1.1 North Sea

The most promising areas for the restoration of *O. edulis* in the North Sea are the Voordelta and to a lesser extent the Frisian Front. The former is already known for its presence of at least one natural reef (Kamermans et al., 2022), while several locations on the Frisian Front have recently been designated for oyster reef restoration. A peculiar observation is the low overall feasibility for restoration on the Oyster Grounds, which historically hosted the North Sea's largest oyster reef (Thurstan et al., 2024). Changes in environmental conditions since the early twentieth century (e.g. changed nutrient and substrate input due to damming of major river inflows) may have partly contributed to this discrepancy (Dickson et al., 2025). However, it is also possible that present-day populations of *O. edulis*, whose DEB parameters were used in this report , are not adapted to the low-nutrient conditions of the Oyster Grounds due to their occurrence closer to the coast. Nonetheless, due to the fact that oysters originating from the south of the Netherlands are likely to be used in restoration projects, this should give a fair impression of the restoration potential of this species.

As a mostly coastal species, the restoration potential for *M. edulis* in the North Sea is concentrated along the Dutch coastline, with particular hotspots near the Wadden islands and especially in the Voordelta. However, our models do not account for the presence of artificial hard substrate (offshore wind turbines, oil and gas platforms, etc.), which has proven to allow for mussel growth in the upper water layers throughout the North Sea and elsewhere within the species' range of occurrence. This indicates that, in the upper few meters of the water

column, the availability of suitable substrate may be its only limiting factor, and the actual suitability range is much larger than what our models suggest. However, the DEB models, specifically based on the food availability near the seabed further indicate that the potential for the development of benthic mussel beds is limited offshore (Rienstra et al., 2024).

4.1.2 Wadden Sea

In the Wadden Sea, restoration could principally focus on the tidal inlet systems of Eierlandse Gat and Vlie, near the island of Vlieland. However, since the species has only recently reappeared in the Wadden Sea and is limited to only a handful of observations, a larger area could be suitable for restoration than what the map suggests. Most likely sites would then be the other tidal inlet systems due to their open exchange with the North Sea and consequent potential susceptibility to larval inflow. Moreover, since *O. edulis* has been found to occur on reefs of *M. gigas* (Christianen et al., 2018), restoration of mixed reefs could be considered, at least in the lower intertidal areas, where *O. edulis* is not completely outcompeted by *M. gigas* (Didderen et al., 2022).

Large parts of the Wadden Sea prove to be potentially suitable for the restoration of *M. edulis*. In recent years, the species has seen a natural expansion, with a record area of mussel reefs in 2024 (CLO, 2026). Assisted recovery may therefore not be needed, although it is as of yet uncertain how long the newly established mussels will survive (personal communication with Max Burgoon, NIOZ). In the Wadden Sea, the most suitable areas on the tidal divides are located at the ends of tidal channels, suggesting that these channels may act as conduits for seed delivery.

4.1.3 Southwestern Delta

Potential sites for restoration of *O. edulis* reefs in the Southwestern Delta are principally found in the Oosterschelde and Lake Grevelingen. Since the species is currently absent from the Westerschelde, no suitability could be calculated in that basin. In the Oosterschelde, restoration should focus on areas relatively close to the storm surge barrier, most notably south of Neeltje Jans. The proximity to the North Sea could also benefit from a potential larval inflow from, and provide a potential source for, nearby (restored) reefs in the Voordelta. As in the Wadden Sea, the lower intertidal parts of existing reefs of *M. gigas* could be suitable for the settlement of *O. edulis*. Similar opportunities for restoration may exist on the *M. gigas* reefs in the Westerschelde.
In Lake Grevelingen, restoration potential is mainly limited by the recurring hypoxic events. As these mostly occur in the deep channels, reefs would ideally be established in the shallower areas near the coast, which are highlighted by the models.

The restoration potential for *M. edulis* has a smaller range than for *O. edulis* in Lake Grevelingen and a larger one in the Oosterschelde. In the latter basin, hotspots near Neeltje Jans and on the Roggeplaat and Galgeplaat indicate that intertidal conditions for mussel growth are suitable up to a larger distance from the North Sea than for oysters. In both basins, the frequent location of highly suitable areas near commercial mussel plots could be an indication that natural reefs are sustained by larval inflow from the aquaculture industry. The pattern for *M. edulis* in the Westerschelde hints at a potential effect of salinity, with the establishment of mussel reefs becoming highly unlikely upriver. As in the Oosterschelde, intertidal areas towards the North Sea are most suitable for potential restoration.

4.2 Ecological considerations of the model results

For a thorough interpretation of the maps, it is important to consider local conditions that are at play, both ecological and anthropogenic. This is well illustrated by the habitat suitability map of *O. edulis* in the Wadden Sea, where its low probability of occurrence is directly related to the very limited amount of observations of the species. No observations were recorded

from its local extinction until 2014, and since then only a handful of records exist even though several monitoring programmes (WOT-MOSKOK, SIBES, MWTL) regularly survey throughout the basin. The concentration of those observations near Vlieland is likely a result of larval inflow through one of the neighbouring tidal inlet systems, rather than a consequence of contrasting conditions with other parts of the Wadden Sea. This also explains why other areas with (slightly) increased probability are located near the tidal inlets. In essence, the map for the Wadden Sea should be interpreted as a probability map for natural settlement of *O. edulis.* While the map does offer some insight into potential restoration sites, it probably underestimates the full range of conditions that could support successful reef restoration.

In the Oosterschelde and Lake Grevelingen, both the models for *O. edulis* and for *M. edulis* were trained on presence data outside of the existing aquaculture plots, because those areas are artificially modified to enhance shellfish production (by adding settling substrate) and are therefore not reliably represented by the environmental data layers. Consequently, some naturally suitable areas may not result in observed presence of the species and the model potentially underestimates the possible relationship between some environmental variables and the probability of the species' occurrence.

What our models for Lake Grevelingen do not explicitly take into account, are the duration and severity of hypoxic events. While these episodes are known to occur primarily in the deeper channels, their temporal extent can vary substantially between years (Prins et al., 2024), and prolonged oxygen deprivation may impair bivalve growth, survival, or reproductive output even in areas that otherwise appear suitable (Kamermans and Saurel, 2022). Short-term tolerance to reduced oxygen levels is likely species- and life-stage dependent, yet the thresholds at which hypoxia becomes limiting remain poorly quantified for both species in this system. As a result, the suitability indices presented here may overestimate the true restoration potential in parts of the lake where low-oxygen conditions persist for extended periods. Incorporating spatially and temporally resolved oxygen dynamics into future modelling efforts would therefore improve the reliability of restoration site selection in Lake Grevelingen.

Finally, our results indicate where new restoration efforts have the best chances to succeed in the current conditions. However, especially the part of the suitability relative to food availability can also change depending on current or future activities implemented in the systems (e.g. increased bivalve aquaculture or restoration activities). Besides site suitability, another factor to account for when developing plans for large-scale bivalve bed restoration is the system's carrying capacity. For example, we know that the Oosterschelde is a fully-mixed system and have therefore not carried out any DEB modelling. In the Oosterschelde, there is already a large grazer population in terms of cultivated shellfish beds. These commercial beds take up a substantial part of the available phytoplankton. How much additional 'natural' shellfish beds the system can accommodate is a question we did not tackle in this research. In an aquaculture context, carrying capacity has been divided into different categories (McKindsey et al., 2006; Ross et al., 2013; Smaal and van Duren, 2019), that can also be transferred to restoration applications: 1) physical carrying capacity, referring to the total area of beds that can be accommodated in the available physical space, 2) the production carrying capacity that is the maximum surface of beds and bivalve stocking density that the system can support, 3) the ecological carrying capacity that is the surface of beds and bivalve stocking density that can be supported without leading to significant changes in ecological functioning and 4) the social carrying capacity which is the amount of aquaculture/restoration that can be developed without adverse social impacts.
A meaningful next step to complement these maps for decision making on future restoration plans would be to assess the ecological carrying capacity of the different (sub-) systems

studied here. Estimating ecological carrying capacity is, however, challenging for two reasons.

The first reason is the definition of ecological carrying capacity itself, or more specifically what is a significant/unacceptable change in ecological functioning. The decision regarding a specific limit ultimately lies with the government. Ecological carrying capacity for bivalve aquaculture has mostly been investigated in terms of primary production (e.g. Dame and Prins, 1998; Troost, 2013) as it forms the base of the food web, and determines how much organic carbon is available to higher organisms. Troost et al. (2025b) suggest an approach to define healthy primary production. In summary, primary production can be considered healthy when it is sufficient, not only in quantity but also in quality (e.g. suitable phytoplankton species), to support ecosystem functioning and species targets, under balanced nutrient-light conditions, and in a way that meets ecological objectives (e.g. Natura 2000, WFD or OSPAR thresholds).

Once these acceptable limits are set, the challenge of assessing the maximum biomass that can be supported by this limit still persists. Assessing carrying capacity requires sufficient data to on the system's primary production rates, water residence times (determining the speed at which food can be "replenished") and information on bivalve clearance rates within these types of systems. Moreover, ecological carrying capacity can have a non-linear relationship to food-availability due to a multitude of biological reactions and interactions (Troost, 2013; Troost et al., 2025b). Therefore, feedbacks of increasing bivalve beds on the primary production itself would need to be accounted for. The last difficulty is to translate the calculated total biomass that can be supported by a specific system to surface of beds that can be restored. This would require knowledge on stocking densities of beds able to naturally settle in these environments. For species that are already re-colonizing (such as *M. edulis* in the Wadden Sea) this is possible, while for species that are extinct and currently absent from these systems, information from other systems will need to be used, which might add extra uncertainty.

4.3 Additional elements to be considered for successful restoration

Some elements were not considered in this study, which also may be very relevant for successful restoration of shellfish beds.

While our models identify several promising areas for the restoration of *O. edulis*, it is important to recognise that physical suitability alone does not guarantee long-term population establishment. Recent work on the Frisian Front demonstrates that larval connectivity may be a major limiting factor for offshore restoration. The dedicated larval dispersal study for this region (Heye et al., 2026) shows that larval retention at the designated sites is low, with larvae rapidly advected out of the area and only minimal exchange occurring between neighbouring restoration sites. This has two implications for the interpretation of our maps. First, areas that appear suitable based on food availability, substrate, or hydrodynamics may still be unable to support self-sustaining reefs if larvae cannot remain in or return to the site. Second, because *O. edulis* is currently largely functionally extinct in Dutch offshore waters, the absence of upstream broodstock means that natural replenishment is essentially absent. Thus, especially in offshore settings such as the Frisian Front, restoration success will depend not only on local conditions but also on metapopulation processes, which remain highly constrained under present circumstances. These findings emphasise that our maps reflect the environmental potential for reef development, but that demographic isolation must be considered when prioritising sites for practical restoration efforts.

In addition to connectivity, the stability of introduced material forms a key ecological and operational constraint on restoration feasibility. Our model results indicate that several

coastal and estuarine systems offer promising environmental conditions for flat oyster recovery. However, offshore and more exposed sites in the North Sea, including the Frisian Front, require careful assessment of local hydrodynamic forces before any large-scale deployment. Findings from the ECOFRIEND project (Bos et al., 2023) revealed that loose oysters, lightweight cages and other unanchored materials are readily displaced, with many elements lost shortly after deployment during field pilots. Hydrodynamic stability modelling for the Frisian Front (Gerritsma et al., 2026) corroborates these observations and shows that typical offshore wave climates may exceed the mobility thresholds of most traditional restoration materials. As a result, restoration opportunities in offshore or dynamic environments depend heavily on the use of robust deployment strategies, such as gabions or spat-on-rock configurations, which were found to provide substantially greater stability under both normal and extreme conditions. For the interpretation of our results, this means that even when abiotic and trophic conditions are favourable, successful reef development may still require active, engineered approaches that prevent displacement during storm events. Thus, the feasibility of restoration is ultimately determined by the intersection of ecological suitability, larval supply, and the physical resilience of deployed structures.

4.4 Methodological considerations and model uncertainty

It is important to consider the shortcomings of the modelling techniques used and the uncertainties arising from both the modelling process and limitations in the data. These methodological limitations cause some uncertainty in the model and the final maps, but it should be stressed that the results are nonetheless considered plausible by the authors and can therefore be used for management purposes.

The different water basins studied in this report differ considerably in terms of data density and quality, which influences model confidence. In the North Sea, environmental data coverage is extensive, and updated sediment maps (Dabekaussen and Meijninger, 2026) greatly improve representation of substrate conditions. However, updated maps of gravel content, or existing locations of stone reefs and other natural hard substrata were not yet available at the time of the analyses. This can particularly impact the habitat suitability ranking in areas such as the Borkum Reef Ground, an area where the oysters appeared to grow relatively well. In the Wadden Sea and Southwestern Delta, environmental data layers were found to be more scarce. Particularly for sediment maps, we had to rely on predictions based on point data, either through predictive methods such as GAM or Random Forest, or through interpolation (Franken et al., *i.p.*). As mentioned before, some of these predictions performed poorly, rendering them unusable for habitat suitability mapping, but it should be stressed that even the remaining ones, especially for the Southwestern Delta, were predicted based only on a limited set of points. The Westerschelde in particular presented a number of methodological challenges. The highly dynamic nature of the estuary is likely to have caused the low performance of the sediment predictions. Moreover, other data layers in this basin also stem from predictions based on a limited set of point data. Due to a lack of available model data, chlorophyll a concentrations were interpolated from only five measuring stations along the estuary, under the assumption that the system is well-mixed and therefore tends to give rise to smooth east-west gradients.

A particular issue arises where the North Sea and Westerschelde meet. The model domain for the Westerschelde is equal to that of the environmental predictor layers used. However, this essentially means that it was limited to the domain of the elevation and exposure time maps, which have a smaller domain than the modelled hydrodynamics layers and use the seaward boundary of the official ecotope maps, equal to the virtual line between Vlissingen and Breskens. The model domain for the North Sea maps ends at the line between Westkapelle and Cadzand, about 10 km further seaward. As a result, a trapezoid covering the estuary mouth and parts of the Vlakte van de Raan is not modelled and a gap persists

between the two maps. This is the largest remaining unmodelled region for habitat suitability of *O. edulis* and *M. edulis* in Dutch coastal and marine waters. Smaller unmapped areas due to limits of the model domain occur along the North Sea coastline, most notably in the Voordelta, and on a few locations where the domain of the Wadden Sea and that of the North Sea do not perfectly align. However, these limitations generally do not prevent meaningful interpretation of regional patterns, as the existing model domains still capture the majority of suitable habitat and allow confident extrapolation where those gaps remain.

The DEB model outcomes are influenced by the environmental forcings taken from the 3D water quality model, which itself carries uncertainties. Although the 3D model is calibrated and validated, its performance varies spatially, with generally higher confidence in coastal areas where observations are more abundant. These uncertainties can propagate into the DEB simulations, particularly in regions where the 3D model is less constrained.

The short forcing periods, three years for the North Sea and one year for Lake Grevelingen, mean that the long-term DEB results reflect present-day conditions rather than long-term environmental variability. While these datasets capture realistic seasonal dynamics, they represent only a snapshot of the system. Consequently, the growth estimates indicate potential under current conditions and do not account for future changes in temperature, hydrodynamics, or other climate-driven factors. This assumption is sufficient for identifying areas with favourable present-day conditions for bivalve restoration but should be kept in mind when interpreting long-term growth potential.

Uncertainties are also linked to the DEB parameterization. Although the model should be generic and one species should be able to be represented by one set of parameters, several parameters are influenced by local environmental conditions and cultivation history. For example, food availability and food quality are affected by site-specific factors such as hydrodynamics, water quality and carrying capacity (Alunno-Bruscia et al., 2001). Physiological adaptation and factors such as biofouling in food-rich areas may further modify feeding performance, while cultivation practices also influence growth (Stechele, 2022b; Saraiva and Kooijman, 2017). In this study, *O. edulis* parameters are based on oysters from the Southwestern Delta, which are adapted to shallow, non-stratified conditions. Growth characteristics may therefore differ slightly from oysters historically inhabiting deeper waters. For *M. edulis*, the DEBGRZ parameters draw on earlier Oosterschelde calibrations (Troost et al., 2010; van Kessel et al., 2022) and were updated with more recent values from Stechele et al. (2022b) to better represent offshore mussel growth.

For scaling the DEB-based length suitability index, the lower threshold for *O. edulis* (2.5 cm) is based on expert judgement of the size at first reproduction, while the 1.2 cm threshold for *M. edulis* is taken from the Add-my-Pet DEB parameter set and reflects the size at puberty. In the suitability maps, areas below these thresholds are classified as unsuitable. The upper bounds (10 cm for *O. edulis* and 4 cm for *M. edulis*) are defined based on observed typical sizes of adult bivalves with reproduction capabilities. However, literature supporting these limits is limited. These assumptions influence the scaling of suitability and should be considered when interpreting the results.

4.5 Recommendations and conclusion

4.5.1 Recommendations on future modelling

1. Periodically update habitat suitability models with new observations and environmental data

The predictive performance of the habitat suitability models is strongly influenced by the availability and spatial coverage of occurrence data. This is particularly relevant for species such as *Ostrea edulis* in the Wadden Sea and *Modiolus modiolus* in the Dutch North Sea, where observations remain scarce. As new monitoring data become available through

restoration projects, national monitoring programmes and international databases, the models should be recalibrated and updated. Regular updates will reduce uncertainty and improve the reliability of restoration prioritisation.

2. Validate predictions using restoration pilots and established reefs
The current assessment is primarily based on habitat suitability and growth potential under present-day conditions. Future restoration projects provide an opportunity to test model predictions against realised restoration outcomes. Systematic monitoring of survival, growth, recruitment and reef development at restoration sites would allow refinement of both habitat suitability models and DEB parameterisations, ultimately improving predictive power and restoration planning.

3. Incorporate connectivity and metapopulation processes into future restoration planning
This study focuses on local habitat suitability but does not explicitly account for larval dispersal and connectivity between restoration sites. Recent work on the Frisian Front demonstrates that demographic connectivity can be a key determinant of long-term restoration success. Future analyses should therefore integrate hydrodynamic connectivity, larval transport and genetic exchange to identify networks of restoration sites that can function as self-sustaining metapopulations rather than isolated reefs. A first project addressing these issues, requested by the Greater North Sea Basin Initiative (GNSBI) and funded by the Nature Regeneration North Sea programme (NN) is currently being executed and expected to deliver results by the end of 2026.

4. Assess restoration potential under future climate conditions
The DEB simulations are based on present-day environmental conditions and do not account for long-term changes in temperature, stratification, oxygen dynamics or primary productivity. Future modelling efforts should evaluate restoration potential under climate-change scenarios to assess the robustness of restoration locations and identify areas that may remain suitable under future environmental conditions. For the southern North Sea, this will be addressed in the Horizon Europe project NID4Ocean.

5. Improve representation of local-scale environmental variability
Several uncertainties identified in this study originate from limitations in sediment maps, local data gaps and unresolved environmental heterogeneity, particularly in the Southwestern Delta and transition zones between model domains. Targeted collection of sediment, oxygen and benthic habitat data in priority restoration areas would improve model performance and support micrositing efforts at the scale relevant for restoration implementation.

6. Complement restoration potential maps with ecological carrying-capacity assessments
The present study identifies where restoration is ecologically feasible, but it does not determine how much reef habitat can be restored without affecting ecosystem functioning. Future work should therefore combine restoration potential mapping with carrying-capacity assessments, particularly in systems such as the Oosterschelde and Wadden Sea where existing shellfish populations already exert substantial grazing pressure on primary production.

4.5.2 Recommendations on management and restoration

1. Protect the most promising restoration areas
Areas identified as highly suitable should be considered in marine spatial planning and protection measures. Activities that may compromise reef establishment, such as bottom-

contact fisheries, dredging, sand extraction, or infrastructure development, should be carefully assessed in these locations.

2. Implement restoration through a phased, adaptive approach with strong monitoring
Given the remaining uncertainties in habitat suitability and ecosystem responses, large-scale implementation should be preceded by pilot projects in the most promising areas. Lessons learned from these pilots can then inform scaling-up efforts and reduce restoration risks. Restoration success should be evaluated over ecological timescales rather than project timescales. Long-term monitoring of survival, recruitment, reef development and associated biodiversity is essential for adaptive management and for improving future restoration efforts.

3. Prioritise connected reef networks rather than isolated restoration sites
Restoration efforts should focus first on areas that not only score highly in habitat suitability models but also have existing populations nearby or are connected to potential larval sources. Such locations are more likely to develop into self-sustaining reefs and require less long-term intervention than isolated restoration sites.

4. Integrate biogenic reef restoration into broader marine spatial planning and ecosystem restoration policies
Since the target species occur across national boundaries, while larval dispersal can connect populations between regions. Coordination between restoration initiatives in the Dutch coastal and marine waters and neighbouring countries would increase the chances of creating resilient reef networks and maximise the return on restoration investments.

4.5.3 Conclusion

This study shows that multiple areas in Dutch coastal and marine waters offer strong potential for the restoration of *O. edulis* and *M. edulis* reefs. For both species, the Voordelta, tidal inlet systems and tidal divides of the Wadden Sea and parts of the Oosterschelde and Lake Grevelingen emerge as promising locations. These areas combine favourable environmental conditions with either existing populations or proximity to suitable larval supply. In contrast, *M. modiolus* appears unsuitable for restoration in Dutch waters, consistent with its historically low presence and the environmental limitations identified by the models.

Despite some uncertainties linked to the used data and methodology, the results are able to highlight that suitable environmental conditions for reef formation and growth remain present at a meaningful scale, and that restoration is both feasible and regionally differentiated. By identifying specific areas where environmental conditions align with the species' ecological requirements, the study provides a practical foundation for planning targeted, basin-specific restoration efforts.

References

Alunno-Bruscia, M., Bourget, E., and Fréchette, M. (2001). Shell allometry and length-mass-density relationship for *Mytilus edulis* in an experimental food-regulated situation. *Marine Ecology Progress Series* 219: 177–188. https://doi.org/10.3354/meps219177

Bennema, F. P., Engelhard, G. H., and Lindeboom, H. (2020). *Ostrea edulis* beds in the central North Sea: Delineation, ecology, and restoration. *ICES Journal of Marine Science* 77: 2694-2705. https://doi.org/10.1093/icesjms/fsaa134

Bennema, F. P. (2022). *North Sea benthos 1902-1912 – Distribution based on Huxley, Wodan and Poseidon surveys data. Second Edition.* MarHis, Leeuwarden.

Beukema, J. J., and Dekker, R. (2022). Bottom-up as well as top-down processes govern zoobenthic secondary production in a tidal-flat ecosystem. *Limnology and Oceanography* 67: 2547-2556. https://doi.org/10.1002/lno.12221

Boerman, R. (2025). *The Impact of Offshore Wind Farms on the Growth of Flat Oysters (Ostrea edulis) and the potential for restoration in the North Sea*. MSc thesis report. Faculty of Geosciences, Utrecht University, Utrecht.

Bos, O., Kamermans, P., Tonk, L., Schutter, M., Maathuis, M., van Gool, A., van der Have, T., Bergsma, J., Raaijmakers, T., van Duren, L., Emmanouil, E., Gerritsma, I., Kleissen, F., and Sas, H. (2023). *Eco-friendly reef restoration pilots in offshore wind farms. Report Project ECOFRIEND 2019-2023*. Wageningen Marine Research, Den Helder.

Christianen, M. J. A., Lengkeek, W., Bergsma, J. H., Coolen, J. W. P., Didderen, K., Dorenbosch, M., Driessen, F. M. F., Kamermans, P., Reuchlin-Hugenholtz, E., Sas, H., Smaal, A., van den Wijngaard, K. A., and van der Have, T. M. (2018). Return of the native facilitated by the invasive? Population composition, substrate preferences and epibenthic species richness of a recently discovered shellfish reef with native European flat oysters (*Ostrea edulis*) in the North Sea. *Marine Biology Research* 14: 590-597. https://doi.org/10.1080/17451000.2018.1498520

CLO. (2026). Areaal mossel- en oesterbanken in de Waddenzee, 1995-2024 (indicator 1559, versie 10, 20 januari 2026), www.clo.nl. Centraal Bureau voor de Statistiek (CBS), Den Haag; PBL Planbureau voor de Leefomgeving, Den Haag; RIVM Rijksinstituut voor Volksgezondheid en Milieu, Bilthoven; en Wageningen University and Research, Wageningen.

Cole, H. A. (1941). The fecundity of *Ostrea edulis*. *Journal of the Marine Biological Association of the United Kingdom* 25: 243–260. https://doi.org/10.1017/S0025315400054710

Craeymeersch, J. A., and Jansen, H. M. (2018). Bivalve assemblages as hotspots for biodiversity. In: *Goods and Services of Marine Bivalves*, edited by Smaal, A. C., Ferreira, J. G., Grant, J., Petersen, J. K., and Strand, Ø., pp. 275-294. Springer Open, Cham, Switzerland. https://doi.org/10.1007/978-3-319-96776-9_14

Craeymeersch, J. A., Schotanus, J., van Asch, M., Capelle, J., Troost, K., and Janse, H. M. (2024). *Draagkracht van de Oosterschelde en westelijke Waddenzee voor schelpdieren*. Wageningen Marine Research, Yerseke.

Dabekaussen, W., and Meijninger, B. (2026). *M10018 MEMO – NHV- Habitat kartering WP2 – Noordzeebrede kartering*. TNO, Utrecht.

Dame, R. F., and Prins, T. C. (1998). Bivalve carrying capacity in coastal ecosystems. *Aquatic Ecology* 31: 409-421. https://doi.org/10.1023/A:1009997011583

Deltares. (2025). *D-Water Quality Processes Technical Reference Manual*. Deltares, Delft.

Dickson, J., Wohl, E., Govers, L. L., Franken, O., Bouma, T. J., Olff, H., Eriksson, B. K., Watson, M. S., Borges, L. M. S., and van der Heide, T. (2025). A review of the historic and present ecological role of aquatic and shoreline wood, from forest to deep sea. *Biological Reviews*. https://doi.org/10.1002/brv.70117

Didderen, K., van der Have, T. M., Bakker, E. G. R., and Japink, M. (2018). *Platte oester Waddenzee – Aanzet strategie en plan van aanpak voor herstel*. Bureau Waardenburg, Culemborg.

Dinesen, G. E., and Morton, B. (2014). Review of the functional morphology, biology and perturbation impacts on the boreal, habitat-forming horse mussel *Modiolus modiolus* (Bivalvia: Mytilidae: Modiolinae). *Marine Biology Research* 10: 845-870. https://doi.org/10.1080/17451000.2013.866250

Franken, O., Holthuijsen, S., Meijer, K., Kleine Schaars, L., Rasch, B., Kooijman, J., van Weerlee, E., Miguel, S., Koolhaas, A., Mosk, D., Dijkstra, A., Greeve, Y., van Walraven, L., Witte, S., Rehlmeyer, K., Dickson, J., Smeele, Q., Bijleveld, A. I., Olff, H., van der Heide, T., and Govers, L. L. *i.p.* Below murky waters: Subtidal benthic species and sediment distributions in the Dutch Wadden Sea. Preprint available at SSRN: https://doi.org/10.2139/ssrn.6307745

Fey, F., Dankers, N., Steenbergen, J., and Goudswaard, K. (2010). Development and distribution of the non-indigenous Pacific oyster (*Crassostrea gigas*) in the Dutch Wadden Sea. *Aquaculture International* 18: 45-59. https://doi.org/10.1007/s10499-009-9268-0

Gercken, J., and Schmidt, A.. (2014). Current status of the European Oyster (*Ostrea edulis*) and possibilities for restoration in the German North Sea. Bundesamt für Naturschutz, Bonn, Germany.Gerritsma, I., Emmanouil, E., and van Duren, L. (2026). *Hydrodynamic boundary conditions for oyster restoration on the Frisian Front*. Deltares, Delft.Groenenboom, J., van der Heijden, L., Markus, A.A., and Laan, S.C. (2020). *Ontwikkeling zesde-generatie modelschematisatie D-HYDRO Grevelingen; Modelbouw, kalibratie en validatie*. Deltares, Delft.

Helmer, L., Farrell, P., Hendy, I., Harding, S., Robertsen, M., and Preston, J. (2019). Active management is required to turn the tide for depleted *Ostrea edulis* stocks from the effects of overfishing, disease and invasive species. *PeerJ* 7: e6431. https://doi.org/10.7717/peerj.6431

Herman, P., and van Rees, F. (2022). *Mapping reef forming North Sea species*. Deltares, Delft.

Hermans, A., Bos, O. G., and Prusina, I. (2020). *Nature-Inclusive Design: A catalogue for offshore wind infrastructure*. Witteveen+Bos, Deventer; Wageningen Marine Research, IJmuiden.

Heye, S., Kleissen, F., and van Duren, L. (2026). *Larval dispersal from potential oyster restoration sites on the Frisian Front*. Deltares, Delft.

Houziaux, J.-S., Kerckhof, F., Degrendele, K., Roche, M. F., and Norro, A. (2008). *The Hinder banks: yet an important area for the Belgian marine biodiversity?* Belgian Science Policy, Brussels, Belgium.

Kamermans, P., Walles, B., Kraan, M., Van Duren, L. A., Kleissen, F., van Der Have, T. M., Smaal, A. C., and Poelman, M. (2018). Offshore Wind Farms as Potential Locations for Flat Oyster (*Ostrea edulis*) Restoration in the Dutch North Sea. *Sustainability*, 10: 3942. https://doi.org/10.3390/su10113942.

Kamermans, P., and Saurel, C. (2022). Interacting climate change effects on mussels (*Mytilus edulis* and *M. galloprovincialis*) and oysters (*Crassostrea gigas* and *Ostrea edulis*): experiments for bivalve individual growth models. *Aquatic Living Resources* 35: 1. https://doi.org/10.1051/alr/2022001

Kamermans, P., Didderen, K., Bakker, E. G. R., and Lengkeek, W. (2022). *Monitoring platte-oesterbank Voordelta 2021*. Wageningen Marine Research, Yerseke. https://doi.org/10.18174/567748

Kooijman, S.A.L.M. (2010). *Dynamic Energy Budget theory for metabolic organization*. 3rd Edition, Cambridge University Press, Cambridge, United Kingdom.

Larsen, P., and Riisgård, H. U. (2016). Growth-prediction model for blue mussels (*Mytilus edulis*) on future optimally thinned farm-ropes in Great Belt (Denmark). *Journal of Marine Science and Engineering* 4: 42. https://doi.org/10.3390/jmse4030042

Lloyd, S. P. (1957). "Least square quantization in PCM". Bell Telephone Laboratories Paper. Published in journal much later: Lloyd, S. P. (1982). "Least squares quantization in PCM". *IEEE Transactions on Information Theory* 28: 129–137. https://doi.org/10.1109/TIT.1982.1056489

MacQueen, J. B. (1967). *Some Methods for classification and Analysis of Multivariate Observations. Proceedings of 5th Berkeley Symposium on Mathematical Statistics and Probability*. Vol. 1. University of California Press. pp. 281–297.

McKindsey, C. W., Thetmeyer, H., Landry, T., and Silvert, W. (2006). Review of recent carrying capacity models for bivalve culture and recommendations for research and management. *Aquaculture* 261: 451-462. https://doi.org/10.1016/j.aquaculture.2006.06.044

Olsen, O. T. (1883). *The piscatorial atlas of the North Sea, English Channel, and St. George's Channels : illustrating the fishing ports, boats, gear, species of fish (how, where, and when caught), and other information concerning fish and fisheries.* London: Taylor and Francis. 118 pp.

Prins, T., Mestdagh, S., and Nolte, A. (2024). *Geïntegreerd meet- en onderzoeksplan voor Grevelingenmeer en Veerse Meer*. Deltares, Delft.

Richardson, C. and Saurel, C. (2003). *Age and growth analysis of native oyster beds in Wales. CCW Contract Science Report No 549 FC 73-02-229*. Countryside council for Wales, Bangor, United Kingdom.Ross, L. G., Telfer, T. C., Falconer, L., Soto, D., Aguilar-Manjarrez, J., Asmah, R., Bermúdez, J., Beveridge, M. C. M., Byron, C. J., Clément, A., Corner, R., Costa-Pierce, B. A., Cross, S., De Wit, M., Dong, S., Ferreira, J. G., Kapetsky, J. M., Karakassis, I., Leschen, W., Little, D., Lundebye, A.-K., Murray, F. J., Phillips, M., Ramos, L., Sadek, S., Scott, P. C., Valle-levinson, A., Waley, D., White, P. G., and Zhu, C. (2013). Carrying capacities and site selection within the ecosystem approach to aquaculture. In: *Site selection and carrying capacities for inland and coastal aquaculture*, edited by Ross, L. G., Telfer, T. C., Falconer, L., Soto, D., and Aguilar-Manjarrez, J. pp. 19–46. FAO/Institute of Aquaculture, University of Stirling, Expert Workshop, 6–8 December 2010. Stirling, the United Kingdom. FAO Fisheries and Aquaculture Proceedings No. 21. Rome, FAO. 282 pp.

Rienstra, J., Vilmin, L., Troost, T., Schneider, L., Kamaldinov, A., and Heye, S. (2024). *Effects of large-scale offshore wind development on trophic transfer pathways in the marine food web*. Deltares, Delft.

Rue, H., Martino, S, and Chopin, N. (2009). Approximate Bayesian inference for latent Gaussian models by using integrated nested Laplace approximations. *Journal of the Royal Statistical Society Series B: Statistical Methodology* 71: 319-392. https://doi.org/10.1111/j.1467-9868.2008.00700.x

Saraiva, S., and Kooijman, B. (2017). Amp Mytilus edulis. Version 2017/11/11.

Smaal, A. C., and Silvert, W. (2008). A simple model for estimation of shellfish carrying capacity. *2008 Annual Science Conference*, Halifax, Canada. https://doi.org/10.17895/ices.pub.25243798

Smaal, A. C., and van Duren, L. A. (2019). Bivalve Aquaculture Carrying Capacity: Concepts and Assessment Tools. In: *Goods and Services of Marine Bivalves*, edited by Smaal, A., Ferreira, J., Grant, J., Petersen, J., Strand, Ø.. Springer, Cham, Switzerland. https://doi.org/10.1007/978-3-319-96776-9_23

Stechele, B., Maar, M., Wijsman, J., Van Der Zande, D., Degraer, S., Bossier, P., and Nevejan, N. (2022a). Comparing life history traits and tolerance to changing environments of two oyster species (*Ostrea edulis* and *Crassostrea gigas*) through Dynamic Energy Budget theory. *Conservation Physiology* 10: coac034. https://doi.org/10.1093/conphys/coac034

Stechele, B., van der Zande, D., Alvera-Azcárate, A., Delbare, D., Lacroix, G., and Nevejan, N. (2022b). Biological site suitability for exposed self-regulating cultivation of blue mussel (*Mytilus edulis*): A Belgian case study. *Aquacultural Engineering* 98: 102264. https://doi.org/10.1016/j.aquaeng.2022.102264

Stephens, D., and Diesing, M. (2015). Towards quantitative spatial models of seabed sediment composition. *PLoS ONE* 10: e0142502. https://doi.org/10.1371/journal.pone.0142502

Thurstan, R. H., McCormick, H., Preston, J., Ashton, E. C., Bennema, F. P., Cetinić, A. B., Brown, J. H., Cameron, T. C., da Costa, F., Donnan, D. W., Ewers, C., Fortibuoni, T., Galimany, E., Giovanardi, O., Grancher, R., Grech, D., Hayden-Hughes, M., Helmer, L., Thomas Jensen, K., Juanes, J. A., Latchford, J., Moore, A. B. M., Moutopoulos, D. K., Nielsen, P., von Nordheim, H., Ondiviela, B., Peter, C., Pogoda, B., Poulsen, B., Pouvreau, S., Roberts, C. M., Scherer, C., Smaal, A. C., Smyth, D., Strand, Å., Theodorou, J. A., and zu Ermgassen, P. S. E. (2024). Records reveal the vast historical extent of European oyster reef ecosystems. *Nature Sustainability* 7: 1719-1729. https://doi.org/10.1038/s41893-024-01441-4

Troost, K., van Asch, M., van den Ende, D., Perdon, K. J., van der Pool, J., van Zweeden, C., and van Zwol, J. (2025a). *Schelpdierbestanden in de Nederlandse kustzone, Waddenzee en zoute deltawateren in 2024*. Wageningen Marine Research, IJmuiden. https://doi.org/10.18174/688163

Troost, T. A., Wijsman, J. W. M., Saraiva, S., and Freitas, V. (2010). Modelling shellfish growth with dynamic energy budget models: An application for cockles and mussels in the Oosterschelde (southwest Netherlands). *Philosophical Transactions of the Royal Society B: Biological Sciences* 365: 3567-3577. https://doi.org/10.1098/rstb.2010.0074

Troost, T. A., and van Duren, L. A. (2013). *Draagkracht voor MZI's in de Oosterschelde*. Deltares, Delft.

Troost, T., van der Linden, A., Dijkman, N., van den Bergh, M., and Holdt, A. (2025b). *Primaire Productie Grote wateren. Een vergelijking van model- en meetmethoden en de relatie met ecologische draagkracht*. Deltares, Delft.

University of Michigan Museum of Zoology. (n.d.). *Mytilus edulis*. Animal Diversity Web. https://animaldiversity.org/accounts/Mytilus_edulis/ (Accessed: 26 March 2026).

Valavi, R., Elith, J., Lahoz-Monfort, J. J., and Guillera-Arroita, G. (2021). Modelling species presence-only data with random forests. *Ecography* 44: 1731-1742. https://doi.org/10.1111/ecog.05615

van der Heijden, L., and Nolte, A. (2022). *Extra validatie zesde-generatie modelschematisatie D-HYDRO Grevelingen*. Deltares, Delft.

van der Meer, J., Franken, O., Glorius, S., van der Heide, T., Troost, K., and van Weerdenburg, R. (2025). Mapping habitat suitability of subtidal mussels *Mytilus edulis* in the Dutch western Wadden Sea. *Ecological informatics* 92: 193458. https://doi.org/10.1016/j.ecoinf.2025.103458

van der Reijden, K. J., Koop, L., Mestdagh, S., Snellen, M., Herman, P. M. J., Olff, H., and Govers, L. L. (2021). Conservation implications of *Sabellaria spinulosa* reef patches in a dynamic sandy-bottom environment. *Frontiers in Marine Science* 8: 642659. https://doi.org/10.3389/fmars.2021.642659

Van Haren, R. J. F., and Kooijman, S. A. L. M. (1993). Application of a dynamic energy budget model to *Mytilus edulis* (L.). *Netherlands Journal of Sea Research* 31: 119-133. https://doi.org/10.1016/0077-7579(93)90002-A

van Kessel, T., van Zelst, V. T. M., Hanssen, J., Vilmin, L. M., and van Duren, L. A. (2022). *Environmental effects of large-scale implementation of offshore wind farms. Further analyses*. Deltares, Delft.

Vilmin, L., Heye, S., Schneider, L., di Paola, F., Kamermans, P., Wijsman, J., and van Duren, L. (2024). *Oyster restoration modelling in the North Sea using Delft3D FM (No. T4.4; FutureMARES)*. Deltares, Delft.

Vilmin, L., Heye, S., Di Paola, F., and Blauw A. (2026). *3D DCSM-FM with water quality: Model set-up and validation*. Deltares, Delft.

Walne, P. R. (1964). Observations on the fertility of the oyster (*Ostrea edulis*). *Journal of the Marine Biological Association of the United Kingdom* 44: 293-310. https://doi.org/10.1017/S002531540002484X

Wood, S. N. (2017). *Generalized Additive Models – An Introduction with R, Second Edition*. Chapman and Hall/CRC, New York, United States. https://doi.org/10.1201/9781315370279

Ysebaert, T., Walles, B., Haner, J., and Hancock, B. (2018). Habitat modification and coastal protection by ecosystem-engineering reef-building bivalves. In: *Goods and Services of Marine Bivalves*, edited by Smaal, A. C., Ferreira, J. G., Grant, J., Petersen, J. K., and Strand, Ø., pp. 253-273. Springer Open, Cham, Switzerland. https://doi.org/10.1007/978-3-319-96776-9_13

Zijl, F., Laan, S. C., Emmanouil, A., van Kessel, T., van Zelst, V. T. M., Vilmin, L. M., and van Duren, L. A. (2021). *Potential ecosystem effects of large upscaling of offshore wind in the North Sea*. Deltares, Delft.

Zijl, F., Zijlker, T., Laan, S., and Groenenboom, J. (2023a). *3D DCSM FM: a sixth-generation model for the NW European Shelft*. Deltares, Delft.

Zijl, F., van Weerdenburg, R., and Laan, S. (2023b). *DWSM: a sixth-generation 3D model of the Dutch Wadden Sea*. Deltares, Delft.

Appendix

Table 5 Additional DEBGRZ-specific mussel parameters used in this study.

Parameter	Units	Value	Description
Vp	$cm^3\ ind^{-1}$	0.0560	Biovolume at start of reproductive age
Vb	$cm^3\ ind^{-1}$	5.60×10^{-8}	Volume at birth
MinSTmp	°C	15	Minimum spawning temperature
GSIupr	-	0.28	Energy threshold to start spawning
kappaA	-	0.9	Assimilation efficiency
kappaI	-	1.0	Ingestion efficiency
rSpawn	d^{-1}	0.02	Gonadal release rate at spawning
Yk	$gC\ m^{-3}$	100	Half-saturation constant for the negative effect of inorganic matter on food uptake
rMor	d^{-1}	0	Reference mortality rate of grazer for individuals of 1 cm at 20 °C
cMor	-	0	Length dependency coefficient for mortality rate
rHrv	d^{-1}	0	Reference harvesting rate of grazer for individuals of 1 cm
cHrv	-	0	Length dependency coefficient for harvesting rate
cAFWC	-	0.4	Conversion coefficient from ash free dry weight to carbon
cWWC	-	0.0224	Conversion coefficient from wet weight to carbon
TC	$gC\ gC^{-1}$	1	C:C ratio
TN	$gN\ gC^{-1}$	0.181	N:C ratio
TSi	$gSi\ gC^{-1}$	0.0	Si:C ratio
SWBen	-	2	Parameter specifying whether grazers are pelagic (0), benthic (fixed to the bottom, 1), or suspended (fixed to some structure at any vertical position in the water column, 2)
PrDet	-	0	Preference of grazer for detritus from the water column
PrDetS1	-	0	Preference of grazer for detritus from the sediment
SFSusp	-	1	Preference of suspension (1) over deposit (0) feeding
SwV1	-	0	Option parameter determining if the simulated grazers represent a cohort (isomorph representation) (0) or a population (V1-morph representation) (1)
FrDetS1	-	0	Fraction of detritus going to sediment
GSIlwr	-	0.1	Energy threshold to stop spawning for grazer

Deltares is an independent institute for applied research in the field of water and subsurface. Throughout the world, we work on smart solutions for people, environment and society.

Deltares

www.deltares.nl